

AN ABSTRACT OF THE THESIS OF

GARY GILMAN OLSON for the Ph. D.
(Name) (Degree)
in Chemistry presented on May 3, 1967
(Major) (Date)

Title: AUTOMATION OF THE PEARL-BENSON METHOD FOR
SPENT SULFITE LIQUOR

Abstract approved


Dr. Harry Freund

An automatic, continuous analyzer has been developed which is suitable for estimating the level of spent sulfite liquors (SSL) in laboratory samples. The analyzer makes use of a version of the Pearl-Benson, or nitroso method, and, in its present form, is useful for samples whose actual SSL solids concentrations are in the range 0 - 100 ppm.

A number of detailed investigations related to the development of the analyzer, but also related to various aspects of continuously flowing analytical streams in general, are discussed. These investigations include consideration of the mechanism by which the pump activates the flowing system and the effects upon flow characteristics which accompany system modification. A rudimentary electrical analog for the pump and its system has been proposed which qualitatively explains the observed behavior of the real system. The response characteristics of an unbroken flowing stream are considered and compared with those expected upon the basis of laminar flow.

Automation of the Pearl-Benson Method
for Spent Sulfite Liquor

by

Gary Gilman Olson

A THESIS

submitted to

Oregon State University

in partial fulfillment of
the requirements for the
degree of

Doctor of Philosophy

June 1967

APPROVED:



Professor of Chemistry
in charge of major



Head of Department of Chemistry



Dean of Graduate School

Date thesis is presented May 3, 1967

Typed by Marion Palmateer for Gary Gilman Olson

ACKNOWLEDGMENTS

The author wishes to express his sincere gratitude to Dr. Harry Freund for his guidance and encouragement during the course of the investigations described in this thesis. He is also grateful to Mr. Roger Blaine for many helpful discussions.

The author is fortunate to have been the recipient of a National Science Foundation Cooperative Graduate Fellowship which helped to support this work. Also gratefully acknowledged is the support received through a grant from the Northwest Pulp and Paper Association.

The author is deeply indebted to his wife, Virginia, whose patience and understanding has been so much appreciated throughout this investigation.

TABLE OF CONTENTS

	<u>Page</u>
INTRODUCTION	1
THE ANALYZER	5
Description	5
Construction Details	13
Support	13
Arrangement of Tubing for Mixing and Waiting	15
Adaptation of DB Spectrophotometer	17
Calibration and Testing	21
Pump Calibration	21
Testing of the Analyzer	23
DETAILED INVESTIGATIONS	29
Type of Flow	29
Mechanism of the Pumping Process	32
Electrical Analog	47
Precision and Accuracy	59
Air Segmentation of the Analytical Stream	63
Response Characteristics	69
SUMMARY	87
BIBLIOGRAPHY	90
APPENDICES	92
APPENDIX I CLARIFICATION	92
APPENDIX II AUTOMATIC SAMPLE SELECTOR	109
APPENDIX III LAMINAR FLOW EQUATIONS	121

LIST OF FIGURES

<u>Figure</u>		<u>Page</u>
1	Schematic flow diagram for analyzer.	8
2	Diagram of debubbler.	10
3	Diagram of constant head reagent supply cup.	12
4	Diagram of input manifold.	18
5	Diagram of flow cuvette.	19
6	Diagram of ported cover for DB Spectrophotometer.	20
7	Representative raw data showing reproducibility.	25
8	Examples of raw data for calibration curve.	26
9	Calibration curve for analyzer.	28
10	Dependence of flow rate on pump speed.	31
11	Dependence of pressure head developed on pump speed.	33
12	Apparatus for studying instantaneous pressures.	34
13	Resistance changes indicating instantaneous pressure changes for various damping combinations.	37
14	Valve operation, Durrum pump.	42
15	Valve displacement, Durrum pump.	44
16	Models of pump and system.	53
17	Waveforms expected of analog model.	55
18	Detector response with segmented and unsegmented analytical streams.	68
19	System response to step changes.	70
20	Dependence of response time on flow rate.	72
21	Dependence of rise time on flow rate.	73

<u>Figure</u>		<u>Page</u>
22	Linear propagation of paraboloid front.	76
23	Comparison of computed and observed response.	78
24	Comparison of computed and "effective" profiles.	81
25	Comparison among "effective" profiles.	82
26	Concentration changes due to diffusion at various times.	84

Appendix
Figure

I-1	Calibration curve for turbidity.	98
I-2	Calibration curve for turbidity.	99
I-3	Fuller's earth settling curve; time profile.	101
I-4	Fuller's earth settling curve; normalized time profile.	103
I-5	Fuller's earth settling curve; vertical profile.	104
I-6	Fuller's earth settling curve; normalized vertical profile.	105
I-7	Composite normalized fuller's earth settling curve.	106
II-1	Diagram of automatic sample selector, top.	112
II-2	Diagram of automatic sample selector, left side.	113
II-3	Diagram of automatic sample selector, front cross section at switches.	114
II-4	Automatic sample selector program.	116
II-5	Schematic wiring diagram for automatic sample selector, programmer, and indicator lamp chassis.	118

AUTOMATION OF THE PEARL-BENSON METHOD FOR SPENT SULFITE LIQUOR

INTRODUCTION

The work which led to the development of this thesis has been to a large extent supported by a grant to Oregon State University from the Northwest Pulp and Paper Association. This work, then, represents an initial portion of a larger project entitled Research on Automatic and Continuous Methods of Chemical Analysis.

The generalized research area under consideration covers investigation of suitable methods for performing continuous and/or repetitive chemical analyses on flowing streams or on samples derived from flowing streams. Special consideration is to be given to these factors: (1) Effluents from the pulp and paper industry are of particular interest. (2) The flowing streams of greatest interest are "natural" (e. g., rivers) rather than "artificial" streams whose compositions are known and/or controlled. (3) A suitable instrumentation system developed through this study should lend itself either directly or through reasonable adaptation to remote, unattended operation for extended periods of time.

Two alternate philosophies of continuous analysis were considered for initial investigation: specific transducers and chemical manipulations.

Specific transducers are perhaps the ultimate in the area of continuous analytical instrumentation. Two well-known examples are the glass electrode for pH and the dissolved oxygen membrane electrode (6). An attempt to develop specific transducers for components of interest, even if successful, would very likely not contribute significantly to the knowledge of techniques required for development of further methods, since the research would be of a very specific nature.

A study of the techniques of chemical manipulations, with or without concentration steps, on the other hand, would be applicable to many methods. In general, most analytical methods involve one or more reagent additions and mixing steps and frequently involve concentration steps as well. Development of a technique for effectively performing such manipulations on samples derived from natural streams would contribute to future related studies.

The problem selected for study was to attempt to render continuous and automatic a version of the Pearl-Benson nitroso method for estimating spent sulfite liquor concentration in water (3).

The Pearl-Benson (P-B) method gives an estimation of lignin sulfonates in water. These lignin compounds are of interest because they are present in spent sulfite liquor (SSL) wastes to the extent of approximately 65% of total solids and are reasonably resistant to biodegradation in waterways. Since they exist in relatively high levels

in the wastes, the lignins would be the last components to disappear from a sample upon continued dilution. Furthermore, since lignins normally don't contribute significantly to the biological oxygen demand of the wastes, following lignin should provide information concerning the dissipation of SSL wastes including the decomposition products of SSL wastes. In addition, the Pearl-Benson method represents an example of a method involving chemical manipulations exclusive of required concentration processes. Inclusion of concentration steps at this time is unattractive. For example, large molecules commonly found in natural streams interfere with ion exchange membranes which might otherwise be used for concentration (12, 13). This method yields a colorimetric readout which may be treated with a suitable light-level transducer, and, by appropriate electronic manipulation, the readout may be presented to the scientists in the desired form (e. g., strip chart or digital printout, or it may be telemetered in computer-compatible code). Finally, the Pearl-Benson method has been in common use by the pulp and paper industry for a number of years, thus a large backlog of data and knowledge of typical interferences exists to assist in the eventual field evaluation of the automatic, continuous analyzer.

The work to be discussed in this thesis has been directed primarily toward the development of a prototype analyzer which will determine lignin levels in synthetic samples prepared in the

laboratory. Some preliminary investigation of the problem of obtaining a clarified sample from a naturally turbid source is discussed in Appendix I. In addition, a dual-beam flow colorimeter is currently being developed in these laboratories (18, p. 60-70) which will be suitable for continuously measuring low levels of absorbing materials in solution.

THE ANALYZER

Description

The Pearl-Benson method for lignins may be resolved into a series of measure and add, mix, and wait steps, followed by measurements of color intensities. Such a summary of the method is outlined below (3).

- I. Determination of total absorbance, A_T
 - A. Measure 50 ml of the sample into a container and add via buret or pipet 1 ml of 10% acetic acid and 1 ml of 10% sodium nitrite solution.
 - B. Mix
 - C. Allow to stand for 15 minutes at room temperature.
 - D. Add via buret or pipet 2 ml of 2 N ammonium hydroxide.
 - E. Mix
 - F. Allow to stand for 10 minutes at room temperature.
 - G. Measure A_T at 430 m μ versus distilled water.
- II. Determination of absorbance of blank, A_B
 - A. Measure 50 ml of the sample into a container and add via buret or pipet 1 ml of 10% acetic acid.
 - B. Mix
 - C. Add via buret or pipet 2 ml of 2 N ammonium hydroxide.

- D. Mix
- E. Add via buret or pipet 1 ml of 10% sodium nitrite solution.
- F. Mix
- G. Allow to stand for 10 minutes at room temperature.
- H. Measure A_B at 430 m μ versus distilled water.

III. Determination of net sample absorbance: $A_S = A_T - A_B$

To create a continuous means for performing a Pearl-Benson analysis, then, one must perform each of these steps continuously.

A laboratory reagent-metering pump may be used to perform the measure and add function. It was felt that the Durrum Dial-A-Pump (Durrum Instrument Corp., Palo Alto, Calif.) would be particularly suited for research attempts to meter reagents. This pump provides 12 individually adjustable channels in which the solution being pumped is in contact only with the tubing through which it flows (e. g., Tygon). In addition, each channel accommodates various tubing sizes for greater adjustability of flow rates, and a factory modification provides for adjustment of the pump rotation rate while holding constant the established ratios between various channels. Thus, if various channels are adjusted so as to pump the desired proportions of reagents to be measured, these may be continuously added to one another by combining the various streams into one at a manifold. This manifold may exit directly into the mixing device.

The mix function may be accomplished by the "repeated inversions" method (19) by causing the analytical stream to flow through helices of tubing whose longitudinal axes are horizontal. Such helices were fashioned from 4 mm Pyrex tubing.

Since flow rate of the analytical stream may be expressed in terms of length of tubing per unit time, waiting periods (as for color development) may be accommodated by providing a suitably long length of tubing. Of course, this tubing may be straight or arranged in a "tortuous path" configuration in order to conserve space.

Based upon the decision to use the Durrum pump to meter reagents, the analytical stream may be visualized as a continuous column of liquid moving along a glass tube containing ports for reagent addition and helices for mixing, and of sufficient length to accommodate the waiting periods required by the analytical scheme. Figure 1 shows a flow diagram for the analytical scheme. Two channels, paralleled with respect to time, were required; one to function in the normal manner as a sample channel and one containing the unknown and all reagents (but with reagents added in reverse order to prevent the nitroso reaction) to serve as a reference channel. These parallel streams pass through the sample and reference cuvettes, respectively, of a dual-beam flow colorimeter, whose output is routed to a strip-chart recorder which serves as a readout device.

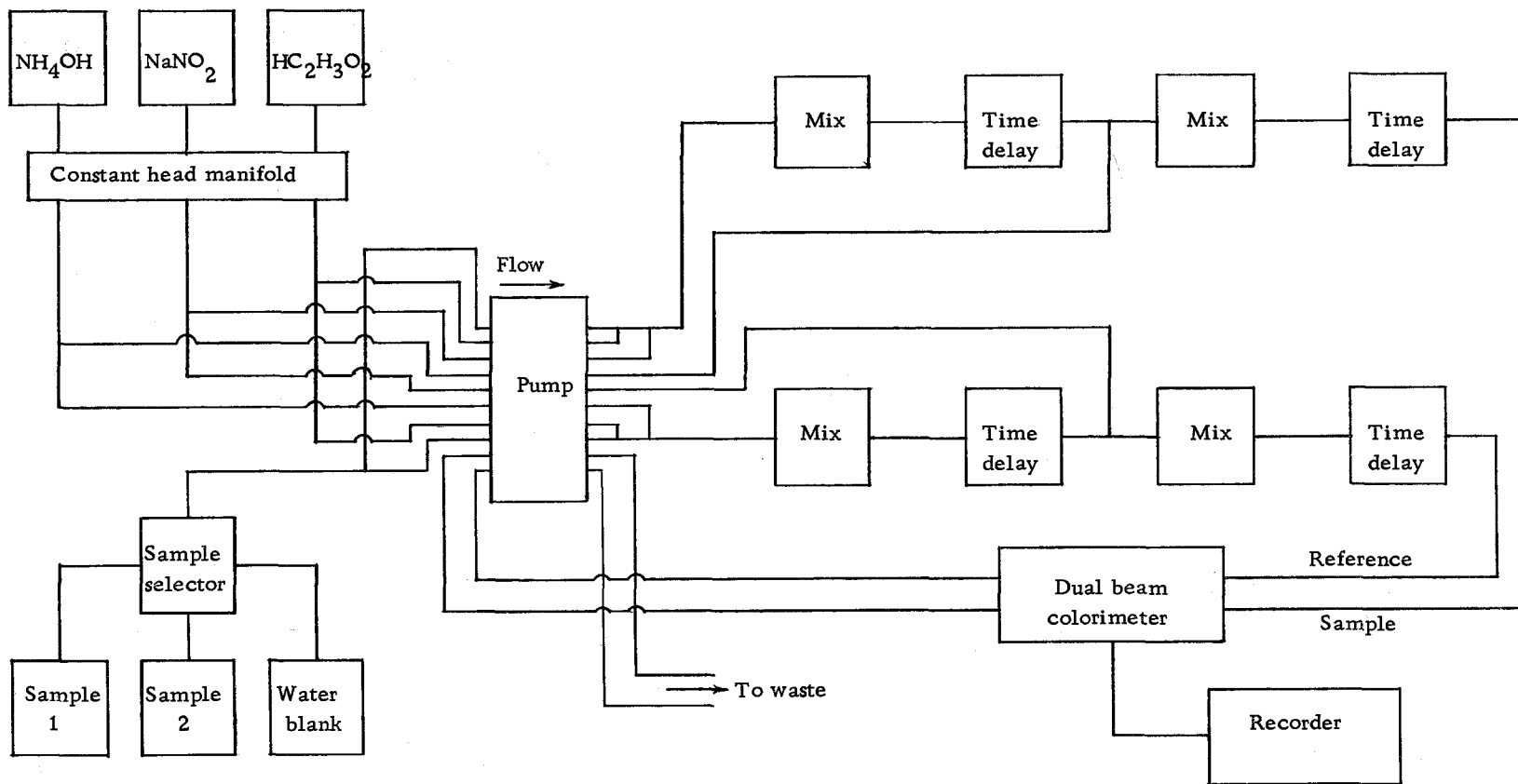


Figure 1. Schematic flow diagram for analyzer.

No continuous flow colorimeter has as yet been developed and found through evaluation to be well suited to measuring the low values of absorbance which will be encountered in natural samples containing lignin. In the interim, until a suitable colorimeter is perfected, it was decided to use the Beckman Model DB Spectrophotometer to perform the differential color measurement. This instrument has the important advantage, at least while the analyzer system is in the development stage, of being tested and stable. This, in effect, suppresses for the present the very large problem of developing and evaluating a colorimeter and allows a concentrated effort to be directed toward the problem of chemical manipulations within the analyzer proper. The use of the DB represents a compromise, however, in that the synthetic lignin samples used during the development of the analyzer must be about ten times the expected concentration range to be found in natural samples. Thus, initially, the analyzer system will be limited by the colorimeter so as to prevent evaluation using actual natural samples.

The DB is equipped with flow cuvettes and liquid is pumped from the exit of each cuvette at a rate slightly lower than the overall flow rate of the system. Two additional channels of the Durrum pump are used for this purpose. Immediately preceding the colorimeter in each analyzer channel is a debubbler (Figure 2), which is allowed to overflow slightly at all times and is open to the atmosphere at the

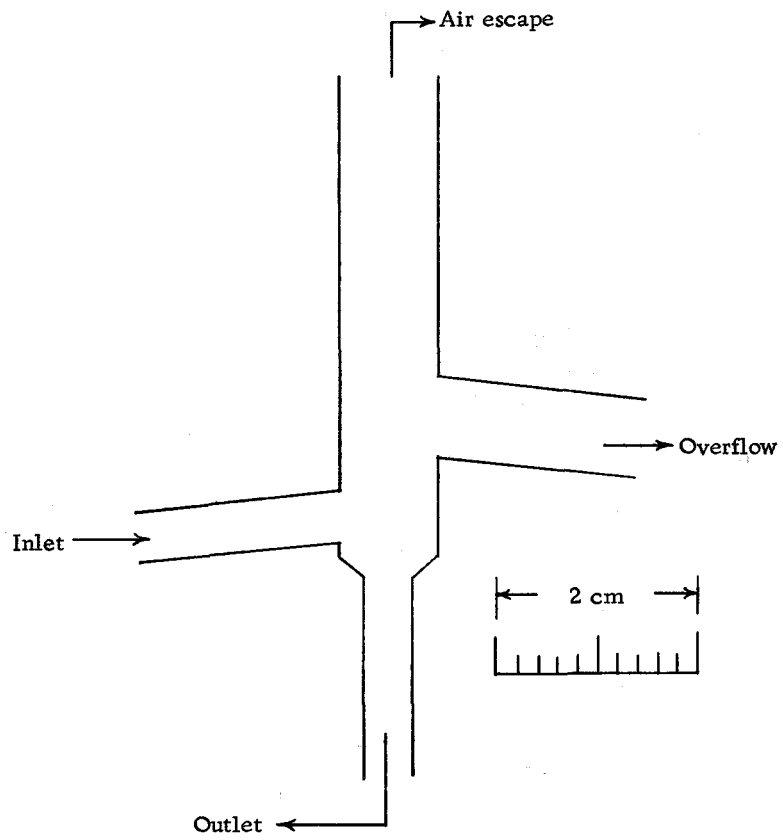


Figure 2. Diagram of debubbler.

top. This device serves to trap and expel from the system occasional unwanted but inevitable air bubbles before they reach the cuvettes. These bubbles arise particularly when a water blank is being run, using water directly from the tap as a source. When this water warms to room temperature upon passing through the analyzer, the dissolved gases become less soluble and appear here and there as bubbles in the analytical streams. A counterpart to this phenomenon would be experienced with a version of this analyzer designed for use in the field, since frequently river water being sampled would be at a lower temperature than the environment in which the analyzer would be located.

Reagents are supplied to the pump from constant head devices (Figure 3) which are fed from closed overhead reservoirs. The reservoirs empty into the cups only as reagent is consumed. The pump is quite sensitive to input head differences, particularly at the extremely low flow rates required in the reagent channels, thus preventing use of a simple open reservoir whose level would decrease as reagent is consumed.

Lignin containing samples were originally selected manually by manipulation of two three-way stopcocks arranged so as to give a choice of sample one, sample two, or water (blank). Later in the investigation an automatic sample selector was constructed (see Appendix II) which consists of a mechanical apparatus to position the

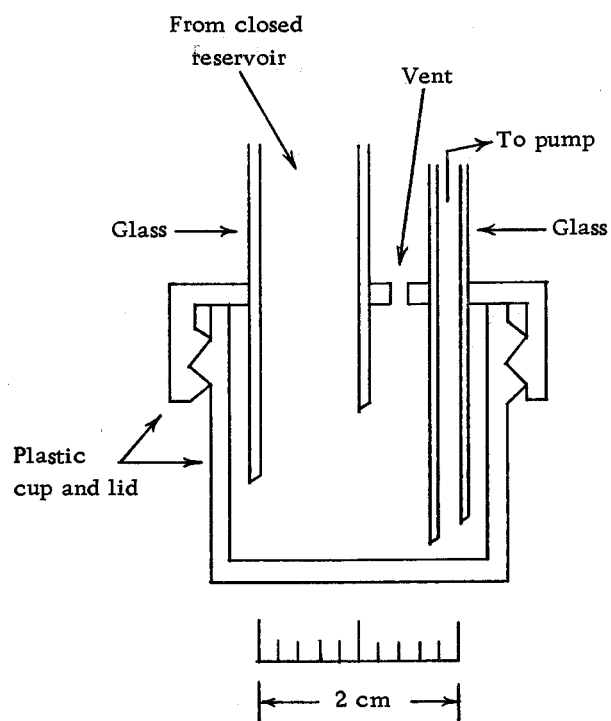


Figure 3. Diagram of constant head reagent supply cup.

stopcocks and a programmer. A 55 minute programmer cycle is used, apportioned equally among the samples and the water blank. A one liter sample reservoir provides enough for three replicate analyses.

Construction Details

Support

To provide a convenient support for the components of the analyzer, a framework was constructed of Handy Angle slotted angle stock (Handy Angle Limited, Grand Buildings, Trafalgar Square, London W. C. 2, England; distributed locally by Oregon Handling Equipment Company, 2949 N. W. St. Helens Road, Portland, Ore.). Perforated 1/8" pressed board sheet was fastened to this framework to provide a platform 12" above the table top, 64" long and 24" deep.

The DB spectrophotometer was placed beneath this platform at one end. The pump was placed at the other end of the platform on a depressed support such that the pump inlet and outlet were approximately at the height of the platform. On the other side of the pump were placed auxiliary pressed board platforms to hold reservoirs, constant head devices, etc.

The overall length of the framework was 96". A vertical panel of pressed board was fastened along the back of this framework,

extending its entire length and 12" above the level of the main platform.

The "instrument table" thus constructed offers several advantages over a similar support constructed, for instance, of wood. Handy Angle provides great flexibility of construction since it is pre-punched with bolt slots, and lends itself to easy changes of design. There is the additional advantage that either the buret clamp end or the rod clamp end of a disassembled Cenco Symmetrical Buret Clamp (No. 12102, Central Scientific Co., 1700 Irving Park Road, Chicago, Ill.) may be fastened directly to the Handy Angle frame by means of a 1/4" x 20 nut or bolt, respectively. Thus all standard ring-stand apparatus is indirectly compatible. The perforated pressed board is also advantageous since it is pre-punched with holes on one inch centers. In addition, a platform may be easily cut or drilled for changes in design without disturbing the apparatus.

A convenient system for securing glass and Tygon tubing to the platforms and framework is to make use of various Weckesser Nylon Fasteners (Cable Clamps and Cable Harnessing System, Weckesser Company, Inc., 5701 Northwest Highway, Chicago, Ill.). These clamps and fasteners, although designed for electronic cable harness assembly, are very useful for the project at hand and can be bolted directly to the pressed board platforms. The adjustable Tab-Loc Cable Clamps (No. TL-28) are useful for securing bundles of tubing;

Ny-Grip Cable Clamps (Type 2) and Half Clips (Type H) may be used to fasten single tubes. A number of parallel tubes may be conveniently supported with End Clips (Type E-1) mounted in End Clip Brackets (Type MB-1). Helices are conveniently mounted with Harness Assembly Clips (Type AC). Since all these clamps and clips are somewhat flexible, a complex tubing structure is less likely to be damaged than if it were supported by a system of rigid clamps.

Arrangement of Tubing for Mixing and Waiting

To estimate the tubing required for each channel (sample and reference), the total hold up time for the P-B method of 15 minutes for the nitroso reaction plus 10 minutes for the oxime formation was considered and approximately 2.5 minutes was allowed each mixing step. Thus a total time from inlet to outlet of about 30 minutes was required. At the expected combined flow rate of about 8 ml/min, this requires about 55 m of 4 mm Pyrex tubing for each channel. About 9 m of this was allotted to mixing helices which were formed to a diameter of 3.5 cm. Thus, in order to obtain a 2.5 minute mix, and 15 minute wait, a 2.5 minute mix and a 10 minute wait, it was calculated that a mixing helix containing 4.6 m of tubing followed by 27.5 m of tubing, 4.6 m of mixing helix, and 18.3 m of tubing would be required for a total time of passage through the system of 30 minutes. These lengths were rounded to the nearest whole length of

standard 1.22 m (48") sections of tubing.

In order to fashion the mixing helices, a mandrel of 28 mm Pyrex tubing was covered with one layer of 1 mm asbestos sheet dampened with water. After drying, the mandrel was supported horizontally between two blocks of wood with V-shaped notches cut to accommodate the mandrel tubing, and a Meeker burner supported by a ringstand was trained on the top surface of the mandrel. The helices were formed about this mandrel by slowly feeding in 4 mm Pyrex tubing and turning the mandrel as the tubing softened. The newly formed helices did not require annealing since the burner was trained in such a way that the 4 mm tubing stayed in the strongly heated zone for a few turns before moving out into the cooler zone where the glass cooled slowly near the flame.

The tubing used for time delay was not bent, but rather, the straight 1.22 m sections were laid side by side. To connect these, glass helices of 1.6 cm diameter were formed from 4 mm tubing and cut each 180° so as to form semicircular connections between adjacent sections of the time delay tubing. All glass-to-glass connections in the analyzer were made by physically butting the glass tubing together inside a short length of Tygon tubing which provides the seal.

A 1/8" polypropylene T-connection (Bel-Art Products, Pequannock, N. J.) was provided just ahead of the second mixing

helix for reagent addition and a manifold was provided ahead of the first mixing helix for introduction of sample and reagents. This manifold (Figure 4) was machined from Lucite and short lengths of 4 mm Pyrex tubing were fastened to it with epoxy cement. Two identical channels were constructed, one to serve as sample and the other as reference channel.

The P-B method specifies reagents in the proportion 50 (sample):1 (nitrite):1 (acid):2 (base). A pump channel was assigned to each reagent in each analyzer channel and connected to the system. These were calibrated so that the reagents are metered in their proper proportions and so that their respective rates are identical in both the sample and reference channels of the analyzer.

Adaptation of DB Spectrophotometer.

A flow cuvette manufactured by Beckman (Assembly No. 96160) has been used in the sample beam of the DB spectrophotometer, and a flow cuvette has been constructed in these laboratories for the use in the reference beam. This consists of a standard Beckman 1 cm Silica cuvette fitted with a machined Lucite top and glass tubes as shown in Figure 5. The assembly was cemented together with Dow Corning Silastic Clear Sealer. A replacement sample compartment cover was constructed for the spectrophotometer (Figure 6) which provides essentially light tight ports for the entrance and exit tubes

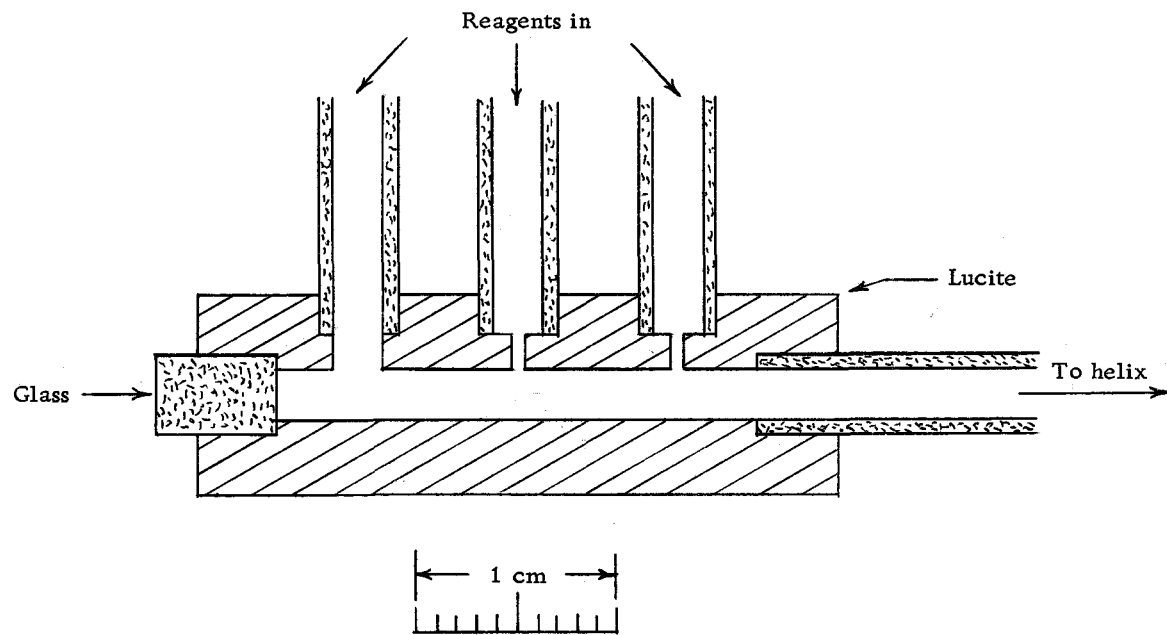


Figure 4. Diagram of input manifold.

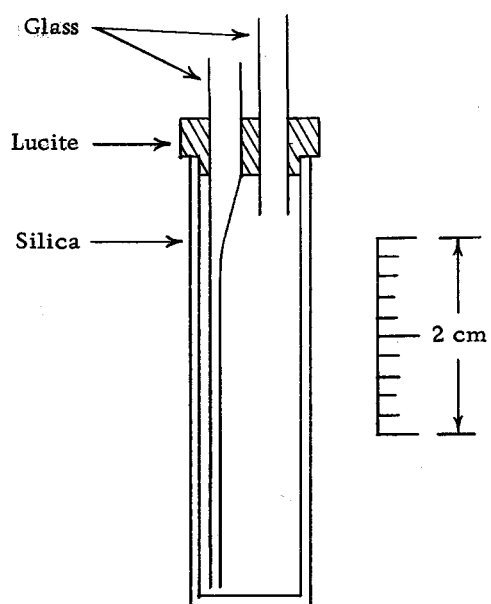


Figure 5. Diagram of flow cuvette.

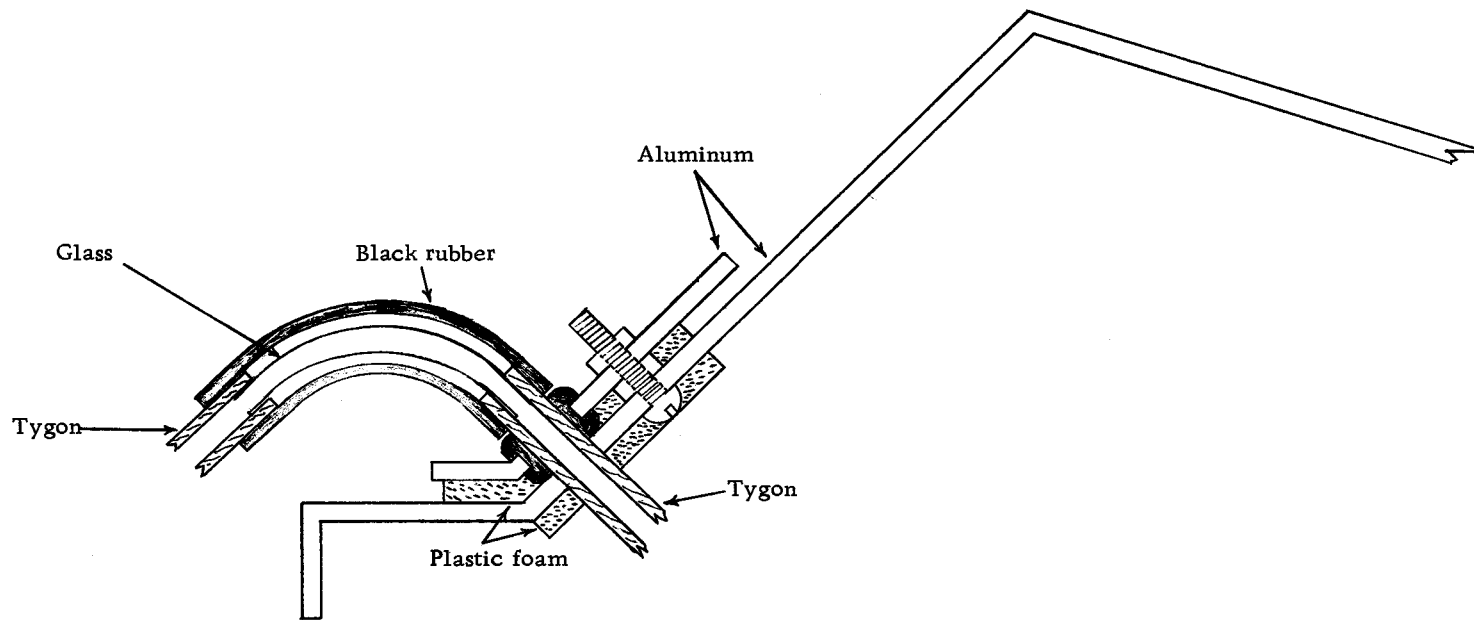


Figure 6. Diagram of ported cover for DB Spectrophotometer.

for each cuvette.

Calibration and Testing

Pump Calibration

To facilitate pump calibration, a system of reservoirs was constructed from 9" lengths of Pyrex tubing. Reservoirs 1 and 2 are 8 mm O. D. tubes, reservoir 3 is a 10 mm O. D. tube, and reservoir 4 is a 45 mm O. D. tube. One end of each reservoir was fitted with a short length of 5 mm Pyrex tubing for an outlet and the other end was left open. The reservoirs were then mounted vertically, with the outlet tubes at the bottom, side by side on a pressed-board support. This pressed-board support had been previously faced with a sheet of 20 x 20 squares per inch coordinate paper to serve as a water level scale for the reservoirs. The entire assembly was supported on a ring-stand by means of clamps secured to the support board.

The reservoir volumes were calibrated and 1, 2, 3, and 4 were found to contain 0.74, 0.74, 1.22, and 34.54 ml/inch of depth, respectively. This gives a volume ratio of 1.00:1.00:1.65:46.7, which is approximately the 1:1:2:50 ratio required of the reagents and sample for the Pearl-Benson method.

Before the procedure for the actual pump calibration can be described, it is necessary to arbitrarily assign pump channel

numbers to the various functions. Note that the sample and reference channels of the analyzer each have several associated pump channels (Figure 1). For a given channel (sample or reference) of the analyzer, let pump channels 1, 2, 3, and 4 be assigned, respectively, to nitrite, acid, base, and sample. Let the pump channel numbers for the analyzer sample channel be designated S and those for the reference channel be designated R. Thus there are eight channels to be calibrated, namely 1S, 2S, 3S, 4S, 1R, 2R, 3R, and 4R.

To proceed with the pump calibration, channel 4S is connected to any source of water and the pump is adjusted to provide a flow rate of about 8 ml/min. After this initial adjustment, channels 4S and 4R are connected to reservoirs 1 and 2, and channel 4R is adjusted to empty reservoir 2 at the same rate as reservoir 1 is being emptied by channel 4S. This technique establishes the common flow rate between the sample and reference channels of the analyzer since reservoirs 1 and 2 contain the same volume per unit depth. Henceforth, the settings for channels 4S and 4R are not changed.

To calibrate the reagent channels of the pump for the sample channel of the analyzer, channels 1S, 2S, 3S, and 4S are connected to reservoirs 1, 2, 3, and 4, respectively. Channels 1S, 2S, 3S, are adjusted to empty reservoirs 1, 2, and 3 at the same rate as reservoir 4 is being emptied by channel 4S. This procedure

establishes the desired ratios among the reagents and sample for the sample channel of the analyzer since the volumes of the reservoirs per unit depth are in the desired ratios. To calibrate the reagent channels of the pump for the reference channel of the analyzer, channels 1R, 2R, 3R, and 4R are connected to reservoirs 1, 2, 3, and 4, and the above procedure is repeated.

It is very important for the output of the pump to be connected into the analyzer during this calibration, since pumping rate varies considerably with back pressure, and this effect is much more pronounced in those channels pumping at low rates. Finally, after the pump is satisfactorily calibrated, it is necessary to clamp the pump adjustment knobs since these adjustments tend to creep to higher rates when the pump is in operation.

Testing of the Analyzer

To illustrate the use of the analyzer, a standard curve was prepared using known concentrations of spent sulfite liquor (SSL) solids.

Synthetic SSL samples were prepared from Orzan A (Courtesy Crown Zellerbach Corp., Camas Wash.). Orzan A is a product prepared by drying SSL and contains approximately 55% ligninsulfonic acid as ammonium lignin sulfonate (5, p. 744).

Powdered Orzan A was dried at room temperature to constant

weight in a desiccator (about 24 hours) over calcium chloride. A stock solution was then prepared by dissolving 1.596 grams of Orzan A in water and diluting to 1.00 l in a volumetric flask. This stock solution of concentration 1596 ppm SSL solids was then diluted volumetrically to prepare several known concentrations in the range 0 - 250 ppm.

Solutions of 10% acetic acid, 10% sodium nitrite, and 2N ammonium hydroxide were prepared according to the usual standards for the Pearl-Benson method (3) and placed in their respective analyzer reagent reservoirs.

Each solution of SSL solids was introduced into the sample input of the analyzer for a total of three separate trials. Figure 7 is illustrative of the strip chart trace obtained. The peak at 20 minutes represents a short rinse; the other plateaus in the figure are self-explanatory. Note that the three plateaus for the 120 ppm solution at 35, 75, and 115 minutes illustrate the extremely good reproducibility of the analyzer for three replicate trials. The raw data used to prepare the calibration curve are summarized in Figure 8, which shows representative sections of the strip chart traces for each solution concentration examined.

At the input to the analyzer, selection among samples of different concentrations was made by means of the stopcocks on the sample selector, hence input changes were "step changes". These step

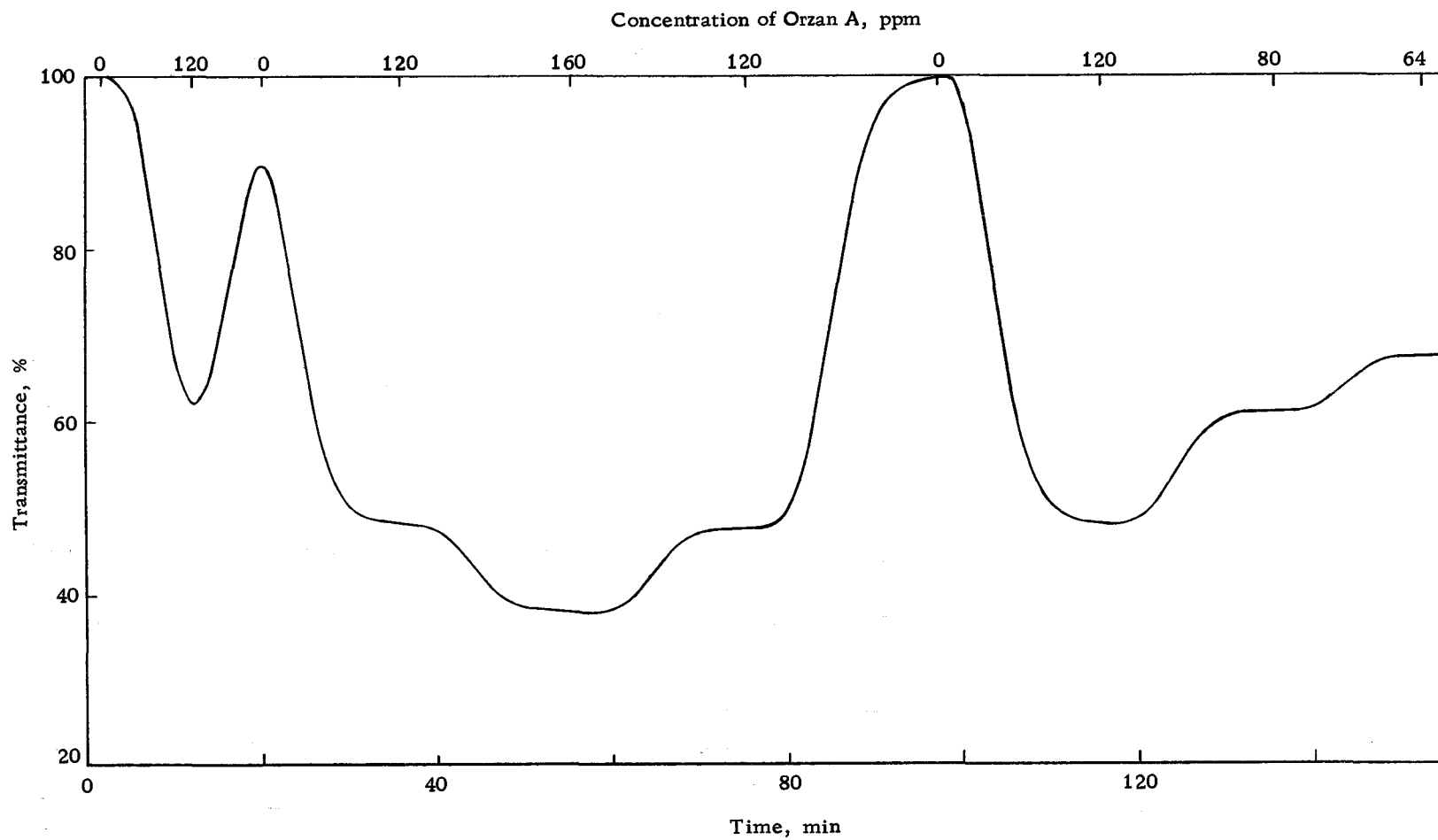


Figure 7. Representative raw data showing reproducibility.

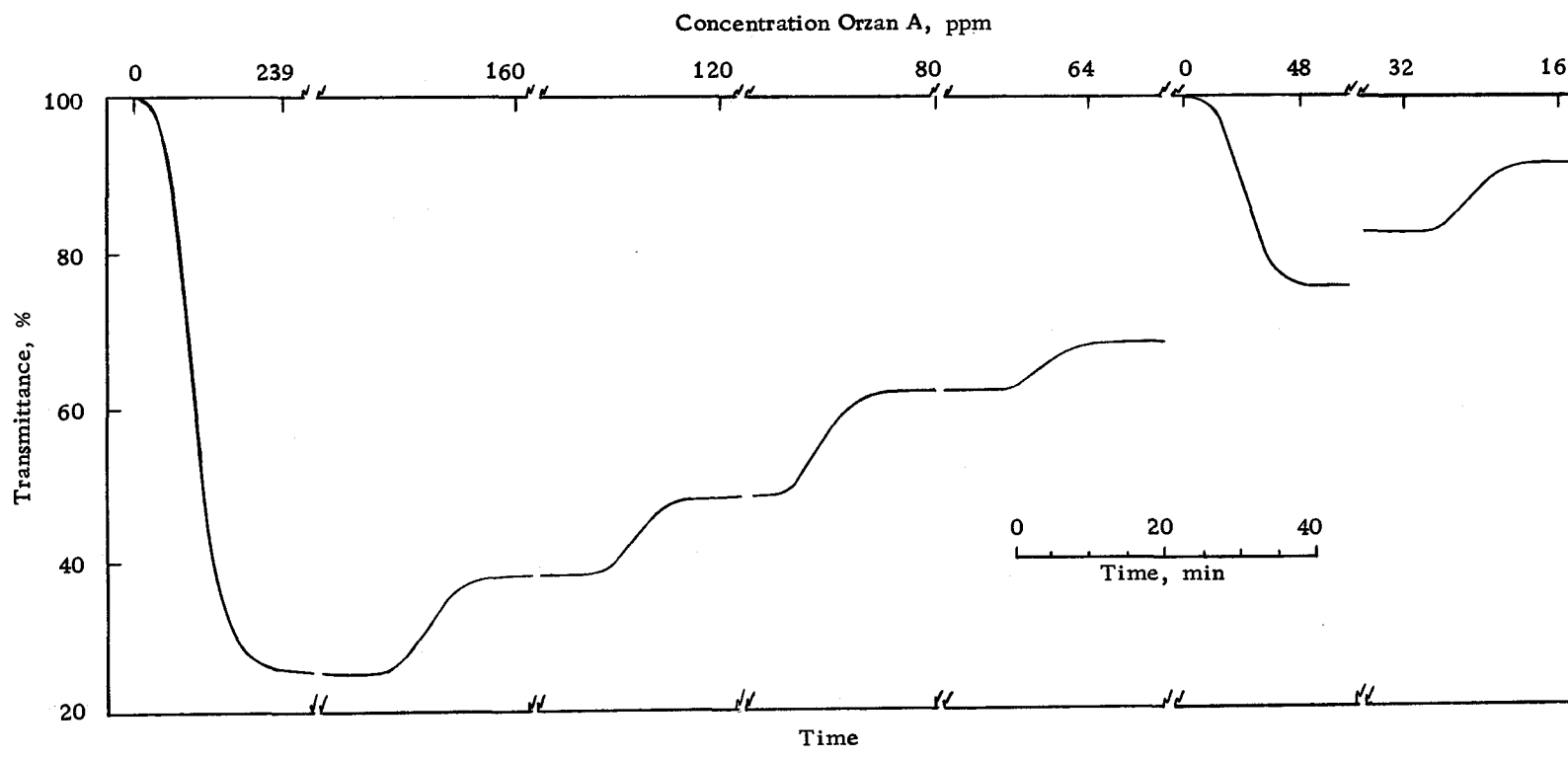


Figure 8. Examples of raw data for calibration curve.

changes are reflected at the output as a sigmoid change of about ten minutes' duration. Note that the duration is relatively independent of the magnitude of the step to be followed. These response characteristics will be discussed in more detail in a later section.

Transmittance values for the various SSL concentrations were taken from the data illustrated in Figure 8, converted to absorbances, and these absorbances were used to prepare the calibration curve shown in Figure 9. This curve indicates that the automated Pearl-Benson determination can be expected to follow Beer's Law to at least 120 ppm SSL solids. Typical values for SSL solids concentration found in natural waters are in the range of 0-20 ppm, which is well within the straight line portion of this curve. For comparative purposes, consult the survey of Pacific Northwest laboratories reported by Felicetta and McCarthy (10). Note that the values given in this survey are reported in ppm of 10% SSL solids. A concentration of 1.00 ppm SSL solids is equivalent to 10.0 ppm of 10% SSL solids.

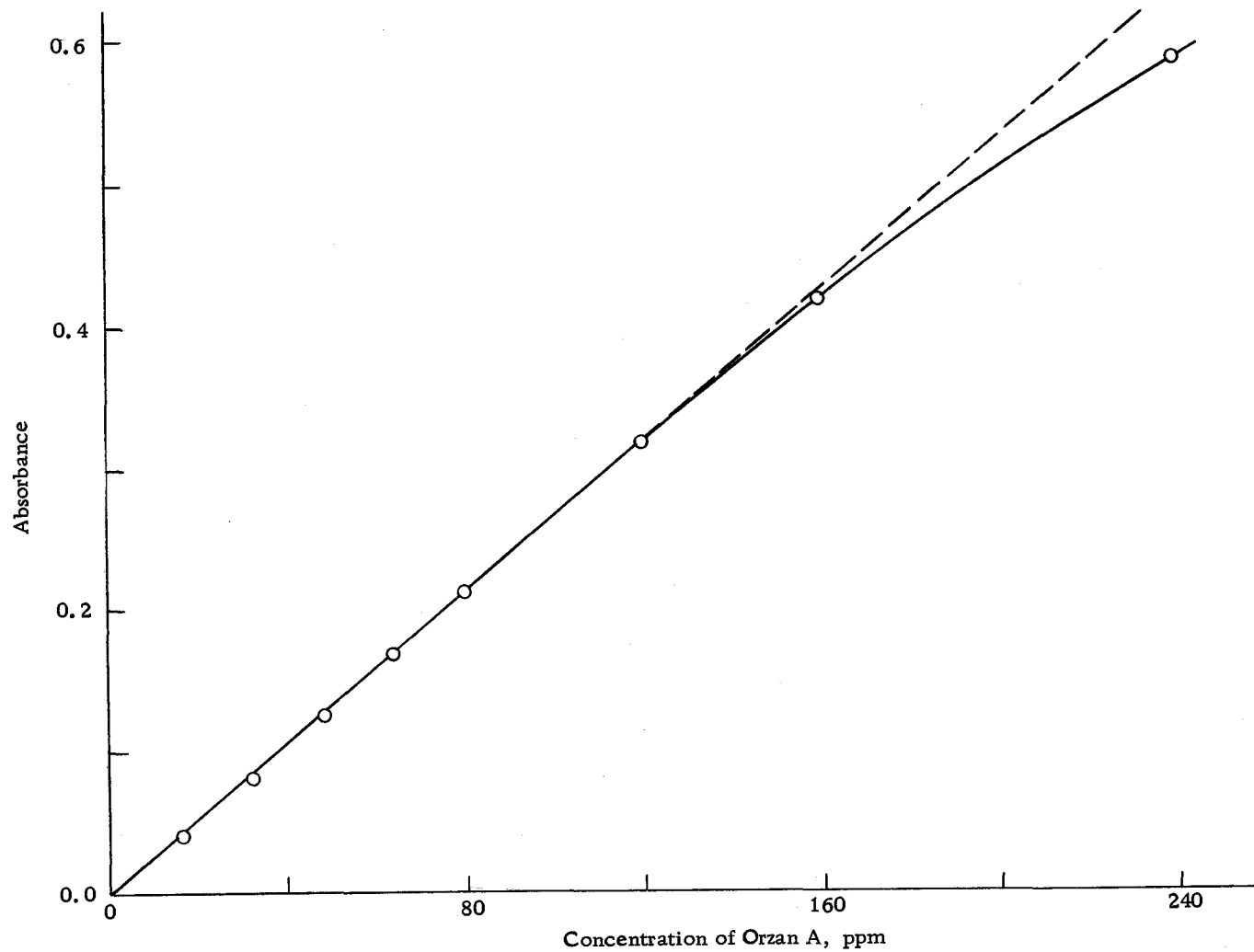


Figure 9. Calibration curve for analyzer.

DETAILED INVESTIGATIONS

Type of Flow

When fluids are pumped through a closed channel such as a pipe or tube, various frictional losses cause a pressure difference to exist between the input and output of this channel. In general, when a liquid flows through small diameter tubing at a relatively low rate, the fluid moves along in an orderly manner parallel to the long axis of the tube (2, p. 26-29). This type of flow is known as laminar, streamline, or viscous flow. The flow is orderly in that the fluid may be visualized as moving along as an infinite number of concentric cylinders. A study of the velocities of these cylinders at different points along the radius of the tube would show that the velocity distribution under these conditions is parabolic, with the highest velocity in the center and a velocity of zero at the wall of the tube. The maximum velocity is 2.00 times the average velocity over the cross-section of the tube. The frictional losses in laminar flow may be thought of as arising from the shear or slipping of these cylinders of different velocity over one another.

As the flow rate is substantially increased, the highest velocity areas in the center of the tube form eddies and, although the regions near the tube walls still behave as in laminar flow, the point of the paraboloid becomes somewhat flattened. This type of flow is known

as turbulent flow. The maximum velocity at the center of the tube drops to about 1.25 times the average velocity, and additional frictional losses occur due to the eddies and erratic flow near the center. This manifests itself by a discontinuity of the pressure as a function of flow rate.

In order to ascertain that we need not concern ourselves with turbulent flow within the range of attainable flow rates, and also to determine the magnitudes of pressures to be encountered using the Durrum pump and 4 mm tubing, three channels of the pump were connected in parallel at the pump output to discharge into about 39 meters of tubing. Although the pump delivers liquid in a pulsatile fashion, the average pressure required to force liquid through a length of tubing can be effectively monitored by connecting a vertical open tube or standpipe to the system through a T-fitting near the pump outlet or input to the tubing system. The height of liquid in the standpipe is a direct measure of this pressure.

The inputs of the pump were connected to a water reservoir and the pump was operated at various speeds to provide different flow rates.

The Durrum pump provides an output rate which is proportional to pump operating speed. Figure 10 illustrates this proportionality for two arbitrary sets of pump adjustments. Thus variation of this speed provides the most convenient method to study pressure

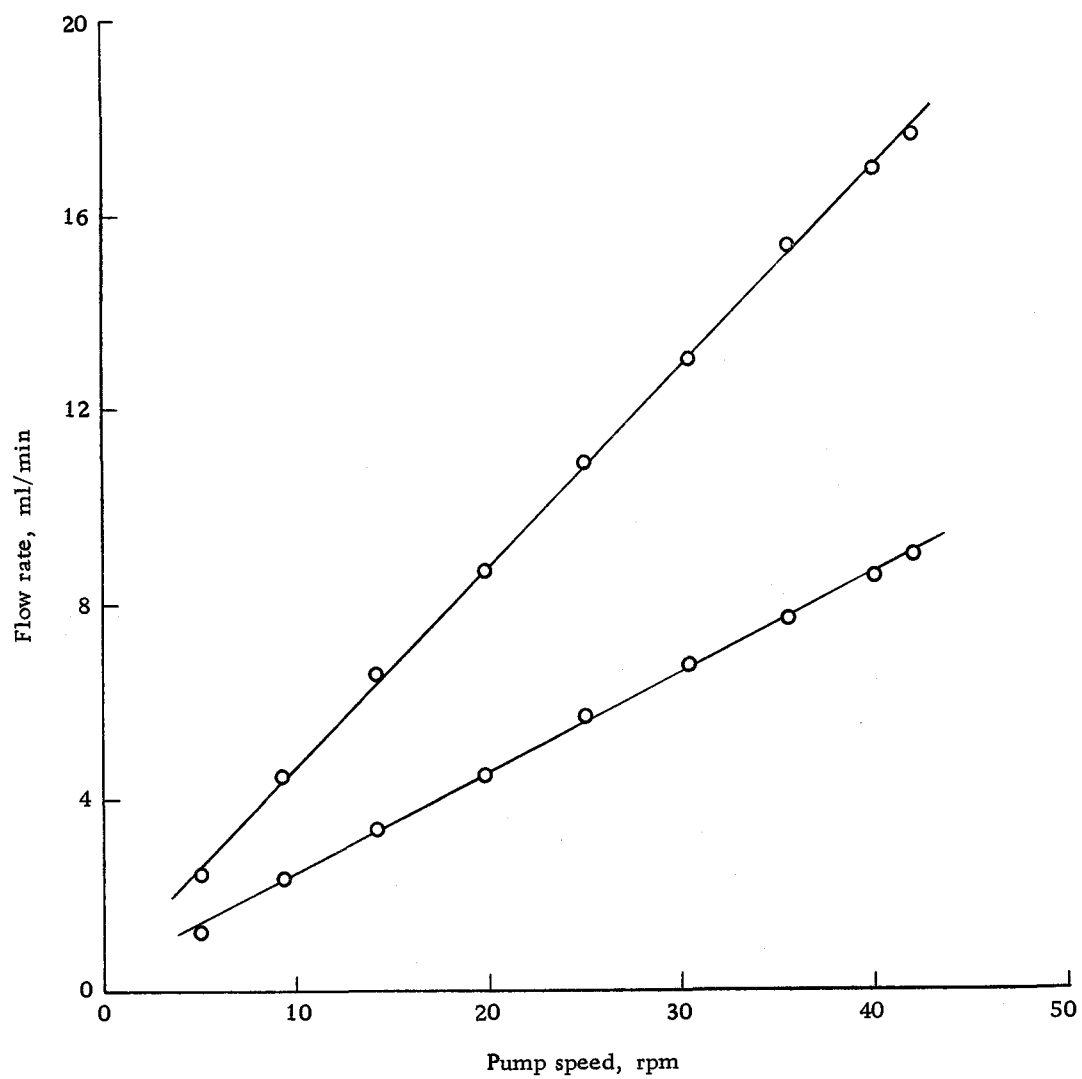


Figure 10. Dependence of flow rate on pump speed.

head developed as a function of flow rate in the system. Figure 11 is a plot of pressure head in terms of cm of water versus pump speed, covering the flow rate range of approximately 0 to 15 ml/min. The pressure intercept approximately represents the height of the outlet above the input. The linearity of the pressure increase with increasing rate is significant because this indicates laminar flow through the tubing in this range of pumping rates. If the flow were turbulent the rate of pressure increase would increase with increasing fluid delivery rate; that is, a plot of pressure against rate would abruptly become exponential at the onset of turbulent flow (20, p. 83).

Mechanism of the Pumping Process

During the pressure measurements described in the preceding section, it was noted qualitatively that the average output rate of the system increased and that the pulsing nature of the output was smoothed somewhat by connecting the standpipe to the system. Thus it was indicated that the standpipe was functioning as a sort of flow damping device within the system. To further investigate the phenomenon, the system described in the preceding section was tapped at various places and fitted with several standpipes.

The resulting system is presented schematically in Figure 12. Standpipes A and B are connected to the same point in the system near the outlet of the pump. They differ in cross-sectional area, A

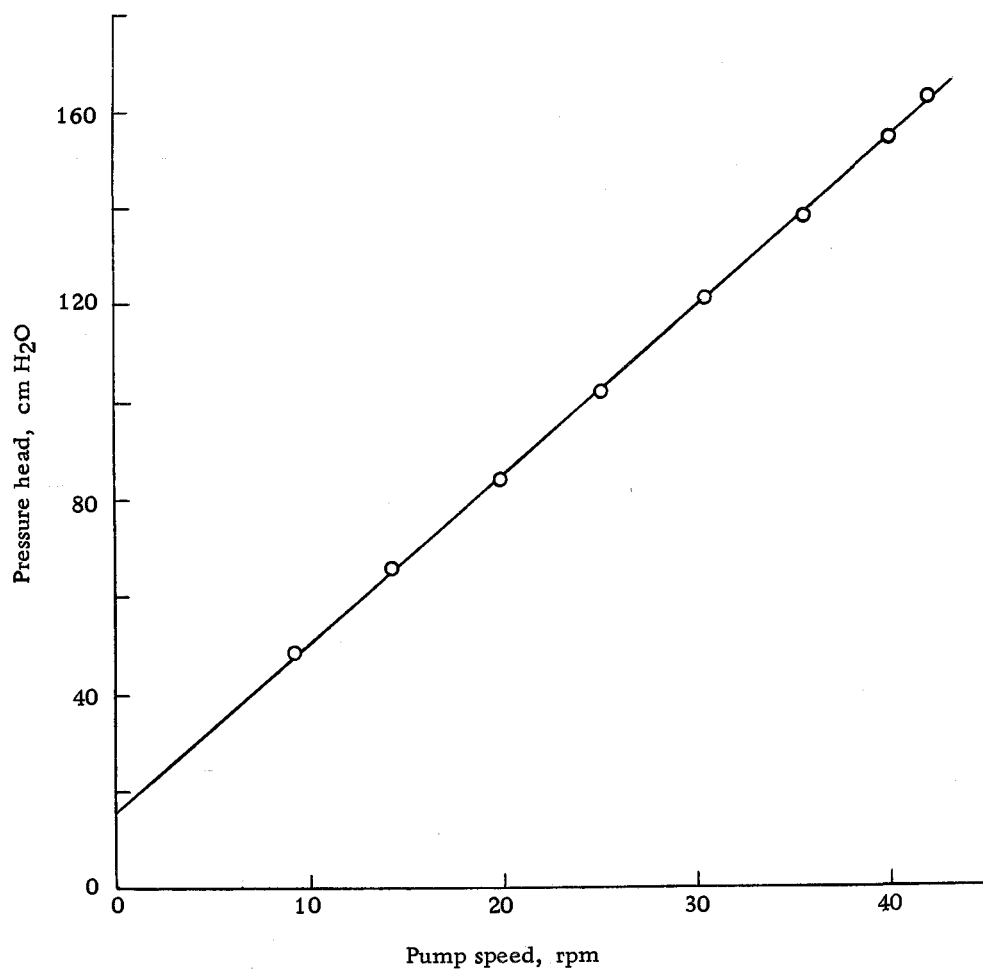


Figure 11. Dependence of pressure head developed on pump speed.

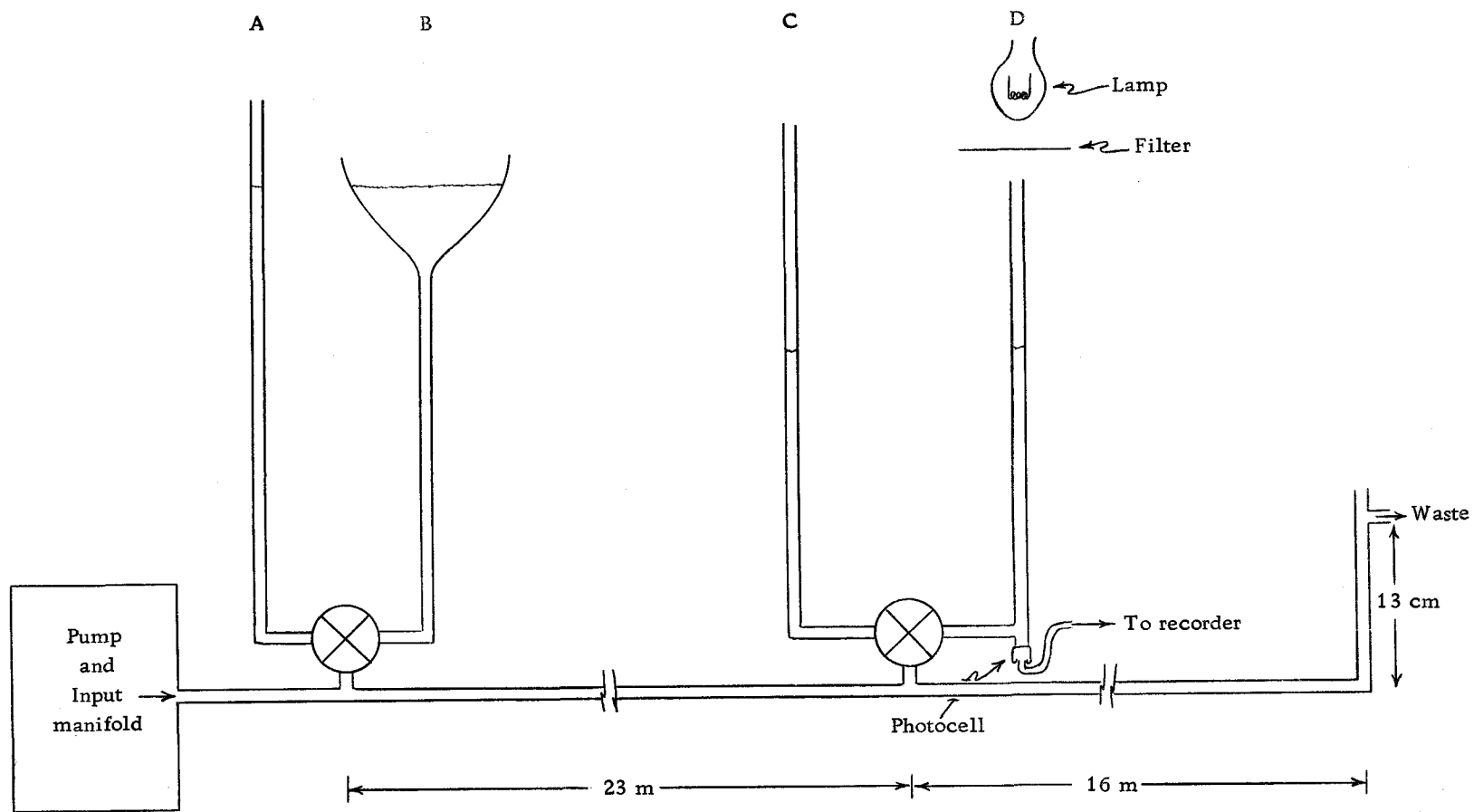


Figure 12. Apparatus for studying instantaneous pressures.

having an area of 0.125 cm^2 and B having an area of about 45 cm^2 . Thus B would tend to hold pressure fluctuations to a minimum since small volumes of liquid delivered from or to this reservoir would have an insignificant effect upon the height of the liquid level. A three-way stopcock provides a means for connecting neither, either, or both A and B to the system. Standpipes C and D, located about 23 meters from the pump outlet, have identical cross-sectional areas of 0.125 cm^2 and may also be connected to the system in any combination by means of a three-way stopcock. To monitor pressure fluctuations, standpipe D was provided with a photoconductive cell (Type 605L, Clairex Corp., New York) at the bottom and a filtered light source at the top. The standpipe is protected against the entry of stray light by a wrapping of black plastic electrical tape. Standpipe C, then, may be used to increase the damping at this point in the system, while also providing a visual estimate of the pressure fluctuations being monitored by standpipe D.

The pump was adjusted so as to pump arbitrary proportions of liquid from each of its three sections. Liquid from all the active pump channels converged at the input manifold and was then introduced to the system with its standpipes. One of the channels pumped potassium dichromate solution, and, since the photoconductive cell was illuminated with blue light, adjustment of the net dichromate concentration provided a means for controlling the resistance range

of the photoconductive cell. An arbitrary dichromate concentration was established so as to provide a photoconductive cell resistance range appropriate for direct monitoring on a Bausch & Lomb VOM-5 recorder. The photoconductive cell responds to a change in light level which in turn is caused by a change in depth of the absorbing column of liquid. This change in depth is caused by a pressure change in the system. Thus the instantaneous resistance of the cell gives an indication of the instantaneous pressure in the system. In Figure 13 are presented copies of representative recorder traces obtained by monitoring the resistance of the photoconductive cell while the pump was operating. Standpipes A, and B, and C in Figure 12 were opened to the system in various combinations and regarded as damping devices. The traces in Figure 13, then, are labeled to indicate the damping combination preceding the monitoring device in standpipe D. The ordinate represents resistance; the abscissa scales in both time and degrees of rotation of the pump are indicated. Qualitatively, it is seen that the resistance fluctuations are cyclic in nature with prominent features appearing at 120° intervals. Qualitatively, also, the greater the damping, the smoother the resistance fluctuations.

Before discussing the information implied by these traces in terms of pressure variation, it is important to note some of the inherent limitations of this pressure monitoring device. (1) The

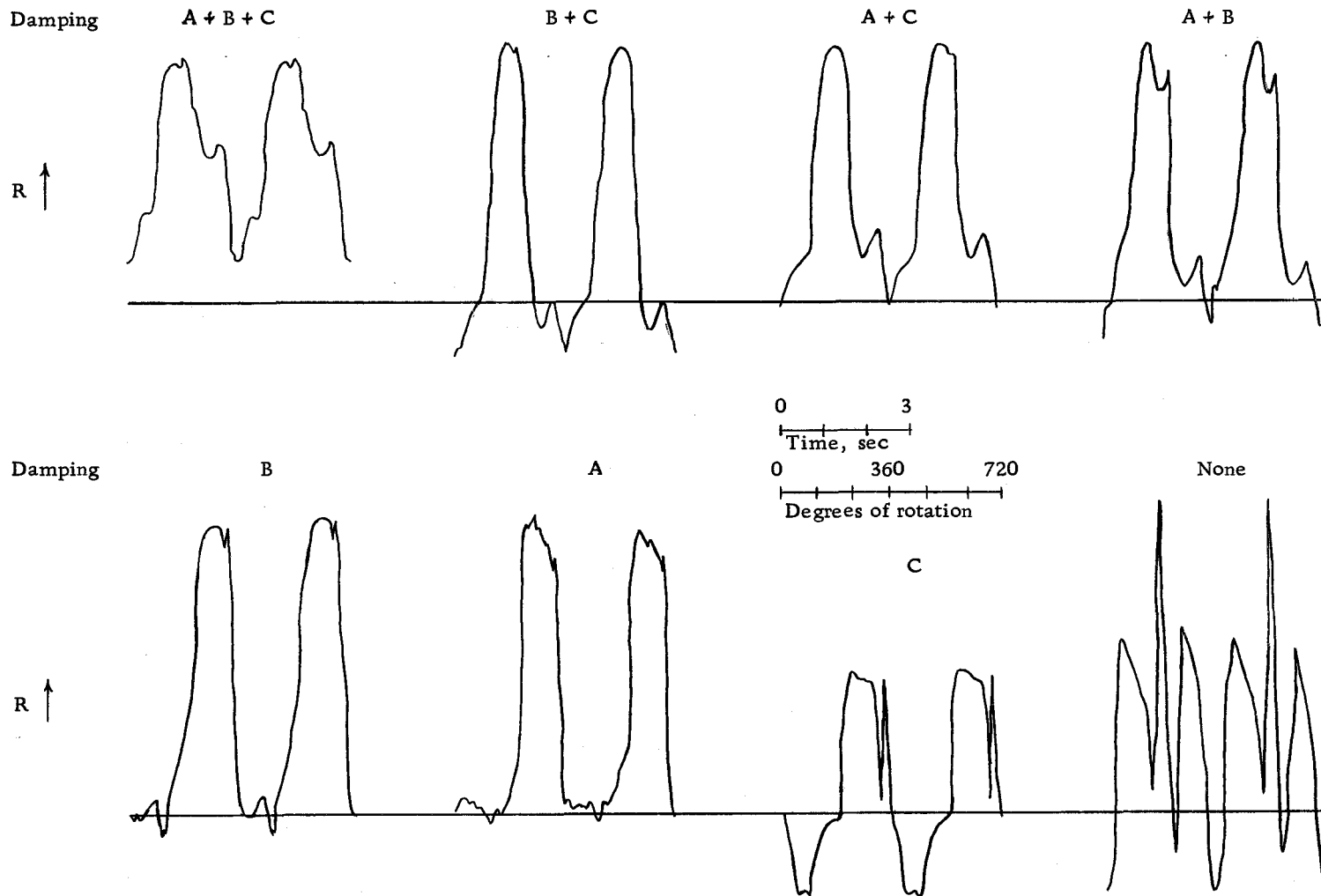


Figure 13. Resistance changes indicating instantaneous pressure changes for various damping combinations.

change in meniscus shape changes the reflectivity of the liquid surface as a whole, thereby altering the effective intensity of the incident light as the depth of the column changes. (2) There is no entirely suitable way to obtain a resistance value for the photoconductive cell which is equivalent to average pressure in the system, thus there is an uncertainty in determining the baseline in Figure 13. (3) Pressure at the monitoring device is related to system flow rate by the impedance to flow exhibited by the remainder of the system. This impedance may not be constant, but rather may be frequency dependent to some extent.

Regardless of these limitations, it is possible to derive useful information from such a monitoring system. It is necessary first to make certain assumptions.

1. Pressure at the monitoring standpipe is proportional to the height of the liquid column, or the pathlength (b). For a given solution of fixed concentration, b is proportional to $\log I_0/I$ where I is intensity at the detector and I_0 is incident intensity. To a reasonable approximation, for a photoconductive cell operating over a narrow range, $\log R$ is directly proportional to $(-)\log I$, where R is the cell resistance (7, p. 11). Thus we can approximate, for constant I_0 , that $\log R$ is proportional to b , which in turn is proportional to P , the pressure head at the monitoring device. The meaning of this is that, as we view Figure 13 in which R is plotted

against time (or angle of rotation of the pump), we must realize that from a pressure point of view, the upper portions of these curves appear to have exaggerated amplitudes and the lower portions are compressed due to the approximate logarithmic relation $\log R = kP$.

2. A depth variation of liquid in the standpipe is attended by a momentary change in the meniscus shape. Because of the attending change in reflectivity of the liquid surface, the effective I_0 is altered. This variation in I_0 would effectively cause the zero pressure reference to fluctuate, i. e., b would become proportional to $(\log R - \log R_0)$. The magnitude of this meniscus effect has not been evaluated, but traces of R against time likely have greater distortion during the steeper portions of the curves. The assumption made then, during the study of these curves, is that their details have less significance than their general shapes and cyclic changes.

3. It will be assumed that the flow impedance of a liquid column is dependent only upon the length of the column. This assumption allows for any reactance or frequency-dependent impedance in the system to be assigned to the standpipes. It is recognized that this is a first approximation only which can be used later to visualize a rudimentary model of the system. The assumption is supported by the linear relationship between average pressure and flow rate discussed previously, but ignores the fact that the resistance to flow of a moving column of liquid is somewhat less than the resistance to

flow of a stationary column. Also ignored is the fact that the direction of flow of a moving column cannot be instantaneously reversed, i. e., a column of liquid has inertia.

4. The baseline in Figure 13 was estimated by extrapolation. It is observed that if, after a steady state is reached, the pump is stopped and the recording of the resistance of the photoconductive cell is continued, the resistance decreases smoothly as the liquid level in the standpipes lowers. The rate of decrease, initially almost zero, becomes larger with increasing time. The extrapolation of this decay of resistance back to zero slope represents the equivalent steady pressure required to cause a flow rate equal to the net flow rate produced by the pump, and thus establishes a baseline for traces such as those in Figure 13.

With the above discussion in mind, we are prepared to examine Figure 13 in greater detail and relate the information there to the nature of the pumping process itself. The pump consists of three sections each operating 120° out of phase with one another. The pressure traces are cyclic in nature and show prominent features at 120° intervals, thus we are looking at composites of three out of phase pressure sources. Several of the less-damped curves show portions below the horizontal line. Since this line represents an estimate of the steady-state pressure, and since the impedance of the liquid column is essentially constant, these negative portions

represent a flow in the reverse direction, i. e., toward the pump. During this time the standpipes serve as reservoirs emptying toward the pump as well as toward the outlet in preference to requiring the reversal of the general direction flow of fluid in the bulk of the tubing. This happens because (1) the standpipes have proportionally lower impedance (impedance is proportional to length) than the rest of the tubing system and (2) there is potential energy stored in the standpipes (due to the pressure head required anyway to force liquid in the forward direction through the remainder of the system). This phenomenon can be confirmed by visual observation of the output. Depending upon the amount of damping there is a near null or even a short period of reverse flow associated with each stroke of the pump.

Let us now examine in detail the mechanism by which liquid is forced through the system by the pump. Figure 14 gives a simplified schematic representation of the valve action of one section of the Durrum pump at each 45° for a complete cycle (360°). In each section of the figure, the tubing through which the liquid flows (not shown) would lie horizontally between a backing plate at the top and the three valves beneath the plate. The small valve to the left functions as the inlet valve, closing the tubing by collapsing it against the backing plate at the proper time during the cycle. The small valve to the right functions in a similar manner as the outlet valve. The

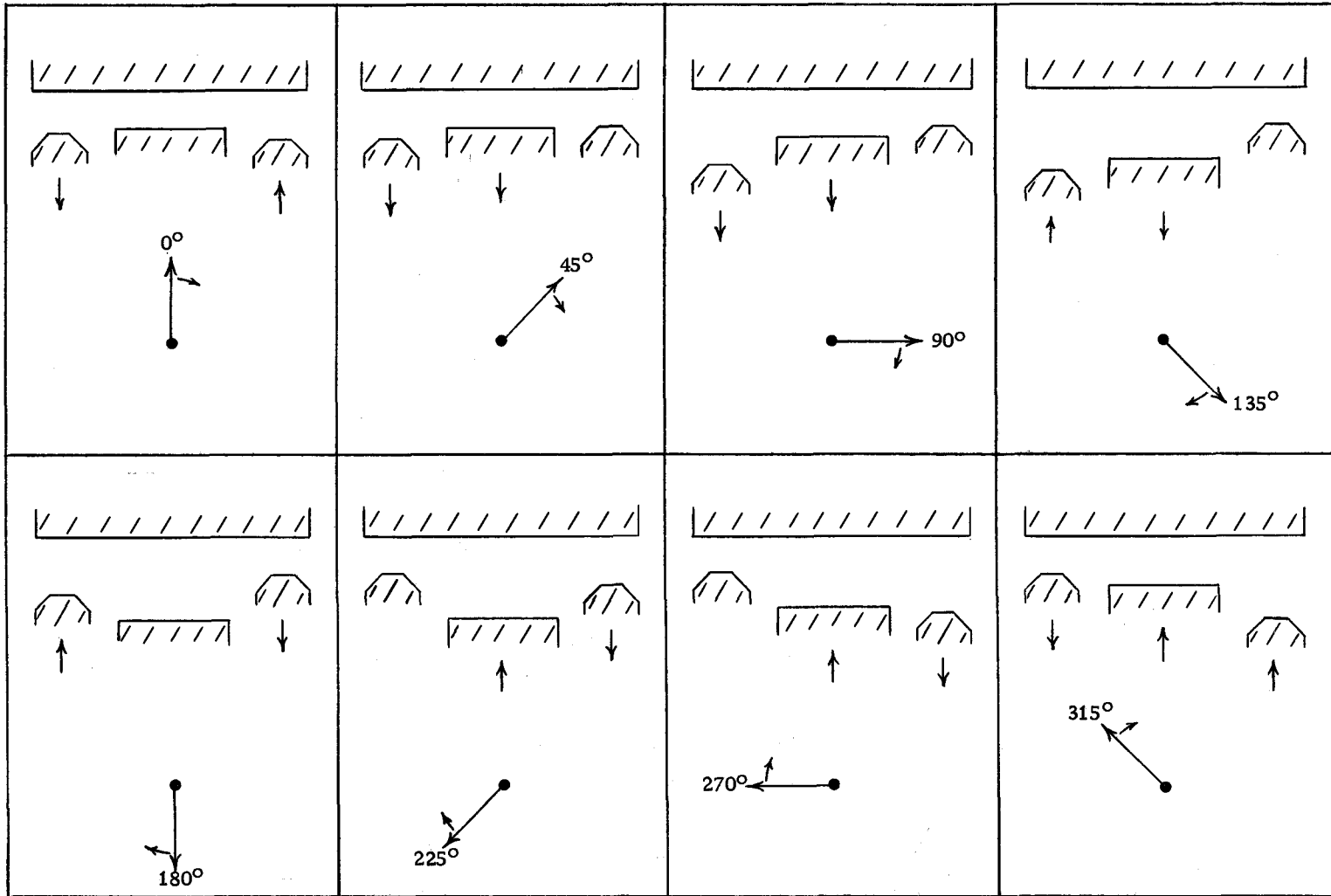


Figure 14. Valve operation, Durrum pump.

longer middle valve is known as the platen and may, in this simplified schematic, be considered to have an adjustable stroke (adjustment not shown). These valves are activated by a camshaft, the extent of rotation of which is indicated below the valves. The small arrows indicate the direction of travel of each valve in each frame of Figure 14. Figure 15 is a graphical representation of this valve action plotted in terms of valve displacement from a reference plane as a function of the angle through which the camshaft has rotated.

Using Figures 14 and 15 as a guide, let us follow the valve action through a cycle, beginning at 0° with the inlet valve opening, the platen closed, and the outlet valve closing. With the outlet valve closed and inlet valve open, the platen begins to release the collapsed flexible tubing lying horizontally between the valves and the upper plate (45°). The expanding tube thus draws in a new charge of liquid (45° through 180°). When the platen has reached its maximum height the outlet closes and the inlet begins to open preparatory to the beginning of a new cycle.

At a typical pump setting, the volume difference caused in the pump tubing by opening and closing the outlet valve may be about $1/3$ of the volume expelled from the pump each stroke by the platen. The outlet valve essentially opens before the platen expels a significant quantity of liquid. Since the expanding tube at the outlet valve requires liquid to fill the volume created by this opening, and since the

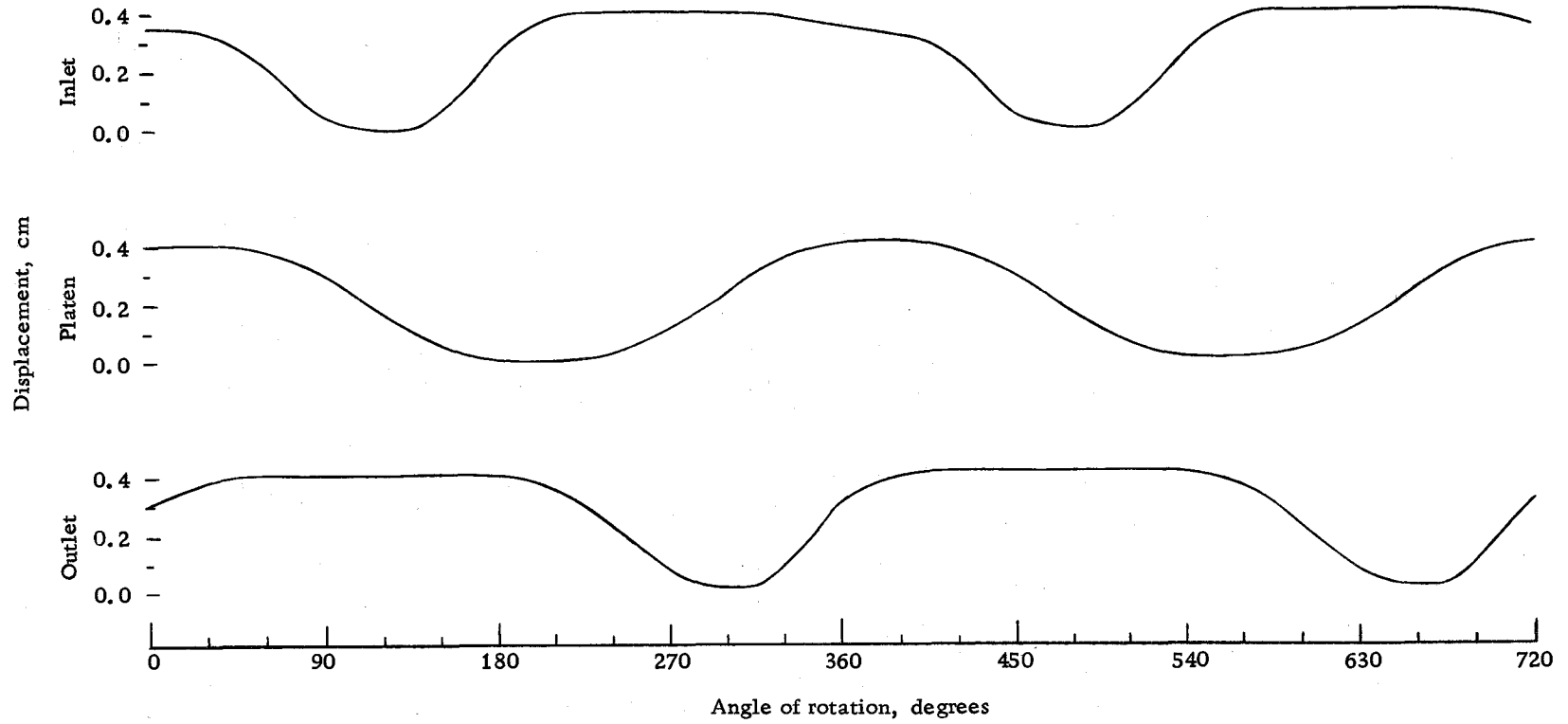


Figure 15. Valve displacement, Durrum pump.

inlet valve is closed at this time, the only source from which to draw the liquid is the system beyond the pump outlet. It is this phenomenon which causes the momentary reverse flow during each cycle.

Reverse flow at the pump can, however, be accommodated by several mechanisms: (1) the flow can be reversed in the entire system, (2) the flexible links in the system can be partially collapsed to compensate for the volume created by opening the outlet valve, or (3) the liquid required for the reverse flow can be supplied from some other source. Such a source must present a lower impedance to reverse flow than the system itself.

The first two mechanisms represent the only ways in which reverse flow can be accommodated when the system consists of a continuous column of liquid with no highly compliant link. Partial collapsing of the flexible portions of the system appears to play a relatively minor role in this reverse flow except to cushion the transition from forward to reverse. Reversing of the entire column of liquid, then, plays a major role as indicated both in Figure 13 and visually.

A standpipe provides an example of a compliant link. Thus, when a standpipe near the pump outlet is opened to the system the third mechanism becomes predominant. The standpipe provides a reservoir which can provide liquid to the pump at low impedance. In greater detail, an idealized standpipe functions as follows: At the beginning of a cycle assume the liquid level in the standpipe provides

the head required to force liquid through the system at the average rate at which the pump delivers the liquid. This level is slowly decreasing as liquid flows from the output. As the outlet valve opens, the standpipe easily supplies liquid to the pump as well as continuing to supply liquid to the system beyond the standpipe. Of course, during this period the liquid level in the standpipe must decrease more rapidly as it supplies liquid both in the forward direction to the system and in the reverse direction to the pump. Note, however, that the flow of the liquid column in the system as a whole has not been required to reverse, but only to decrease.

Now as the platen of the pump begins to expel liquid, the system and the standpipe accept this liquid. The standpipe accepts liquid until its level reaches a point which represents a pressure head equivalent to that required to force liquid through the system at the rate at which the pump is delivering liquid. Since the standpipe damped the output by accepting a surge of liquid at the beginning of the pump delivery, the system output flow did not have to accommodate an abrupt increase. When the pump platen stops delivering liquid, the standpipe liquid level still provides a pressure head so as to continue delivering liquid to the system, using the standpipe itself as a reservoir. As the liquid level in the standpipe decreases, the flow at the system outlet again diminishes, and presently a new cycle begins. It can be seen, then, that the standpipe serves two functions.

It provides the reverse flow required by the pump when the outlet valve opens, and it also cushions or damps the forward surge of liquid from the pump, thus smoothing the outlet flow.

Electrical Analog

It is appropriate at this point to generate a model which will serve as a rudimentary electrical analog of the pump and its fluid system. In general, such a model is potentially useful in a number of ways. An important aspect of a model for our immediate purpose is to examine the nature of the system from a different point of view, making use of electrical components whose functions are more carefully defined than those of the fluid system. A carefully conceived model also can lend itself to a detailed mathematical analysis since techniques for analyzing electrical circuits are well developed upon a sound theoretical basis. Further, such a model can lend itself to optimization studies, simulating experimental conditions with a model constructed from readily available electronic components. With such a device, then, one could vary parameters, including time, and systematically perform many experiments rapidly, easily measuring the resulting changes in variables with ordinary test instruments.

Before beginning the development of the model it is important to identify the analog quantities which correspond to various

components and variables in the fluid system. Pressure in a fluid system represents potential energy and its logical electrical analog is electrical potential or voltage. Flow rate in a fluid system represents a change (appearance or disappearance) of quantity per unit time; its analog is change of charge per unit time or current. Resistance is the electrical analog of the frictional resistance to flow exhibited by a horizontal column of liquid confined in a length of tubing; thus pressure is proportional to flow rate by frictional resistance (see Figures 10 and 11) and, of course, voltage is related to current by the proportionality factor resistance (Ohm's Law).

A standpipe (sufficiently high) will serve to store liquid rather than transport it; the amount of liquid stored in a given standpipe will be dependent upon the applied pressure exerted on the liquid from within the system. That is, the depth (thus quantity) of liquid in the standpipe will increase until the pressure exerted by the liquid in the standpipe due to its head is equal to the applied pressure. Similarly, a capacitor will store electrical charge, current flowing into the capacitor until the voltage across the capacitor is equal to the applied potential. If liquid stored in a standpipe is connected to a system providing frictional resistance to flow, a flow rate will be established dependent upon the pressure head remaining and the resistance to flow offered by the system, until no head remains. Similarly, if a charged capacitor is allowed to discharge through a resistor, current

will flow dependent upon the potential remaining and the magnitude of the resistance.

Within a fluid system there exists a zero-reference pressure level which will be assumed to be the level of the reservoir from which the pump draws liquid. When liquid is discharged to waste, it will be assumed to return to this reference level; the zero-reference pressure level is analogous to electrical ground. The pump serves as a source of pressure (potential energy) to the system; and electrical voltage source supplies a potential to an electrical system.

Criteria to be satisfied by the electrical analog model are as follows: (1) The model will consist of a section identifiable as the source (analogous to the pump) and a section identifiable as the load (analogous to the fluid system associated with the pump). (2) The voltage waveform at the output of the source will resemble the pressure waveform at the output of the pump. (3) The source will be subdivided into three sections operating 120° out of phase with one another. Each of these sections will contribute a pulsatile voltage whose negative component has a maximum amplitude about $1/3$ that of the positive component. (4) An optional filter or damping device will be included which will account for increased flow rate and a smoothed output. (5) The load will present a constant impedance to the source except when the optional filter is connected to the device.

From the knowledge that a given section of the pump provides

alternate positive and negative pressure pulses, it is logical to assume that the pump model will include an A. C. source. Reference to Figure 15 indicates that since the output valve is closed during nearly half the cycle (at least 45° through 180°), the output of the pump would of necessity be zero during this period. Since the outlet valve is fully open and the platen is closing from 285° through 360° , the output would be positive during this period. In the actual pump, then, the observed negative output could occur only during the period 180° through 285° during such a time that the opening of the output valve has not been compensated by a corresponding closure of the platen. Thus, qualitatively, the output of one section of the pump would be zero from 45° to 180° and positive from 285° to 360° . At some time during period 0° to 45° would be a transition from positive to zero; the period 180° to 285° would include a transition from zero to negative, a period of negative output, and a transition from negative through zero to positive.

This output waveform could be plotted and expressed in terms of a Fourier series expansion. (Techniques for Fourier analysis of repetitive waveforms are treated in many electronics texts. See for example Malmstadt and Enke (15, p. 552-554) or Cohen (8, p. 309-315).) A Fourier series is the sum of an infinite number of terms, each involving a constant multiplied by the sine or cosine of the fundamental frequency or its harmonics. Thus the pump could

be represented, to whatever degree of accuracy desired, by the appropriate parallel combination of an appropriate number of sources, each representing an individual term in the Fourier series.

Since the objective at this point is to generate a rudimentary model, it is felt that attempts to describe the pump as a source based upon a Fourier analysis would be premature. Rather, we can make a major simplification by assuming that each pump section contains a simple sinusoidal source and that the pump output is a simple sinusoid except that the maximum amplitude of the negative portion is attenuated to $1/3$ the maximum amplitude of the positive portion. Thus the output will be positive from 0° to 180° and negative from 180° to 360° . This assumption does, however, preserve the qualitative observations that the pump provides an alternating pulsatile pressure which reaches a negative value about $1/3$ of the magnitude of the maximum positive value at some time during each cycle, and which has a net positive average value.

The important advantage to be gained by this assumption is that a section of the pump can be represented by a single sinusoidal A. C. source. However, since the positive portions are of greater magnitude than the negative portions, there must be an imperfect diode intimately associated with the A. C. source. This can be represented by a perfect diode shunted with a resistor. The perfect diode has zero resistance in the forward direction and effectively shorts the

shunt resistor when the source output is positive. However, the diode acts as an open circuit in the reverse direction. Hence when the source output is negative, its amplitude is attenuated by the shunt resistor, which functions in conjunction with the load as a voltage divider. The load on the pump due to the long length of horizontal tubing will be represented in the model by a simple resistance. The three out-of-phase sections of the pump model will be connected in parallel ahead of the load resistance. All sources, the load, and measurements will be referenced to electrical ground. The optional damping device will be represented by a capacitor shunting the load.

A schematic diagram of the electrical model for the pump and its fluid system is presented in Figure 16 as well as an abbreviated schematic diagram of the real system drawn to the same format for ease of comparison.

Let us now discuss the detailed operation of the model thus generated and later relate it to the operation of the real system.

First consider only one section (source, diode, and shunt) to be connected to the load. The instantaneous voltage e of the source, is given by $e_1 = E_1 \sin\theta_1$, where the subscript one refers to the first section and where E is the maximum output voltage and θ corresponds to the angle in degrees through which the pump has rotated. Since the diode represents a short circuit when the source voltage is positive, the summing point voltage e_s will be e from

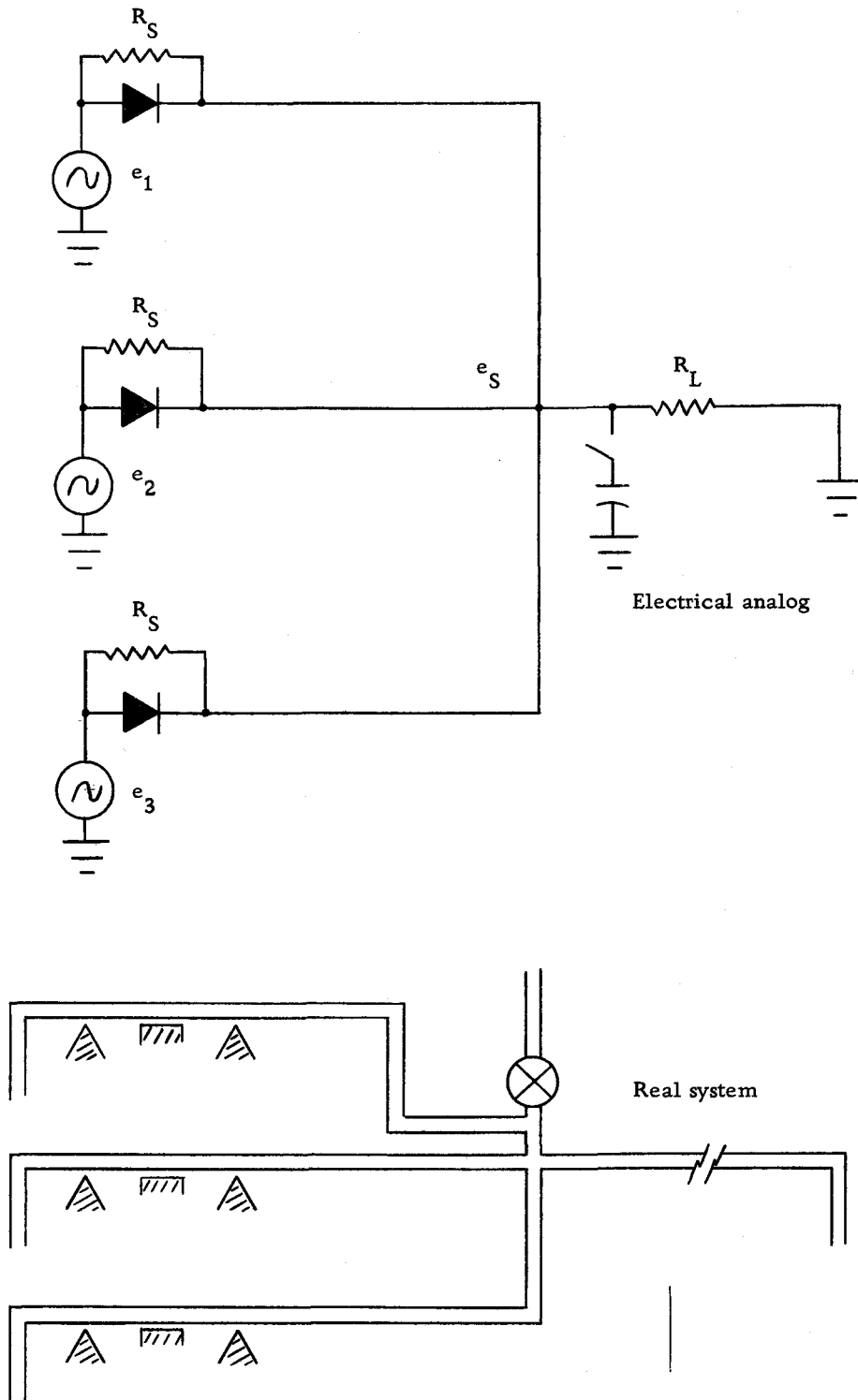


Figure 16. Models of pump and system.

0° to 180°. When the source voltage is negative, the diode is reverse biased and e_s is only a fraction of e determined by the voltage divider established by the load resistance R_L and the shunt resistance R_s . Consistent with the criteria established for the model, the negative amplitude of e_s will be 1/3 of e from 180° to 360°. Since during the negative half cycle, $e_s = e R_L / (R_L + R_s) = e/3$, it can be seen that this condition can only be met when $R_s = 2R_L$. A similar consideration of either section two or section three individually would also lead to the conclusion that $R_s = 2R_L$.

To establish the proper phase relationship among the sources, referred to section one, $e_1 = E_1 \sin \theta$; $e_2 = E_2 \sin (\theta - 120^\circ)$; $e_3 = E_3 \sin (\theta + 120^\circ)$. For the purpose of illustration, let $E_1 = 1.0$, $E_2 = 0.5$, and $E_3 = 0.2$. Referring now to Figure 17, curves A, B, and C represent the waveforms of e_s when e_1 , e_2 , and e_3 , respectively, are considered individually, the others being open circuited in each case.

Now consider the three sections connected in parallel to the load. At any time, the most positive source will forward bias its diode and reverse bias both other source diodes, thus the waveform of e_s when all sources are connected to the load will be defined by the most positive of (e_1, e_2, e_3) plotted as a function of θ (curve E in Figure 17).

When the capacitor representing the damping device is

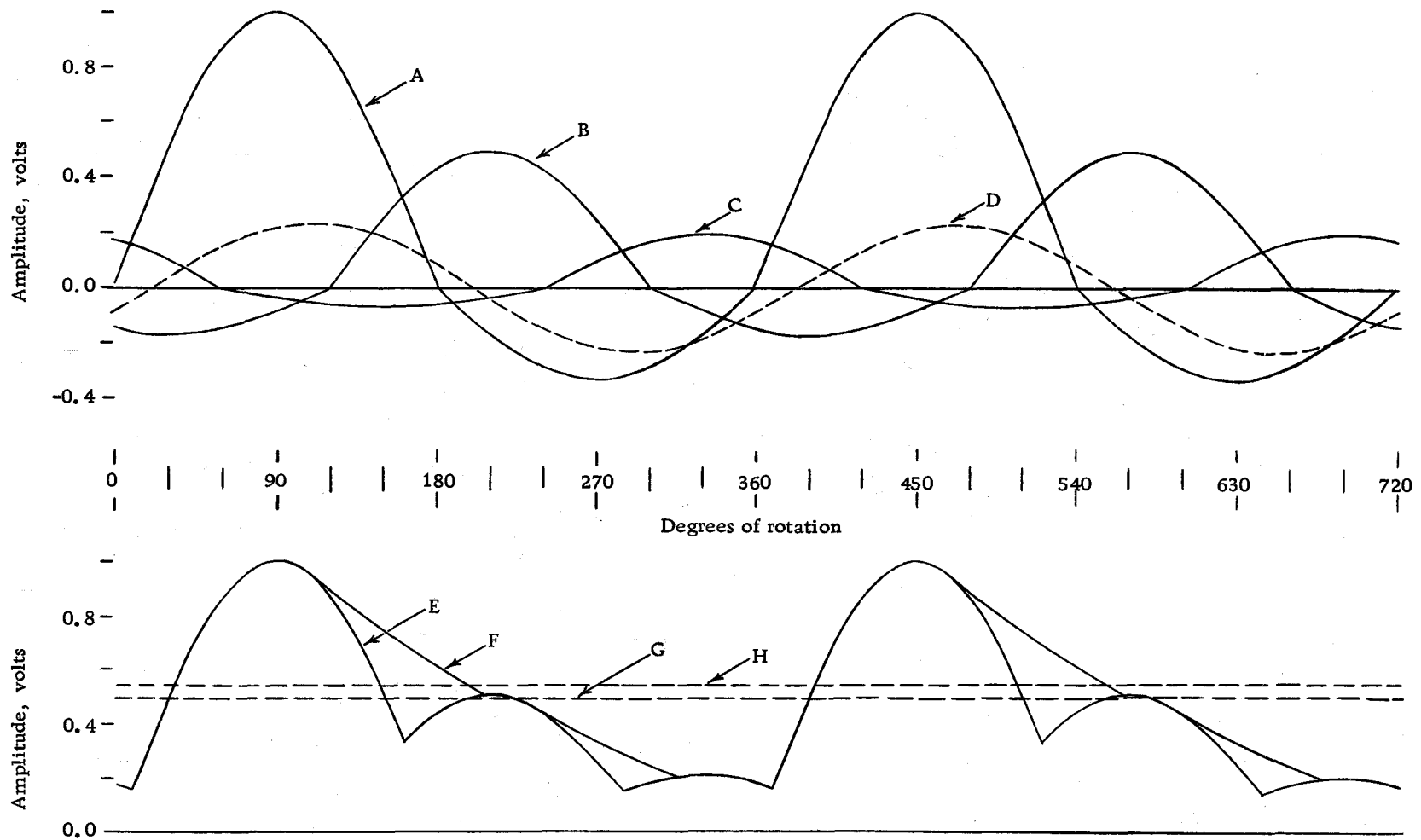


Figure 17. Waveforms expected of analog model.

connected to the model, the operation is as described below. At any time that a source voltage is more positive than any other source or the voltage on the capacitor, that source will control e_s . On the other hand, at any time e_s is more positive than any source due to the accumulated charge on the capacitor, e_s will decay exponentially at a rate determined by the various resistances, and source and ground potentials.

The Thevenin equivalent source voltage e_{eq} toward which the capacitor discharges is $e_{eq} = (e_1 + e_2 + e_3)/3$. Thus

$$\begin{aligned} e_{eq} &= [\sin\theta + 0.5 \sin(\theta - 120^\circ) + 0.2 \sin(\theta + 120^\circ)] / 3 \\ &= 0.1221 \sin(\theta - 21.79^\circ). \end{aligned}$$

Curve D in Figure 17 is a plot of e_{eq} . The equivalent resistance R_{eq} through which the capacitor discharges toward e is given by $1/R_{eq} = 1/R_{s1} + 1/R_{s2} + 1/R_{s3}$; since each $R_s = 2R_L$, then $R_{eq} = 2R_L/3$. Of course the capacitor is simultaneously discharging toward zero through R_L .

In general, for the decay of the voltage on a capacitor between the limits E_o and E_f , the difference between the initial voltage E_o and the voltage e at any time is given by

$$\Delta e = (E_o - E_f)[1 - \exp(-\Delta t/RC)],$$

where Δe is the voltage difference and E_f is the final voltage

toward which the capacitor is decaying. The quantity $\Delta t/RC$ may be regarded as the "number of time constants' duration" that the discharge is allowed to continue, Δt representing total elapsed time and the product of resistance through which the discharge proceeds and capacitance of the capacitor RC representing the time constant of the circuit in seconds.

If, for illustration, $R_L C$ is arbitrarily equated with $1/f$ where f is the frequency of the sources in seconds⁻¹, Δt may be expressed by $\Delta\theta/360f$. Thus

$$\Delta t/R_L C = \Delta\theta/360$$

and

$$\Delta t/R_{eq} C = 3\Delta t/2R_L C = \Delta\theta/240.$$

It follows that for the circuit under consideration, during an incremental θ ,

$$\Delta e_s = (e_s - 0)[1 - \exp(-\Delta\theta/360)] + (e_s - \bar{e}_{eq})[1 - \exp(-\Delta\theta/240)],$$

where \bar{e}_{eq} is the mean value of e_{eq} during the incremental θ and $\Delta\theta$ is the size of the increment. The first term relates to the decay toward the equivalent source voltage through its equivalent resistance.

Thus, the new value e_s' at the end of any increment is given by

$$e_s - \Delta e_s, \text{ or}$$

$$e_s' = e_s \exp(-\Delta\theta/360) - (e_s - \bar{e}_{eq})[1 - \exp(-\Delta\theta/240)].$$

Curve F in Figure 17 is a plot of the waveform expected of the model when the capacitor is connected in shunt with R_L . It is apparent upon comparison of curve E with curve F that such a capacitive filter smooths the waveform significantly and raises the average level somewhat. The dashed lines G and H in Figure 17 represent the average levels of curves E and F, respectively.

The electrical analog model which has been described in some detail above is intended to demonstrate, in an idealized way, the main features of the behavior of the real pump and the fluid system being considered here. The model is recognized to be rudimentary, however, and thus would not precisely duplicate the behavior of the real system. A major simplification was introduced in assuming the simple waveforms used in the model. Further, the model indicates that the source has zero output impedance when a diode in any section is forward biased, i. e., when a diode is conducting, the source voltage is perturbed neither by any other section of the source nor by the load. This is, to a degree, unrealistic since the real pump possess output impedance. That is, when the output is opened directly to waste, i. e., short circuited, the pump does not approach infinite flow rate. Finally, no detailed investigation has been made of changes in load, pump displacement setting, or pump speed setting; without such investigations, the model cannot be represented as one which simulates pump behavior under conditions in which these variables might

be changed.

Nevertheless, the model does contribute to the understanding of the mechanism by which the standpipe functions and illustrates the pulsing nature of the pump output. Most importantly, perhaps, such a model illustrates the usefulness of a systematic approach to the investigation of pump behavior and suggests that more sophisticated models might be proposed which would have the practical use of investigating various parameters with an analog device in preference to investigating the real system.

Precision and Accuracy

When continuous analytical systems are under consideration, the traditional concepts precision and accuracy must be applied very carefully. It is appropriate, then, to discuss the applicability and relative importance of these concepts to continuous systems.

With respect to reagent metering, for instance, the designation continuous implies that the same thing is being done in the same way all the time (continuously) rather than each time (repetitively). Discrete samples of the metering process do not exist as such. Thus, the traditional use of the term precision to indicate agreement among trials or samples becomes rather meaningless. There is however, a type of precision which becomes important, and this is the precision which refers to agreement among time-integral samples of the

process under consideration.

For example, comparison of several 80 ml samples, each collected over a period of about 600 seconds, for the purpose of determining errors of precision would actually represent a comparison among time-integrals. If the total quantity collected, 80 ml, were divided by the number of some unit times of interest which have elapsed, e. g., ten minutes, then a metering rate, 8 ml/min, would present itself for comparison. It cannot be too heavily stressed that the rate, 8 ml/min, represents only one-tenth the integral of the metering rate over ten minutes. Consequently, there is no basis for predicting instantaneous rate from the average rate data thus collected.

Now consider a process, such as reagent metering by the Durum pump, which, although not continuous on a fractional-second time scale, appears to behave continuously when examined on a several-minute time scale. Recalling the instantaneous flow rates studied in a previous section, it becomes apparent that if one were to compare the quantities of liquid delivered in each of several randomly selected one-second time intervals, at a pump rotation rate of 40 cycles per minute, the precision would appear to be very poor. Indeed, the comparison would be among quantities of liquid delivered in only $2/3$ of a cycle. The system would not even appear to be continuous, but rather quite erratic within the frame of reference of

one-second intervals. In contrast, if the sampling interval were changed slightly to 1.5 seconds to coincide with the time required for one cycle, depending upon the ability of the pump to recycle faithfully, quantities delivered might exhibit excellent precision and the pump would be considered to be continuously delivering a reproducible amount per cycle. If the sampling intervals were further increased to 25 minutes at a pump rotation rate of 40 cycles per minute, each sample would contain 1000 times the quantity per cycle. These samples would be time-integrals and any resolution of these to predict the reproducibility per cycle would be only speculation.

On the other hand, if the pump operates continuously and is not grossly erratic, comparisons of precision among the averages of various 25 minute (1000 cycle) samples could hardly vary significantly, thus errors of precision become vanishingly small and would not need to be considered in first approximation.

To extend the concept of the time dependence of precision a step further, suppose 25 minute samples were collected on several successive days. Their precision might again be rather poor, the difference between samples, though, probably would show a trend implying a systematic change (e. g., tubing wear, etc.) or random or cyclic changes (e. g., temperature fluctuations, etc.). This type of imprecision is more properly termed drift and several analogous examples could be drawn from familiar electronic equipment. It can

be concluded, then, that to a first approximation, errors of precision need not be considered in continuous systems provided the time interval of interest is sufficiently large to include many cycles, yet not so large as to reflect undesirable drift.

When one reflects upon typical standard analytical methods, he is struck by the coincidence that almost without exception, colorimetric procedures, in particular, specify addition of an integral number of milliliters of reagent to a sample whose size is expressed in a round number of milliliters. Color development times are often expressed in an integral number of minutes. Careful consideration of such procedures will result in the realization that the accuracy with which these measurements are carried out is seldom important to more than one significant digit. If the procedure specifies a pipetted sample of 50.0 milliliters, almost always any quantity from 40 to 60 ml would be quite satisfactory if one would adhere to the 0.2% precision tolerance implied by 50.0 and make any computations according to the sample size actually drawn. In a continuous system where the computations are made by comparison with a standard curve prepared under the same operating conditions and where errors of precision are vanishingly small, it can be concluded that the accuracy of following the procedure is rather unimportant.

Perhaps the case has been slightly overstated here, but it is intended to illustrate that in continuous system, as errors of

precision tend to become vanishingly small, errors of accuracy become proportionally less important. With regard to precision errors resulting from drift, the somewhat naive but usually valid assumption is made that drift resulting from change in speed or temperature, or from tubing wear, will affect all channels in the same proportion, restoring errors of precision of proportioning to near zero.

Air Segmentation of the Analytical Stream

The philosophy of segmenting the analytical stream with air bubbles is based upon two fundamental considerations which frequently offer a significant advantage in continuous monitoring schemes.

First, the presence of regularly spaced uniform air bubbles in a stream resolves the overall stream into a series of discrete samples moving along one after the other. Thus, any concentration gradient introduced more or less retains its integrity throughout the instrument. This technique was introduced by Skeggs (19) for the purpose of preventing mechanical mixing between sequential samples or between a sample and a sequential water blank, and is extensively employed by users of the Technicon Auto Analyzer (Technicon, Research Park, Chauncey, N. Y.) for that purpose.

Secondly, if a segmented analytical stream is made to flow through a helix whose longitudinal axis is horizontal, the discrete

samples will be subjected to repeated inversions, which action constitutes an effective mixing mechanism within each segment, while allowing little forward or backward transfer from one segment to another.

Properly handled, then, the air segmentation technique can provide an analytical system that provides prompt and thorough mixing after introducing reagents and presents a stream to the readout detector whose properties faithfully reflect variations in concentration of the component of interest at the input. The air segmentation technique presents, however, some extremely important limitations when an attempt is made to reduce the philosophy to practice.

Consider for the purpose of illustration the following system. Two active channels of the pump were connected through a manifold to the input end of approximately 39 m of 4 mm Pyrex tubing, the output end of which was opened to waste. One of the active pump inputs was connected to a water reservoir, the other left open to the atmosphere so as to pump air. The channels were adjusted to provide about the same average rate of flow.

First regard the system at rest and assume the tube's segmented column of fluid to consist of equally spaced air and liquid bubbles. Now if the pump is started, it is observed that although additional fluid is being injected at the head end of the tube, because of the high degree of compliance of the air segments, the column

appears to present a large static resistance to flow. Although each displacement of the water channel platen injects the equivalent volume of water, a displacement of the air channel serves partly to compress the air in the tubing ahead of the manifold and only partly to inject air into the system at the resulting higher-than-atmospheric pressure. As the process continues, it is observed that all the air segments become compressed, the air segments closer to the input to the greater extent, the newly injected air bubbles become progressively smaller, and the exit end of the column at first does not move at all. Eventually the exit end of the column begins to move, and since the dynamic resistance to flow is substantially less than the static resistance, the entire column begins to surge forward. Driven by the compressed air bubbles within the column, the column moves at a rate greatly exceeding the input rate until the pressure throughout the system drops to some level near atmospheric pressure, at which time flow stops and the surge cycle begins again. This oscillatory surge phenomenon continues for some time before damping out and occasionally appears to spontaneously begin again even when the system is not knowingly disturbed. A reasonable conclusion seems to be that an air segmented column of liquid being driven by a pulsating pump is an inherently unstable system tending toward uncontrollable oscillations.

To illustrate the deleterious effect of this surging phenomenon,

a T-fitting was inserted about 23 m from the inlet end of the tubing through which potassium dichromate solution or water could be metered at will by a third active channel of the pump. The output of the tubing system was connected through a debubbler (Figure 2) to a flow-cuvette inlet in the DB Spectrophotometer. A portion of the stream was then pumped through the flow cuvette by a fourth active channel of the pump connected to the outlet of the cuvette, and the transmittance was measured at 370 m μ . The flow rate of the reagent (potassium dichromate) channel was adjusted so that, on the average, each liquid segment within the main stream receives one small pulse of reagent and that the output level was about 40% T. It can be seen that during the time when the portion of the column opposite the reagent injection port is moving slowly or not at all, those liquid segments will receive several pulses of reagent, and while the column is surging past the port, several segments may receive no reagent at all. When we further include the consideration that the segments rapidly become nonuniform in size and spacing, while the reagent continues to be metered at regular intervals, it becomes apparent that the net effect, on segment by segment basis, is highly nonuniform reagent proportioning.

It is important to realize that a careless consideration of metering process here could result in an assumption that reagent proportioning is satisfactory. If for instance a mass balance is obtained by

measuring the disappearance of sample and reagent and appearance of waste over several consecutive ten minute intervals, the proportioning may appear to be very reproducible because of the integrating nature of such measurements.

The practical result of this nonuniform reagent proportioning is a rather large fluctuation or noise at the detector, which renders the technique useless without further controls. Figure 18 includes a plot of transmittance versus time illustrating the unwanted noise at the detector resulting from this uncontrolled oscillation.

If an unsegmented stream is considered, its compliance is drastically reduced. Deformation of the column can occur only at flexible plastic tubing connections, but not within the column itself, since water can be considered to be incompressible. Mixing helices still serve to mix reagents by repeated inversions, although the efficiency is somewhat lower. Reagent proportioning becomes more precise, and any imperfections in this proportioning are smoothed by forward and backward diffusion, since the column is unsegmented. Of course, short-term fluctuation in sample concentrations are also smoothed. This may be an advantage for this particular project, while the lengthening or response time to a step change will not offer a serious disadvantage. Also shown in Figure 18 is a plot representing the very noise-free signal at the detector obtainable with a non-segmented liquid analytical column.

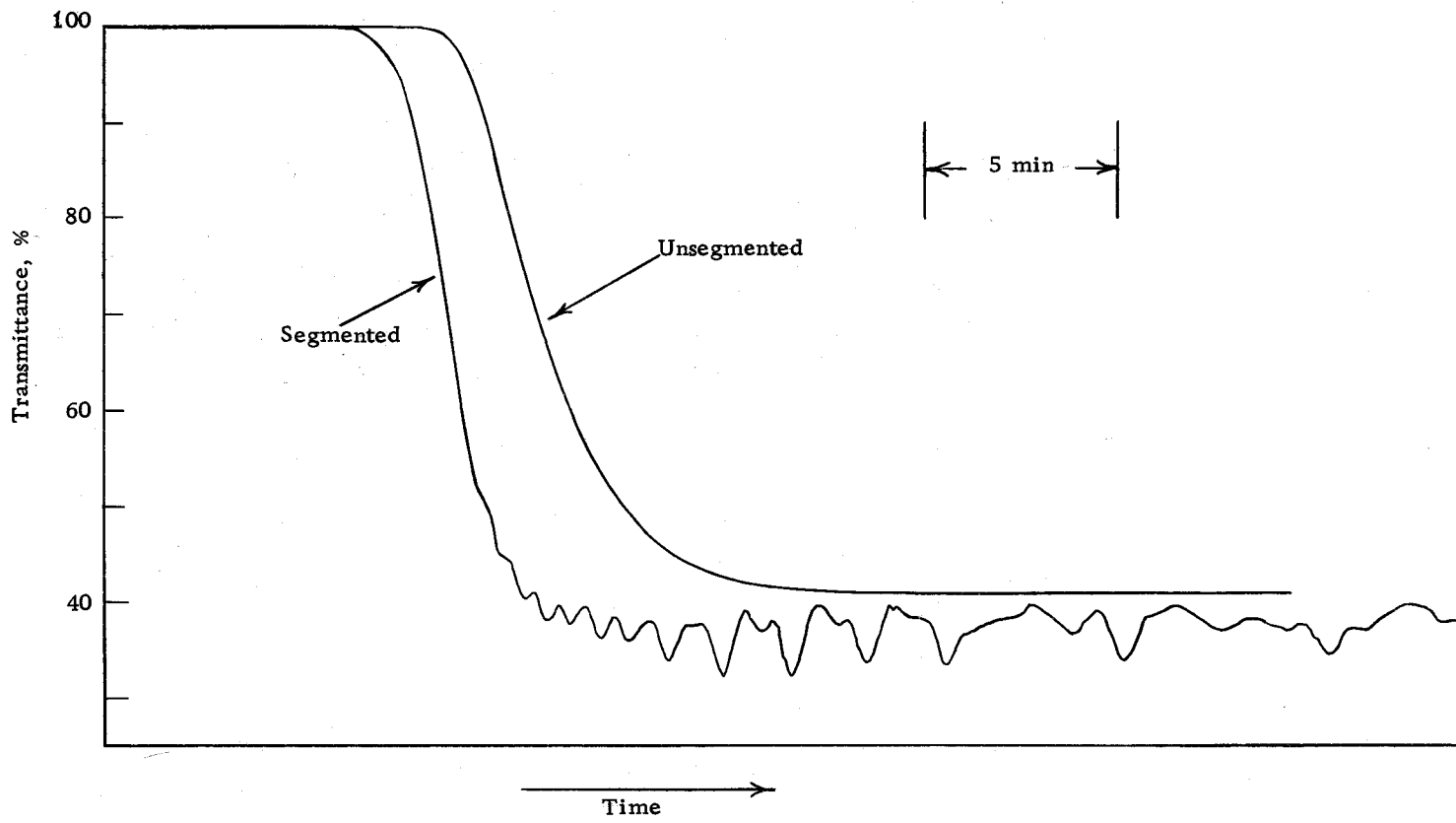


Figure 18. Detector response with segmented and unsegmented analytical streams.

Response Characteristics

In order to study the response characteristics of an unsegmented liquid stream an arbitrary system 39 m long was constructed using 4 mm Pyrex tubing. This system provided for the pumping of water as the major portion of the liquid stream and the introduction of either water or a colored material (e. g. , potassium dichromate) in low proportions through a reagent channel. Thus while the system was in operation step changes could be initiated by switching from water to colored material or vice versa. To detect overall system response to these changes, a Beckman DB Spectrophotometer was fitted with a Beckman flow cuvette (Assembly No. 96160) and its output signal recorded on a strip chart.

A family of curves is presented in Figure 19 which indicates the nature of the overall system response to step changes at various system flow rates. These curves were derived from strip-chart traces of transmittance by converting several points of each of these traces to absorbance values and then normalizing the curves to a common time origin and common absorbance change (0.0 to 1.0 in this case). It may be seen that the response is sigmoid in nature and, as the flow rate increases, the overall response is faster and the change from 0.0 to 1.0 more nearly resembles the step input.

It is helpful at this point to define terms to be used below.

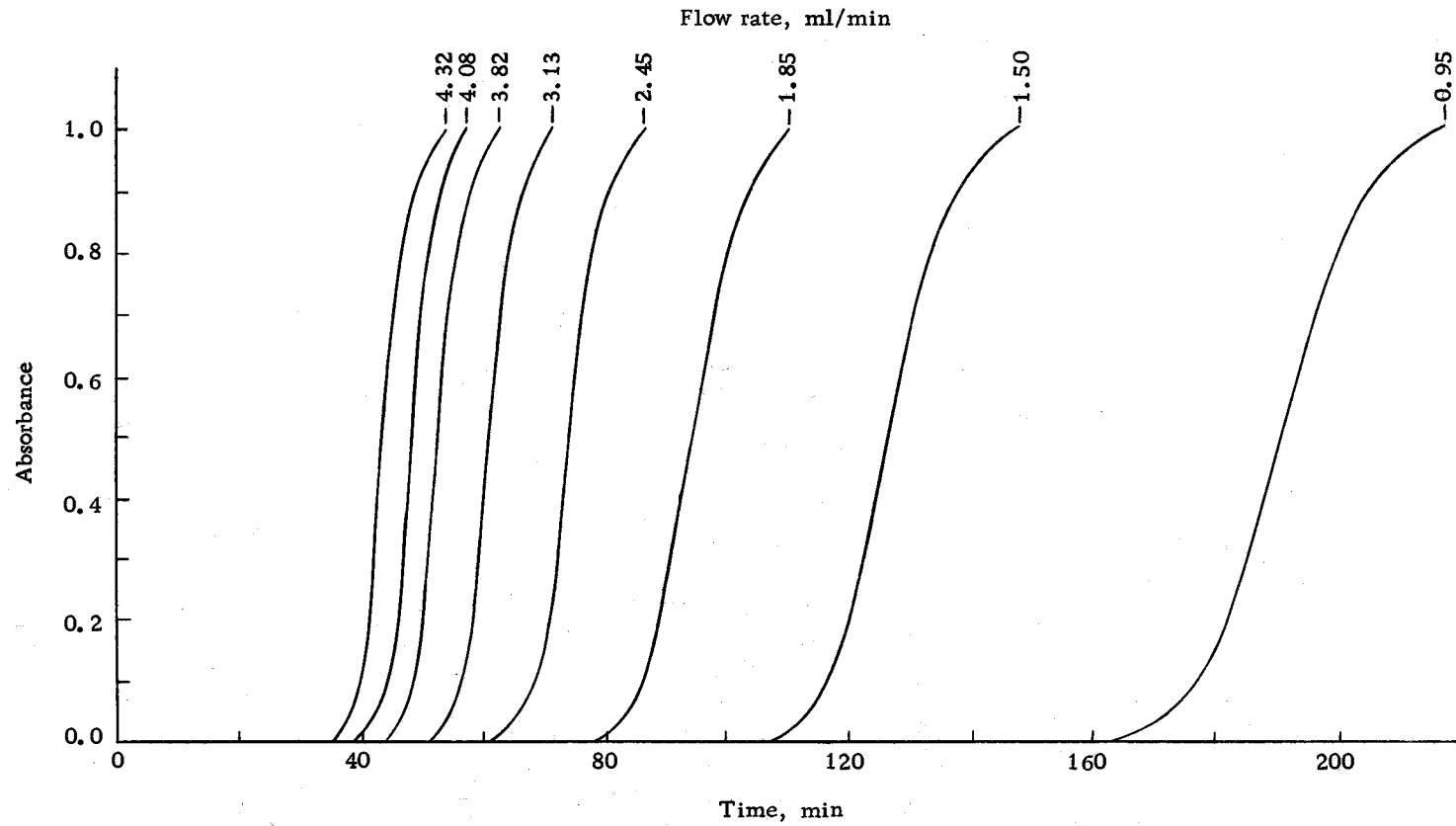


Figure 19. System response to step changes.

Response time is arbitrarily considered to be the interval between the time of initiation of a step change at the input and the time of appearance of 90% of the ultimate change at the output (e. g. , the response time of the instrument at 4. 32 ml/min is 49. 0 min). Rise time refers to the time interval during which the output is changing and is arbitrarily considered to be the interval between the appearance of 10% and the appearance of 90% of the ultimate output signal (e. g. , the rise time of the instrument at 4. 32 ml/min is 9. 0 min). Thus the response time of the instrument at a flow rate of 4. 32 ml/min is 49. 0 min, which includes a rise time of 9. 0 min.

Examination of Figure 19 indicates that response time decreases with increasing flow rate, as does rise time. Figures 20 and 21 are, respectively, plots of response time and rise time versus flow rate. Each of these curves may be fit by an equation of the form $t = (A/R) + B$, where t is time in minutes, R is flow rate in ml/min, and A and B are constants. The net units for A are ml and those for B are minutes.

It may be established, then, for the arbitrary system under consideration here, that response time is given by

$$t_{\text{response}} = \frac{190 \text{ ml}}{R} + 5.6 \text{ min}$$

and rise time is similarly given by

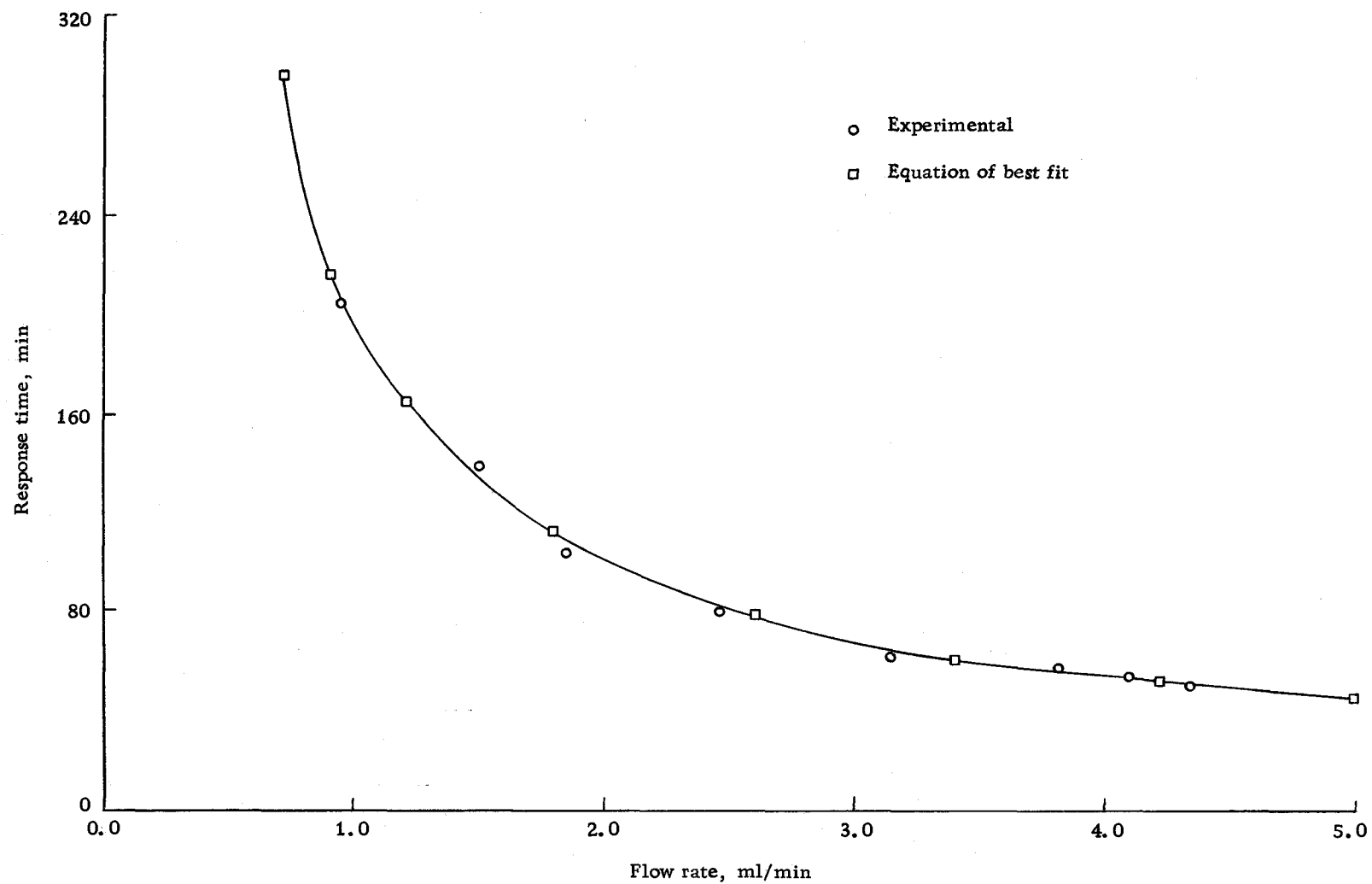


Figure 20. Dependence of response time on flow rate.

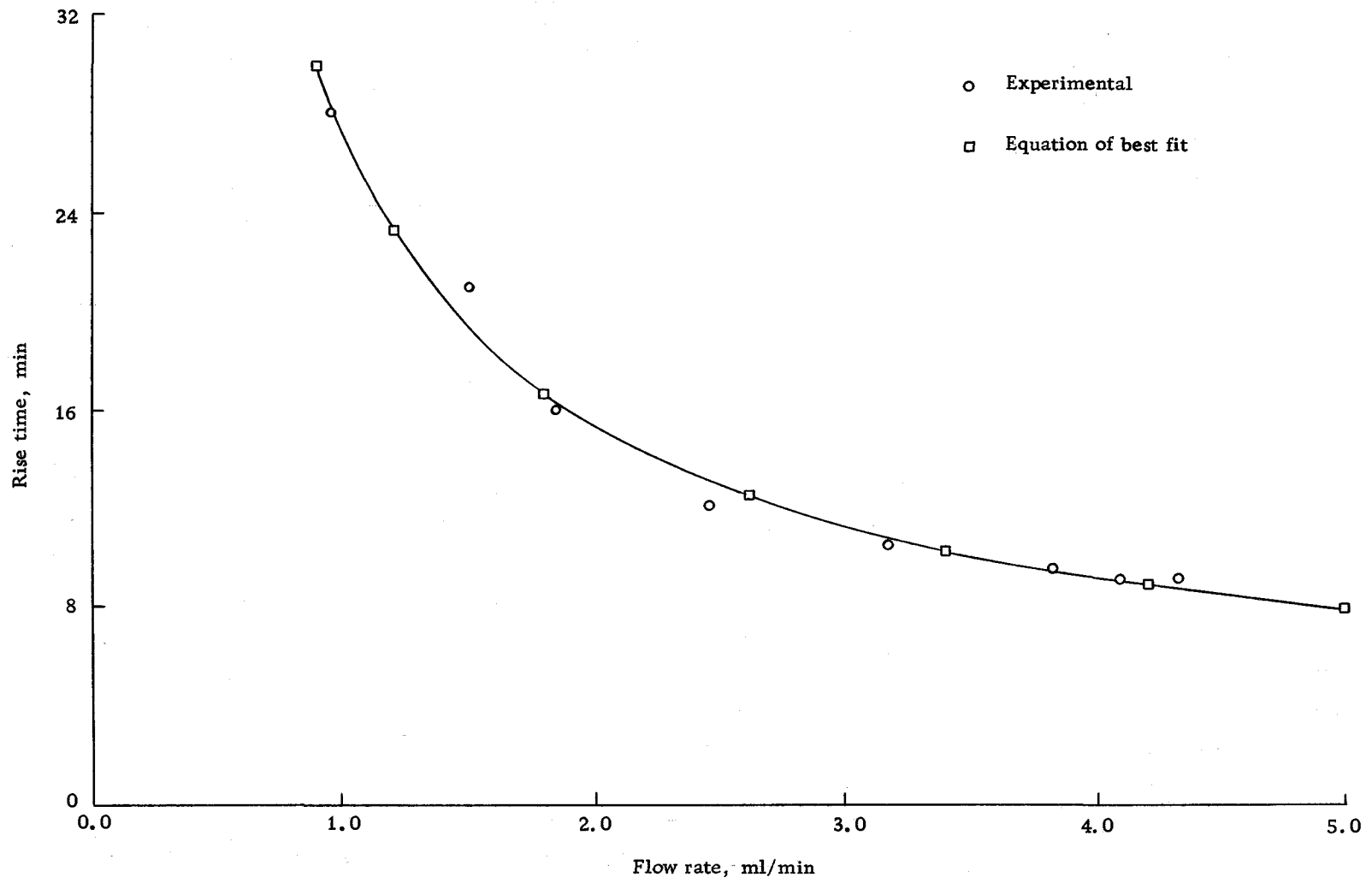


Figure 21. Dependence of rise time on flow rate.

$$t_{\text{rise}} = \frac{24.3 \text{ ml}}{R} + 3.1 \text{ min.}$$

It is felt that an insufficient number of parameters have been examined to assign a definite significance to the constants A and B. It is important to point out, however, that the values for B were established by taking the time-intercept in plots of time versus rate⁻¹, where the best straight line fit of the data points was estimated by the least squares method. The B values may reflect an experimental uncertainty and thus have no real significance.

The equation $t = (A/R) + B$ describes the hyperbola $t' = A/R$ where $t' = t - B$ (merely a shift of the t origin). It is this hyperbolic relationship between t and R that is of particular significance to this discussion, since it is clearly indicated that, within the range studied, there exists no best flow rate for best response or rise time. That is, there is no minimum in the response or rise time function of flow rate, but rather a reciprocal relationship, e. g., doubling rate halves time. This, of course, applies strictly only to t' or t - B, and if B is real, the reciprocal relationship is not exact.

It will be recalled from an earlier section of this thesis that laminar flow is believed to exist within the system in the flow rate ranges under consideration. It is appropriate, then, to compare the observed shape of the response curves with the shape expected

in a system with only laminar flow.

Under conditions of laminar flow, there exists within the tube a parabolic velocity distribution, with the highest velocity along the center of the bore and zero velocity at the tube walls. Thus it follows that if a "plug" of identifiable fluid (e. g., of different color) is introduced into the tube and laminar flow continues, then this plug, if its leading edge was originally planar, will develop a parabolic profile in the tube, i. e., the fluid nearest the wall will not move and the fluid at the center of the bore will move the greatest distance in a given time.

It may be shown (see Appendix III) that the longitudinal distance x that any point a radial distance r' from the center of the bore has traveled in time t is given by

$$x = (2 F t / \pi r^2) [1 - (r'^2 / r^2)]$$

where F is the average flow rate in ml/min and r is the radius of the tube; x , r , and r' have the units cm. Figure 22 illustrates the propagation of this parabolic front in a 4 mm Pyrex tube (I. D. = 0.24 cm) at a flow rate of 4.0 ml/min. Note that the longitudinal time scale is plotted in meters which effects a compression factor of 2500 in the horizontal direction.

Now consider a window of length dx located at a distance $x = 3900$ cm from the origin. Assume the liquid ahead of the

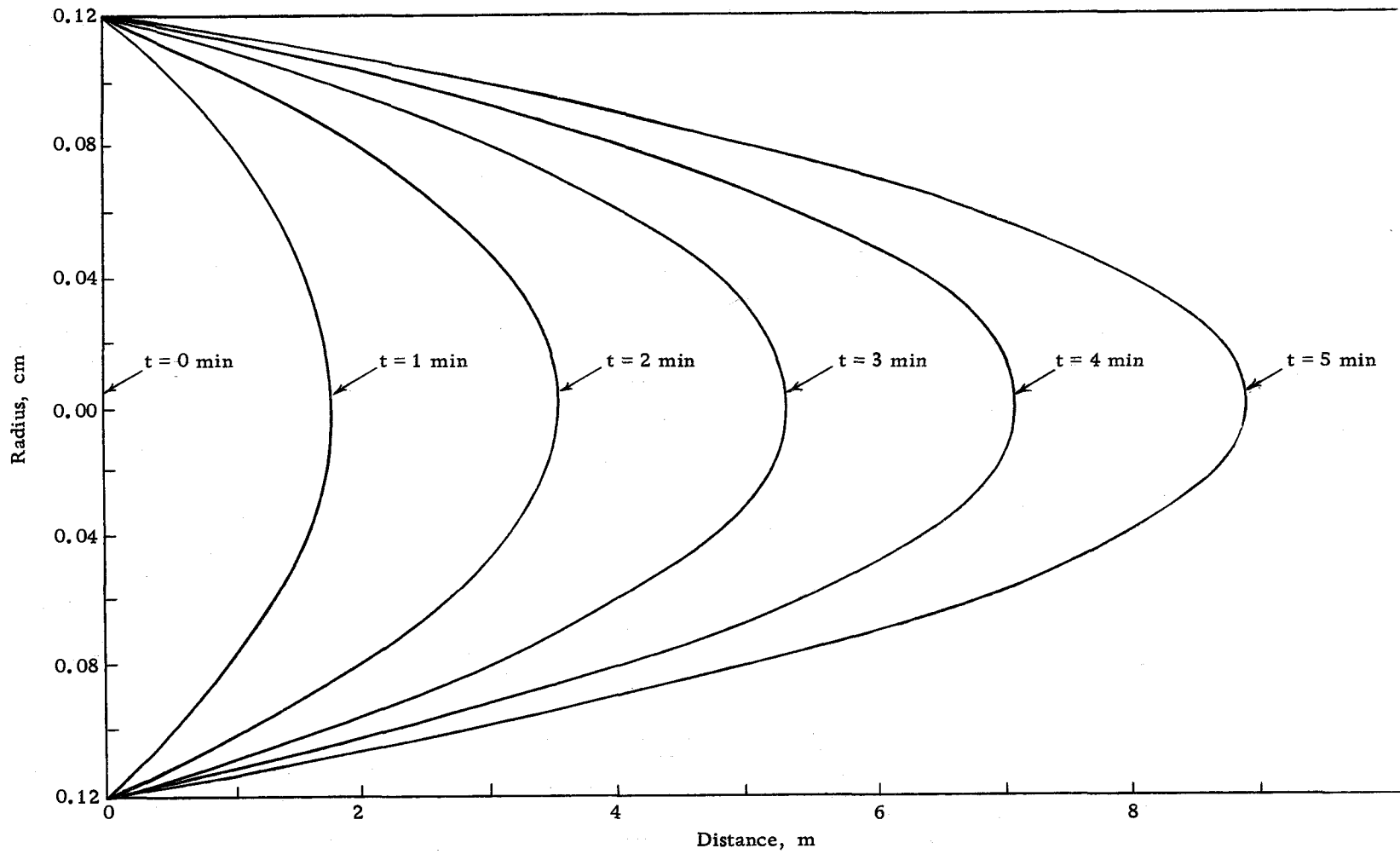


Figure 22. Linear propagation of paraboloid front.

parabolic front has a transmittance of 100% ($A = 0$) and the liquid behind the front has a transmittance of 10% ($A = 1$). If the window of length dx is viewed end-on (in the x direction), there will be observed a disk of radius r' , whose transmittance is 10%, located centrally in a disk of radius r , whose transmittance is 100% (e. g., consider a cross-section taken at 8 m in Figure 22).

The "window" described above will represent the flow cuvette in the spectrophotometer in the instrumental system of tubing whose length is 39 m. The cuvette pathlength of 1.0 cm may be approximated very closely by dx if x is 3900 cm. It will be assumed that the actual shape of this 1.0 cm pathlength cuvette is relatively immaterial in view of its tiny fraction of overall system length.

Now further assume that the detector scans a circular area of πr^2 . The net transmittance T reported by the detector will be given by

$$T = 0.1(r'^2/r^2) + 1.0[1 - (r'^2/r^2)].$$

Thus the transmittance which would be expected of perfect laminar flow, as a function of time is expressed by

$$\begin{aligned} T &= 0.1[1 - (\pi r^2 x/2Ft)] + 1.0[\pi r^2 x/2Ft] \\ &= 0.1 + (0.45 \pi r^2 x/Ft). \end{aligned}$$

In Figure 23, absorbance ($A = (-) \log T$) is plotted for the perfect laminar flow as well as observed absorbance for the

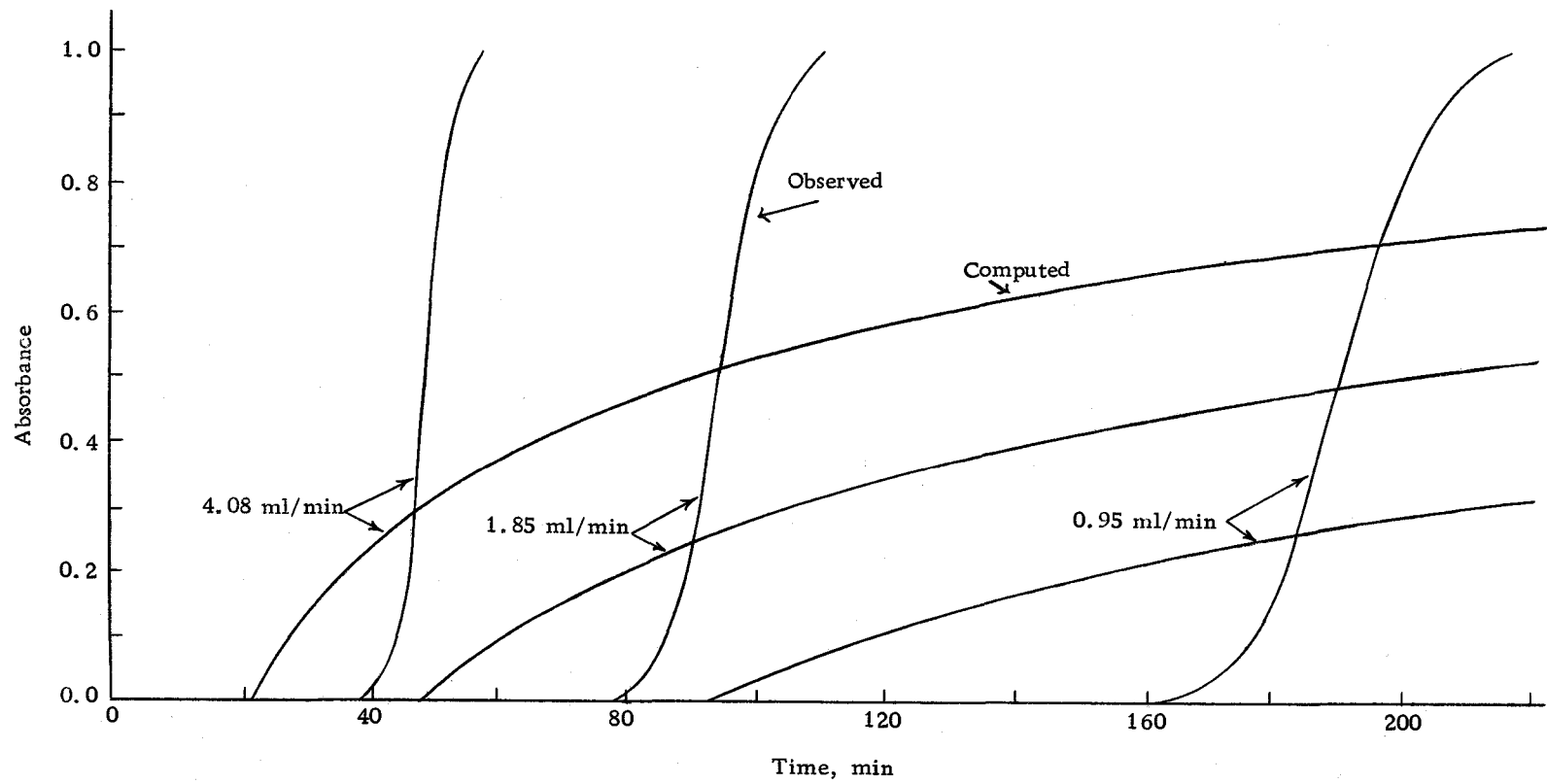


Figure 23. Comparison of computed and observed response.

experimental system for three different flow rates. The observed sigmoid response appears to bear little resemblance to the response computed on the basis of perfect laminar flow.

Nevertheless, it must be emphasized that the computation for perfect laminar flow has made no allowance for mixing between the liquid of $A = 0.0$ and that of $A = 1.0$. It is reasonable to say that in any real system there would be mixing to some extent, as by diffusion, across the interface of the regions of different concentration.

To rationalize the difference in appearance of the observed and calculated response curves in terms of mixing (diffusion), let us examine the data at hand from a different point of view. Consider the "effective profile" that would be necessary to produce the observed response, i. e., what would be the profile of a front separating absorbances of 0.0 ahead and 1.0 behind, that would produce the observed response. If this "effective front" is assumed to have cylindrical symmetry, as does the computed profile, then the r' value corresponding to a T may be determined at various t values taken from the observed data by rearranging the equation for T discussed above. For a tube of radius $r = 0.12$ cm,

$$r' = [(r^2/0.9)(1 - T)]^{\frac{1}{2}}$$

thus we may plot r' versus t from the observed data where r' is the radius of the "effective profile" at any time. Similarly, we may

plot r' for the computed laminar flow profile as a function of t from

$$r' = r[1 - (\pi r^2 x/2Ft)]^{\frac{1}{2}}.$$

Naturally only real values of r' will be considered. The time t_0 corresponding to $r' = 0$ is given by $t_0 = \pi r^2 x/2F$.

The "effective profiles" thus estimated and their corresponding computed laminar flow profiles are plotted in Figure 24 for the same three flow rates considered in Figure 23. All values of t for each laminar flow profile and its corresponding "effective profile" were divided by the respective t_0 values to superimpose the computed profiles for the purpose of comparing the "effective profiles" with one another. In conjunction with Figure 24, consideration is given Figure 25, which is a plot of these same "effective profiles", this time normalized to a common origin on the basis of " t_0 " for each "effective profile".

Now consider diffusion in general. Linear diffusion in static systems has been thoroughly treated in the literature (18, 19), and, in general, Fick's First Law states that the quantity of material which diffuses across an area is proportional to the difference between the concentrations in two adjoining areas infinitely near. It is not attractive to attempt to rigorously treat diffusion in the dynamic system at hand, but qualitative advantage can be taken of several results of treatments of diffusion under various

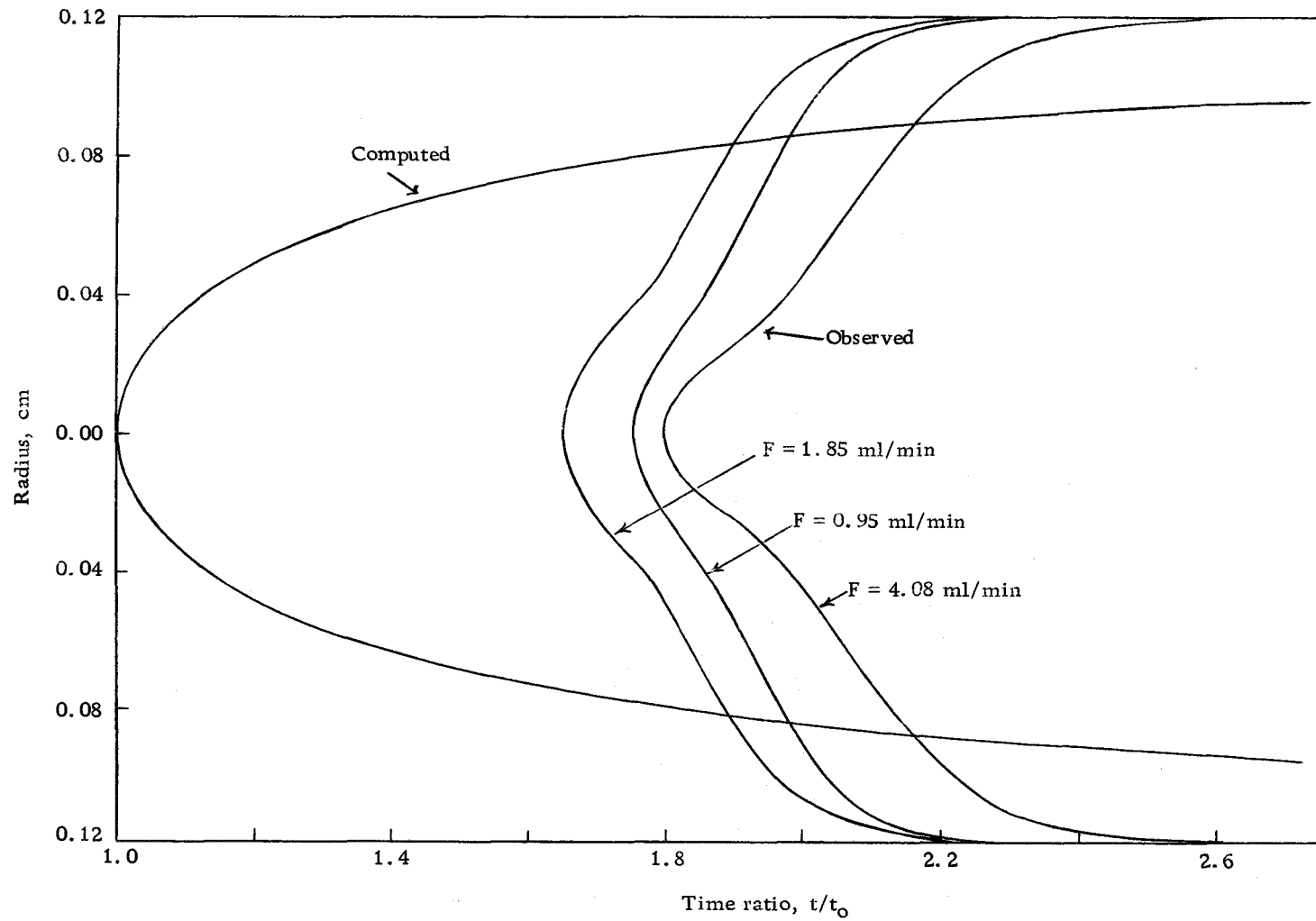


Figure 24. Comparison of computed and "effective" profiles.

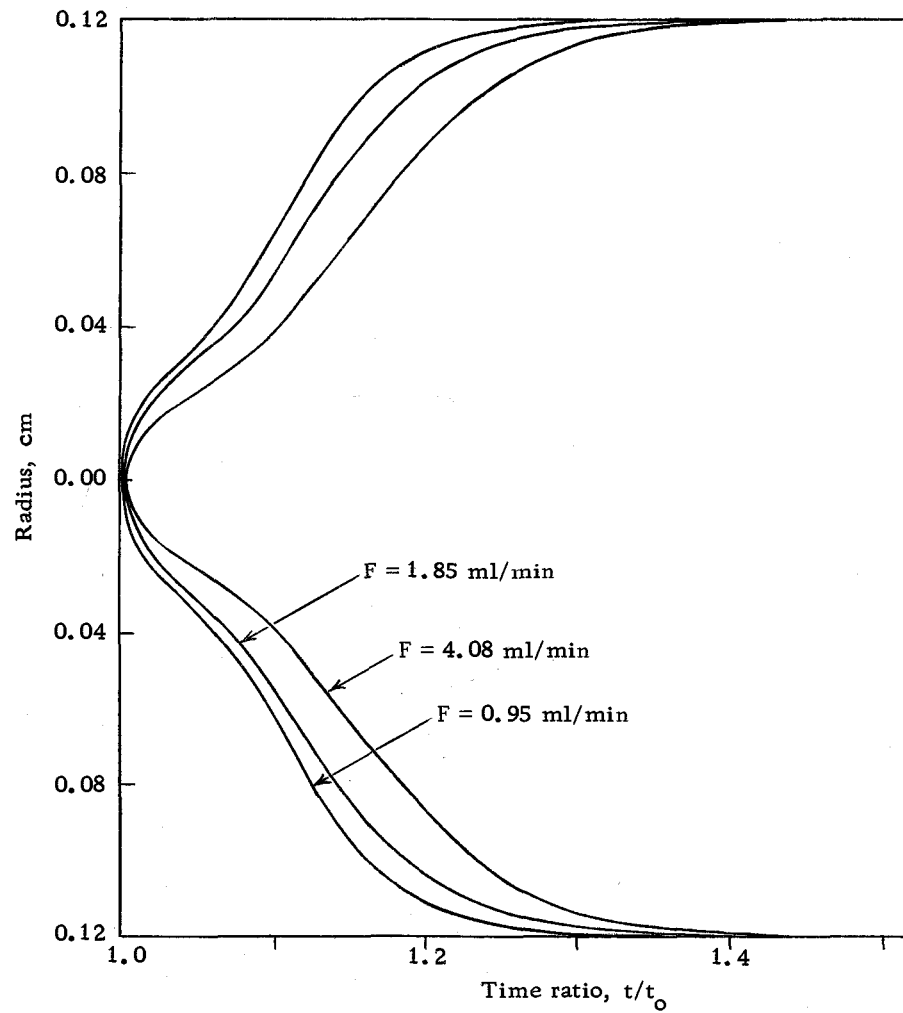


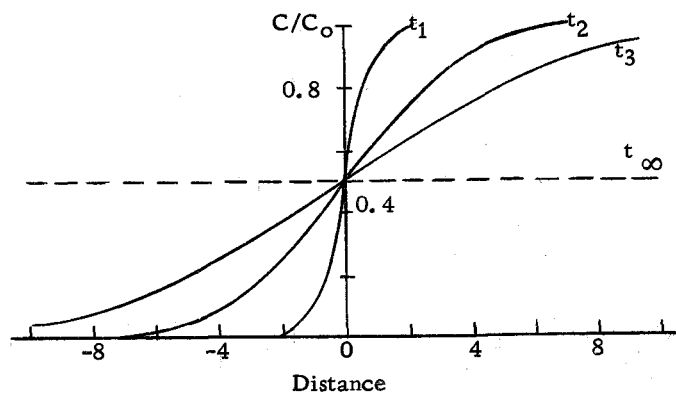
Figure 25. Comparison among "effective" profiles.

static conditions.

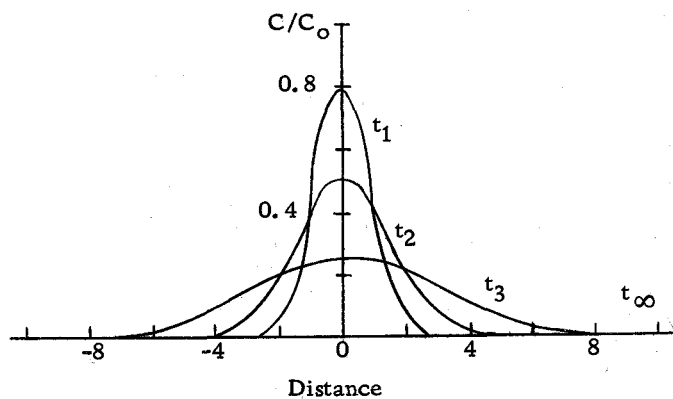
1. Diffusion of solute from solution into solvent: If an infinitely long tube is considered, with solution in the positive direction and solvent in the negative direction, and with an imaginary boundary at the origin, diffusion as time elapses would produce the relative concentrations plotted in Figure 26a. The location of the concentration mean remains at the origin and the relative concentration of all points approaches 0.5.

2. Diffusion of solute from a thin layer of solution into solvent: Again consider an infinitely long tube with solvent in both the positive and negative directions and solution only in a thin layer at the origin. Diffusion as time elapses would produce the relative concentrations plotted in Figure 26b. The location of the concentration mean remains at the origin and the relative concentration at all points approaches zero.

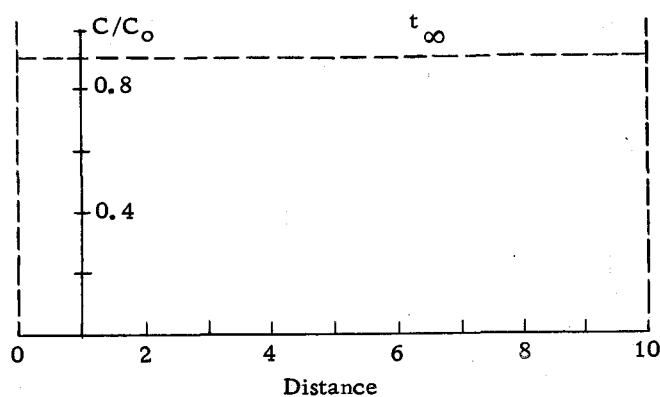
3. Diffusion of solute from solution into solvent with finite boundary: Consider, for example, a tube ten units long with solvent from 0.0 to 1.0 and solution from 1.0 to 10.0. Diffusion as time elapses would ultimately produce a uniform relative concentration of 0.9 throughout the tube (Figure 26c). The location of the concentration mean does not remain at the origin and the relative concentration at all points approaches a value determined by the fraction of the tube originally filled with solution.



(a) Across boundary



(b) From thin layer



(c) Across boundary toward finite limit

Figure 26. Concentration changes due to diffusion at various times.

Now look once again at Figure 22 and recall that there is a compression factor of 2500 on the distance axis. Thus the parabolic profile would be very elongated when its front has traveled 39 m. If the paraboloid is divided into three portions, the effect of diffusion normal to the surface of the paraboloid may be considered. Because this paraboloid is so extremely elongated, the diffusion normal to the surface will be essentially perpendicular to the long axis of the tube.

First consider the section of the paraboloid whose surface is near the center of the tube. This will be the leading portion of the paraboloid, e. g., radius 0.00 to 0.06 cm. The solution contained in this section of the paraboloid will be a long thin spike and should diffuse circularly much as a thin layer of solution would diffuse linearly. Thus in consideration of condition (2) above, diffusion would cause the leading point of the paraboloid to be blunted to a large extent as suggested in Figure 26b. It is felt that this lateral diffusion of a spike would qualitatively account for the blunt leading edge of the observed "effective profiles" plotted in Figure 24.

Now consider the trailing section of the paraboloid, e. g., radius 0.09 to 0.12 cm. In this region condition (3) above would govern the diffusion, since the tube wall lies rather close to the boundary across which diffusion is taking place. In addition, the solution near the boundary is continuously being replaced (recall the

"sliding concentric cylinders" concept of laminar flow). Thus diffusion of solute from the relatively large bulk of continuously renewed solution into a small amount of solvent would cause the concentration in the solvent to approach that of the solution. This appears to qualitatively account for the observation that the "effective profile" appears sooner than predicted from the computed profile in the regions near the tube walls.

If the central section of the paraboloid is considered, e. g., radius 0.06 to 0.09 cm, this appears to be a transition region between the two phenomena discussed above and would most nearly correspond to condition (1) for diffusion.

This explanation of the shapes of the observed "effective profiles" based upon diffusional mixing may be further supported by reference to Figure 25. It is seen that the "effective profiles" demonstrate a regular change of shape with changing flow rates. At the lowest flow rate, i. e., the most time elapsed during which diffusion can proceed, the profile is most blunted along the leading portion and least tapered (or most advanced) near the walls of the tube. At the highest flow rate, i. e., least time elapsed, the leading portion is least blunted and the trailing edge is most tapered. That is, diffusion changes the profile proportionally least in the short elapsed time of the higher flow rate.

SUMMARY

An automatic, continuous analyzer has been developed which is suitable for estimating the level of spent sulfite liquors (SSL) in laboratory samples. The analyzer makes use of a version of the Pearl-Benson, or nitroso method (3), and, in its present form, is useful for samples whose actual SSL solids concentrations are in the range 0 - 100 ppm.

The analyzer functions by metering reagents into an analytical sample stream with a laboratory multi-channel metering pump. This analytical stream is then propelled by the pump through 4 mm Pyrex tubing, where the reagents are mixed upon flowing through helical tubing configurations and the stream is delayed for color development by flowing through a suitably long tube arranged in a tortuous-path configuration. This analytical stream, in parallel with a suitable reference stream then flows through the cuvettes of a Beckman DB Spectrophotometer adapted to function as a flow colorimeter. The output signal of the DB is then recorded on a stripchart recorder.

There are a number of detailed investigations related to the development of the analyzer. While applicable to the problem at hand, these investigations represent efforts to establish the relative importance of a number of aspects of continuously flowing analytical streams in general.

An important consideration developed here is that the detailed mechanism by which the pump activates the flowing system accounts for certain apparent pressure and net flow anomalies, e. g., net flow increases when a standpipe is connected to the system. This suggests that the components of the system must be considered in relation to one another as well as individually. Toward this end, a rudimentary electrical analog model of the pump and its system has been proposed. It is felt that the development of a comprehensive model with accurate analogous functions to the real system would provide a particularly suitable systematic approach to general study of system behavior.

A discussion has been presented which suggests that certain aspects of precision and accuracy are of little practical consideration in a continuous flowing system such as the one at hand.

Also discussed are the advantages of a continuously unbroken analytical stream over an air segmented stream for the long hold up times required of the analyzer and relatively slow concentration changes expected of natural samples.

Finally, the response characteristics of such an unsegmented continuously flowing stream are considered and compared with response expected upon the basis of laminar flow.

The research reported in this thesis represents a portion of a continuing project dealing with continuous monitoring of pulp and

paper mill wastes in natural waterways. Work currently in progress in these laboratories is being directed toward the development of a suitable flow colorimeter (18, p. 60-70) which will respond in the approximate range 0 - 20 ppm full scale as required for typical natural samples in this area (10). The analyzer described here should be readily adaptable to some ultimate instrument suitable for field use by optimizing component layout and determining long-term reliability.

BIBLIOGRAPHY

1. American Public Health Association, American Water Works Association, and Water Pollution Control Federation. Standard methods for the examination of water and wastewater. 11th ed. New York, American Public Health Association, 1960. 626 p.
2. Badger, Walter L. and Warren L. McCabe. Elements of chemical engineering. New York, McGraw-Hill, 1931. 625 p.
3. Barnes, C. A. et al. A standardized Pearl-Benson, or nitroso, method recommended for estimation of spent sulfite liquor or sulfite waste liquor concentration in waters. Tappi 46:347-354. 1963.
4. Black, A. P. and Sidney A. Hannah. Measurement of low turbidities. Journal of the American Water Works Association 57:901-916. 1965.
5. Brauns, F. E. and D. A. Brauns. The chemistry of lignin. Supplemental Volume (Covering the literature for the years 1949 to 1958). New York, Academic Press, 1960. 804 p.
6. Carritt, Dayton E. and John W. Kanwisher. Electrode system for measuring dissolved oxygen. Analytical Chemistry 31:5-9. 1959.
7. Clarex Corporation. Photoconductive cell design manual. New York, 1966. 16 p.
8. Cohen, Andrew R. Outline of linear circuits and systems. Part 1. New York, Regents Publishing Co., Inc., 1965. 320 p.
9. Cox, Charles R. Laboratory control of water purification. New York, Case-Shepperd-Man, 1946. 386 p.
10. Felicetta, Vincent F. and Joseph L. McCarthy. Spent sulfite liquor: X. The Pearl-Benson, or nitroso, method for the estimation of spent sulfite liquor concentration in waters. Tappi 46:337-347. 1963.
11. Hochgesang, Frank P. Nephelometry and turbidimetry. In: Treatise on analytical chemistry, ed. by I. M. Kolthoff and P. J. Elving. Part I, Vol. 5. New York, Interscience, 1964. p. 3289-3328.

12. Ionics Incorporated. Nepton ion exchange membranes. Cambridge, Mass., 1964. 2 p. (Bulletin AR111).
13. Katz, William E. Preliminary evaluation of electric membrane processes for chemical processing applications. Paper presented at the eighth annual all-day meeting, Separation processes in practice, sponsored by the Philadelphia-Wilmington Section, American Institute of Chemical Engineers and The School of Chemical Engineering, University of Pennsylvania, 1960. 24 p.
14. Knight, A. G. The measurement of turbidity in water. *Journal of the Institution of Water Engineers* 4:449-456. 1950.
15. Malmstadt, H. V. and C. G. Enke. *Electronics for scientists*. New York, Benjamin, 1963. 619 p.
16. Meehan, E. J. Fundamentals of spectrophotometry. In: *Treatise on analytical chemistry*, ed. by I. M. Kolthoff and P. J. Elving. Part I, Vol. 5. New York, Interscience, 1964. p. 2753-2803.
17. Neurath, Hans. The investigation of proteins by diffusion measurements. *Chemical Reviews* 30:357-394. 1942.
18. Olson, Gary, Roger Blaine and Harry Freund. Progress report on research on automatic and continuous methods of chemical analysis. Corvallis, Oregon, Oregon State University, Dept. of Chemistry, 1966. 70 numb. leaves.
19. Skeggs, Leonard T. An automatic method for colorimetric analysis. *American Journal of Clinical Pathology* 28:311-322. 1957.
20. Walker, William H. et al. *Principles of chemical engineering*. 3d ed. New York, McGraw-Hill, 1937. 749 p.
21. Williams, J. W. and L. C. Cady. Molecular diffusion in solution. *Chemical Reviews* 14:171-217. 1934.

APPENDICES

APPENDIX I

CLARIFICATION

Discussion of Turbidity

When seeking to establish a continuous colorimetric monitoring system for some constituent of a flowing stream, it is necessary to consider the clarity of this stream.

The use of a dual beam colorimeter in the monitoring scheme is intended to automatically compensate for the presence of materials other than the desired constituent which absorb radiation at the wavelength of interest. Such an instrument presents to the output the ratio of the intensity of light transmitted by the sample to the intensity of light transmitted by the reference material. Subject to the conditions that all species present are either ideal absorbers (obey Beer's Law) or non-absorbers; and that the compositions of both sample and reference are identical except that the sample also contains an absorber of interest; it may be assumed, then, that the value of the ratio will be dependent only upon the amount of material of interest in the sample (16, p. 2789). Furthermore it is not unreasonable to cautiously extend the assumption into the realm of species exhibiting properties not strictly absorptive in nature, but nevertheless impeding the passage of light through the sample.

The property of a sample which causes light to be scattered and absorbed rather than transmitted is normally referred to as the turbidity of the sample. For suspended materials of the same nature and particle size, the degree of turbidity is related to the quantity of suspended matter at low levels (11, p. 3291), the degree of turbidity referring here to the decrease in transmission of light by these turbid samples compared to similar samples containing no suspended particles. Black and Hannah (4, p. 903) emphasize that "The total intensity . . . of light scattered from turbid water. . . [depends] on such factors as the number, size, shape, and refractive index of foreign particles and on the wavelength of the exciting light." It is reasonable to assume, then, that samples of the same turbidity resulting from the suspension of identical amounts of suspended materials of the same nature and particle size would have the same light transmission. If this is the case, the application of dual beam philosophy is sound here and can indeed be used to obtain significant colorimetric data in spite of turbidity.

Differential transmittance measurements are practical, for example, with the Beckman DB Spectrophotometer provided that the reference sample transmits about 50% or more of the incident light. Other instruments will limit at different values of reference transmittance depending upon the method used for electronically comparing reference and sample signals within the instrument and converting

such a comparison to an output.

Two considerations which become limiting factors in any scheme in which it is intended to derive meaningful colorimetric data while ignoring turbidity are (1) the sample and reference must have the same turbidity resulting from the same amount of the same suspended materials, and (2) the reference may have its transmittance reduced, due to both the presence of absorbing species (in solution) and the presence of turbidity, only to the extent allowed by the design of the particular colorimeter or spectrophotometer used to collect such data.

Working Standard for Turbidity

In practice, turbidity is the cloudiness produced in a sample by the presence of suspended materials peculiar to the local area from which the sample is drawn, and any attempt to clarify this sample, of course, would have to be directed at removing these specific materials. Nevertheless, to provide a common reference material, a turbidity unit has been defined (9, p. 139) as ". . . the degree of cloudiness produced by one milligram of fuller's earth in one liter of water, which is equivalent to 1.0 ppm." The cloudiness of a turbid sample from a natural source, which may contain various suspended materials as clay, silt, micro-organisms, etc., can then be arbitrarily expressed in terms of turbidity units. This expression makes possible a rather loose comparison among samples from

various sources. The instrument generally accepted as a secondary standard by workers in this field is the Jackson candle turbidimeter (1, p. 261), whose scale is graduated in turbidity units. The only practical use of this instrument, in general, lies in the preparation of tertiary standard solutions. The tertiary standards, then, may finally be compared with the unknown by visual estimation or in a suitable colorimeter.

Since some light is absorbed and some is scattered by a turbid solution, it is not strictly correct to refer to the absorbance of a turbid solution. Nevertheless, a turbid sample does attenuate the light, both through absorption and scattering, so that only a portion of the incident energy finds its way to the detector of the colorimeter. At low levels, the relation $I = I_0 \exp(-\tau l)$ holds (11, p. 3293-3294) where I_0 is incident intensity, I is intensity after passage through the turbid sample, l is the length of the sample, and τ is a turbidity coefficient describing the extinction of the incident light by the turbid solution. The turbidity coefficient varies with concentration (amount of suspended material) and the nature of the suspended material.

Since absorbance is generally defined from the point of view of energy reaching the detector as $A = \log I_0/I$, it is appropriate to deal with absorbance in the case of turbid solutions, where $A = \tau l$. It is important to realize, however, that this is a definition of convenience and does not in any way imply that the overall mechanism of light attenuation in a turbid solution is limited to true absorbance. Finally,

absorbance of a turbid sample, as defined, may be expressed as a function of concentration by replacing T with kc where k refers to the nature of the suspended material and c is expressed in suitable concentration units. A plot of A versus c should be a straight line with a slope of kl at low concentrations indicating that only single scattering occurs, and the curve should deviate toward the concentration axis as double and multiple scattering becomes appreciable (11, p. 3294).

Brief laboratory studies have been carried out to gain some further understanding of turbidity and clarification problems. As it was not of particular importance for the purpose of these studies to express turbidity in terms of the usual turbidity units, working standards were prepared in the following manner. An arbitrary suspension of fuller's earth in water was prepared. A portion of this suspension was volumetrically diluted to half its concentration, and the process was repeated until a series of several suspensions were obtained by serial dilution, each containing half the weight of fuller's earth of the preceding suspension. Aliquots of the first few suspensions were evaporated to dryness and the residues weighed, thereby making possible designation of the concentration of each suspension in parts per million fuller's earth. The transmittance of 430 m μ light by each suspension was then measured, using a Bausch and Lomb Spectronic 20.

The absorbance plotted as a function of concentration for the series of suspensions described above yielded a useful calibration curve (Figure I-1). The absorbance is essentially a straight line function of turbidity (ppm) below about 350 ppm fuller's earth (Figure I-2), and shows the expected deviation toward the concentration axis at higher levels.

Settling Studies

In investigations in which turbidity is determined, either as an end in itself, or as insurance that the turbidity level is below that which would interfere with some colorimetric procedure, the technique of allowing a turbid suspension to settle for some period of time is in common use.

The recommended Pearl-Benson procedure (3) prescribes a 12 to 24 hour settling period after which the clear sample is decanted or pipetted away from any sediment in the bottom of the container. The American Standard Methods (1, p. 262) recommend that, as a part of the procedure for preparing standard suspensions, a fuller's earth (or other) suspension be allowed to settle for 24 hours, after which the supernatant is removed without disturbing the sediment at the bottom of the vessel. Knight (14), in investigating the propriety of using a material such as fuller's earth to prepare standard suspensions, reports that after 24 hours' settling, four different

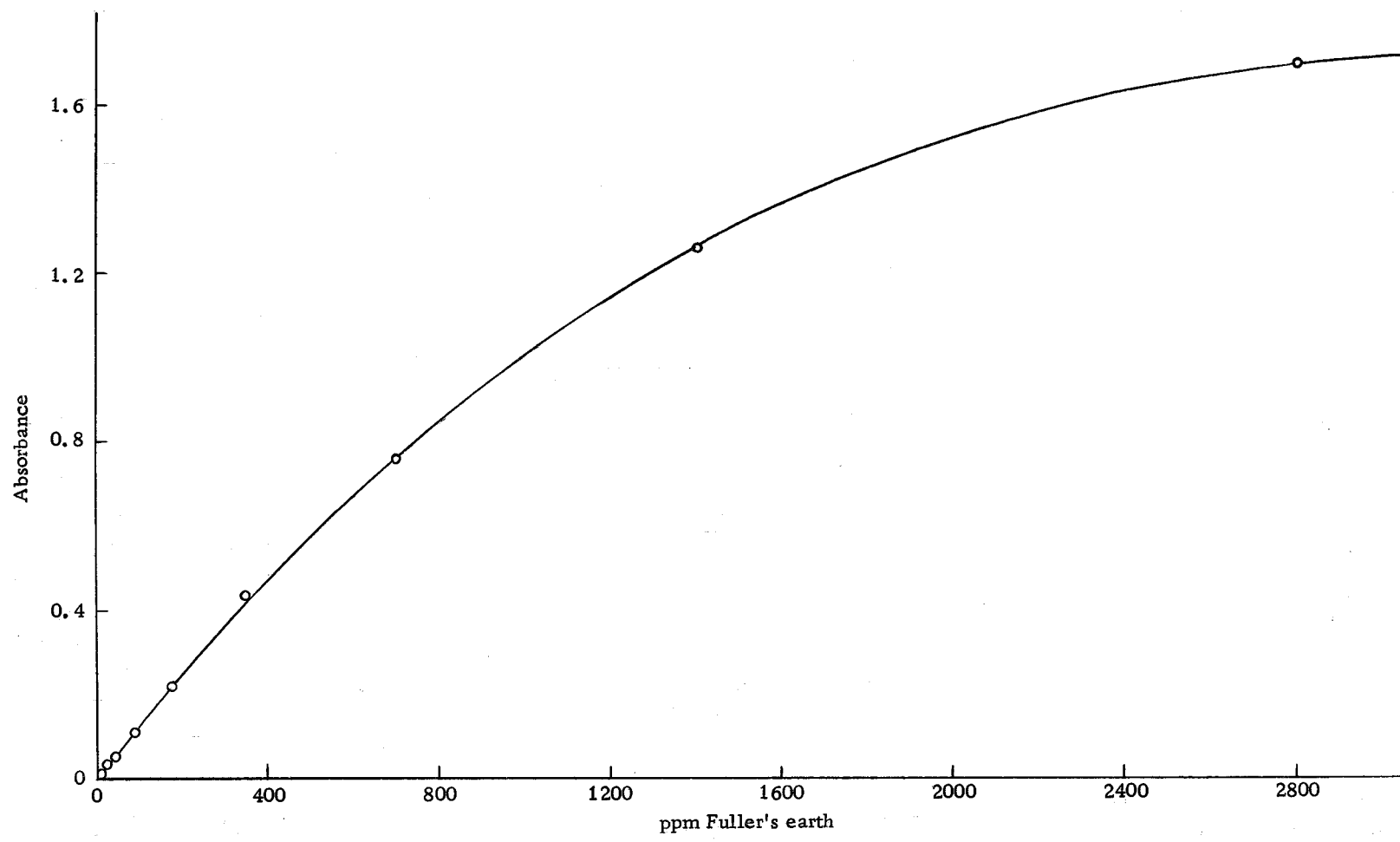


Figure I-1. Calibration curve for turbidity.

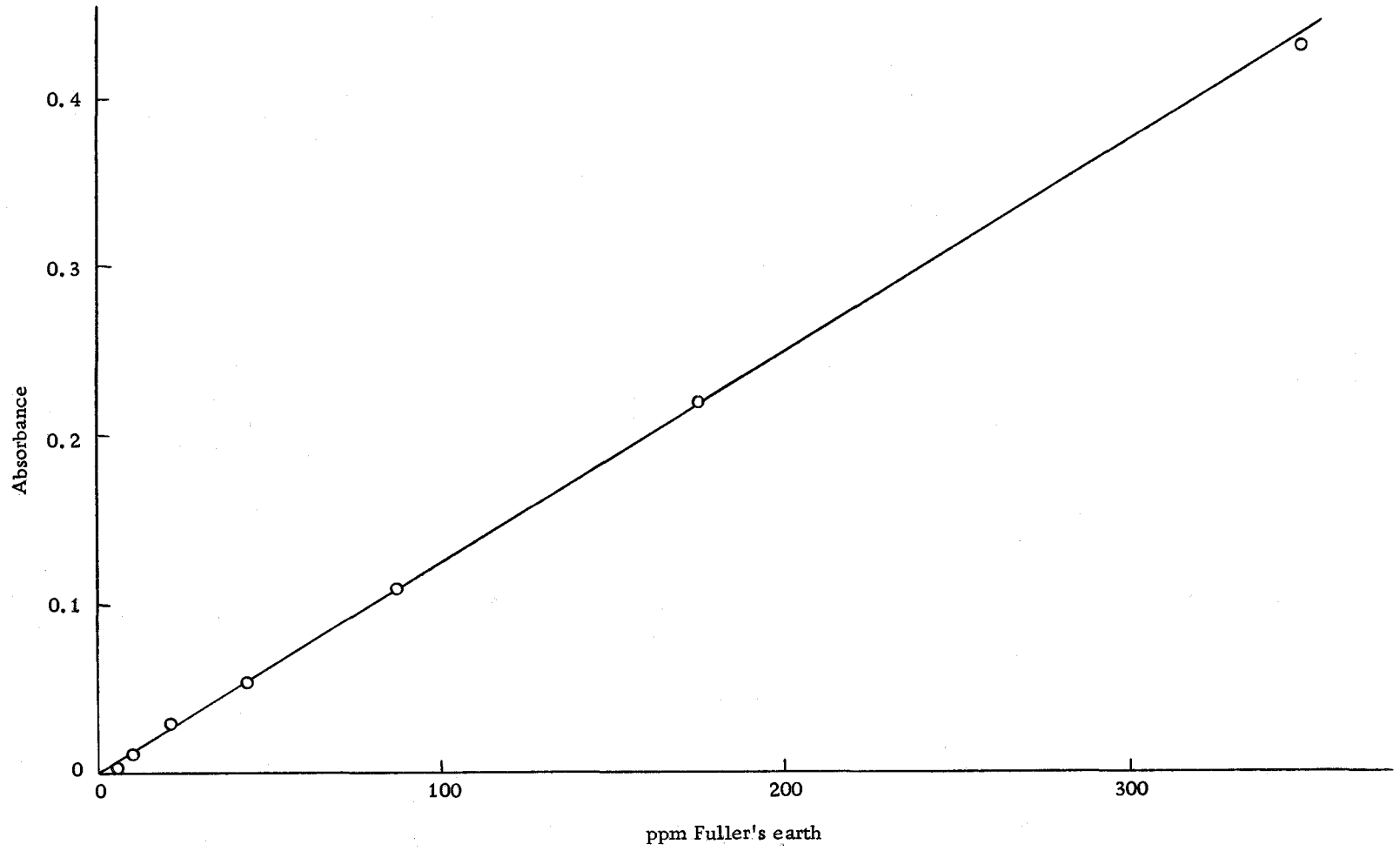


Figure I-2. Calibration curve for turbidity.

commercial samples of fuller's earth yielded turbidities of 120 ppm, 400 ppm, 620 ppm, and 1966 ppm by weight.

Even though a settling technique would likely not be applicable to a continuous analytical scheme, it seemed important to the appreciation of clarification problems to investigate briefly the settling process itself. An experiment was designed to examine what happens during this settling process with respect to the turbidity profile of the vessel and the change of turbidity with time at a given point on this profile. Two arbitrary suspensions of fuller's earth were prepared in carboys and the vessels were placed out of direct sunlight on a concrete floor. This probably represents best conditions under which samples would be allowed to settle overnight with respect to relative lack of vibration and absence of thermal convection currents.

Carboy 1 was prepared with an initial concentration (C_{o1}) of 3000 ppm of fuller's earth by weight, and carboy 2 with $C_{o2} = 500$ ppm.

Aliquots were withdrawn at intervals at a point slightly below the surface, but at a point reproducible with respect to distance (21 cm) above the bottom of each container. The concentration of fuller's earth in each aliquot was estimated by comparing its transmittance at 430 m μ with the standard curve in Figures I-1 and I-2. These data represent a time profile of undisturbed settling of fuller's earth suspensions with respect to time, and are plotted in raw form in Figure I-3. These data were normalized to percentage of original

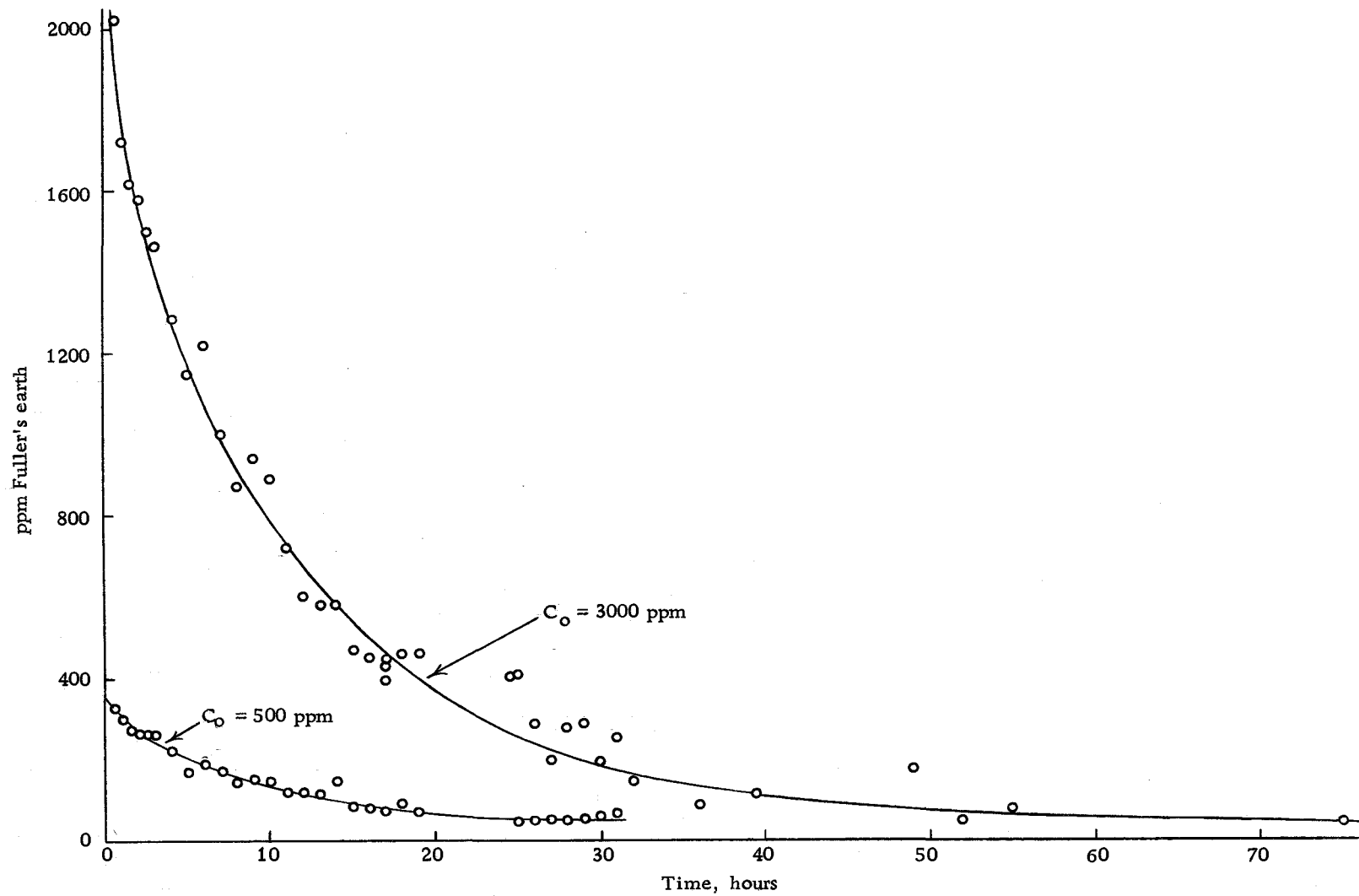


Figure I-3. Fuller's earth settling curve; time profile.

concentration remaining and are presented in this form in Figure I-4.

Note that the data from the two separate experiments are indistinguishable when normalized to a common reference. This indicates that percentage of material which has settled at any time is independent of the original number of particles, when the nature and size distribution of the suspended material are held constant.

To determine a vertical profile of the vessels, aliquots were taken from various depths within each carboy at 17 hours. These aliquots were all collected within ten minutes, thus time was held constant within about one percent. The concentration of fuller's earth in each aliquot was estimated in the manner described above, and the raw data are plotted in Figure I-5. These were again normalized to percentage of original concentration remaining and are presented in Figure I-6. Again it is noteworthy that the data may be represented by a single curve, indicating that settling is independent of the number of particles present.

Figure I-7 summarizes the above data in a composite three dimensional representation suggesting the shape of the surface on which concentration may be found as a function of both distance above the bottom of the container and time.

The data obtained in these experiments are of little importance in themselves, since they only give specific information regarding

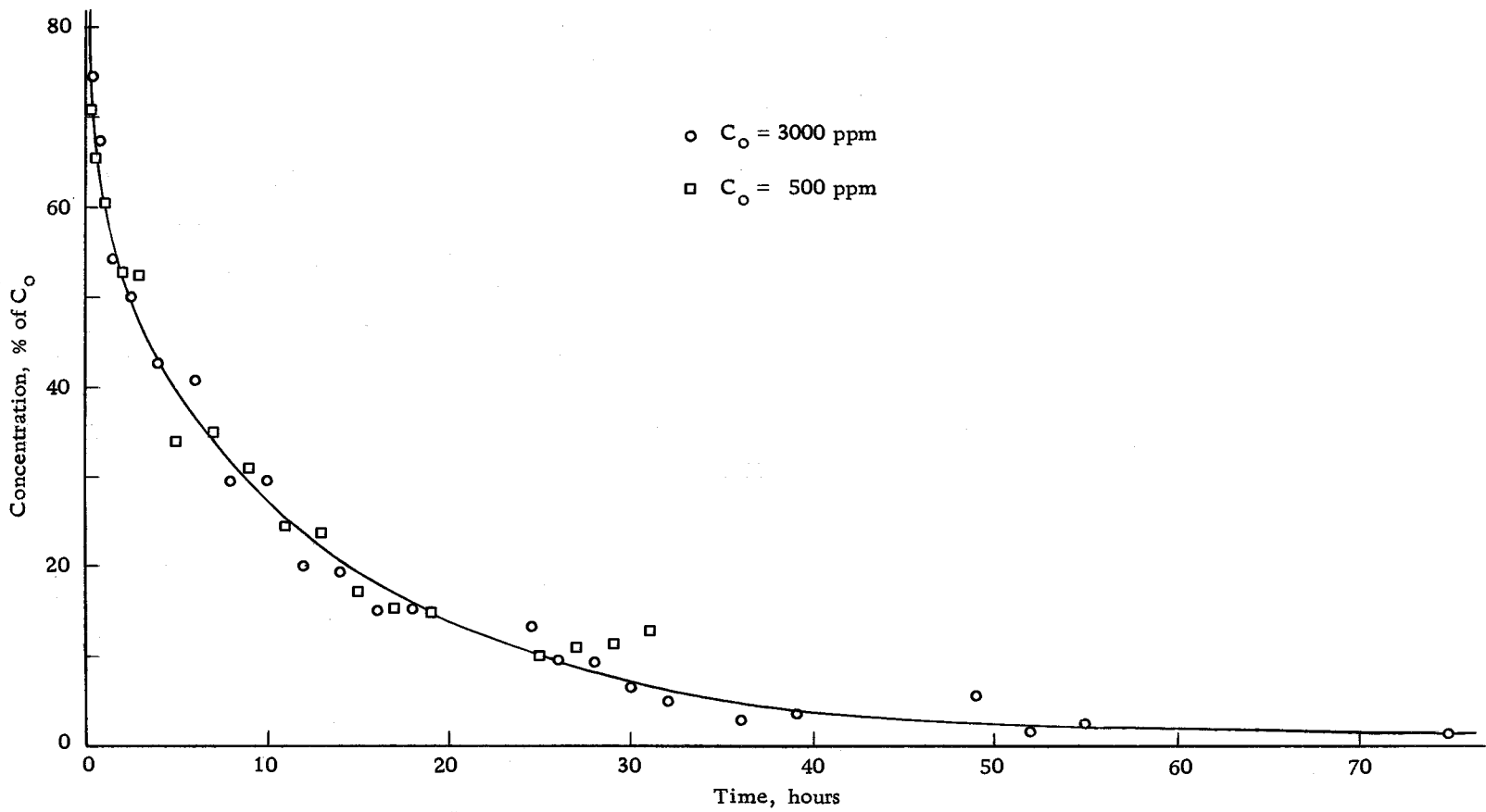


Figure 1-4. Fuller's earth settling curve; normalized time profile.

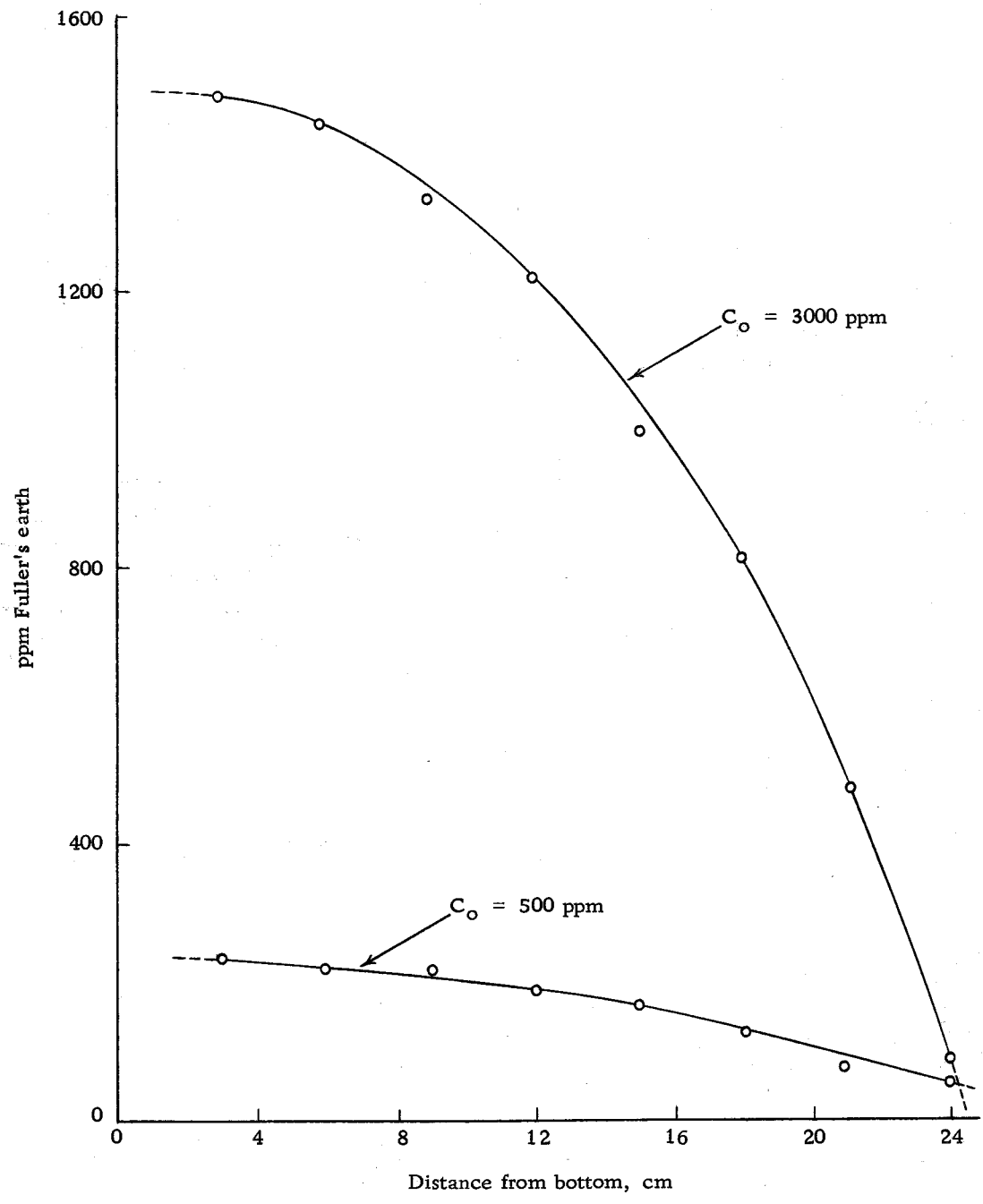


Figure I-5. Fuller's earth settling curve; vertical profile.

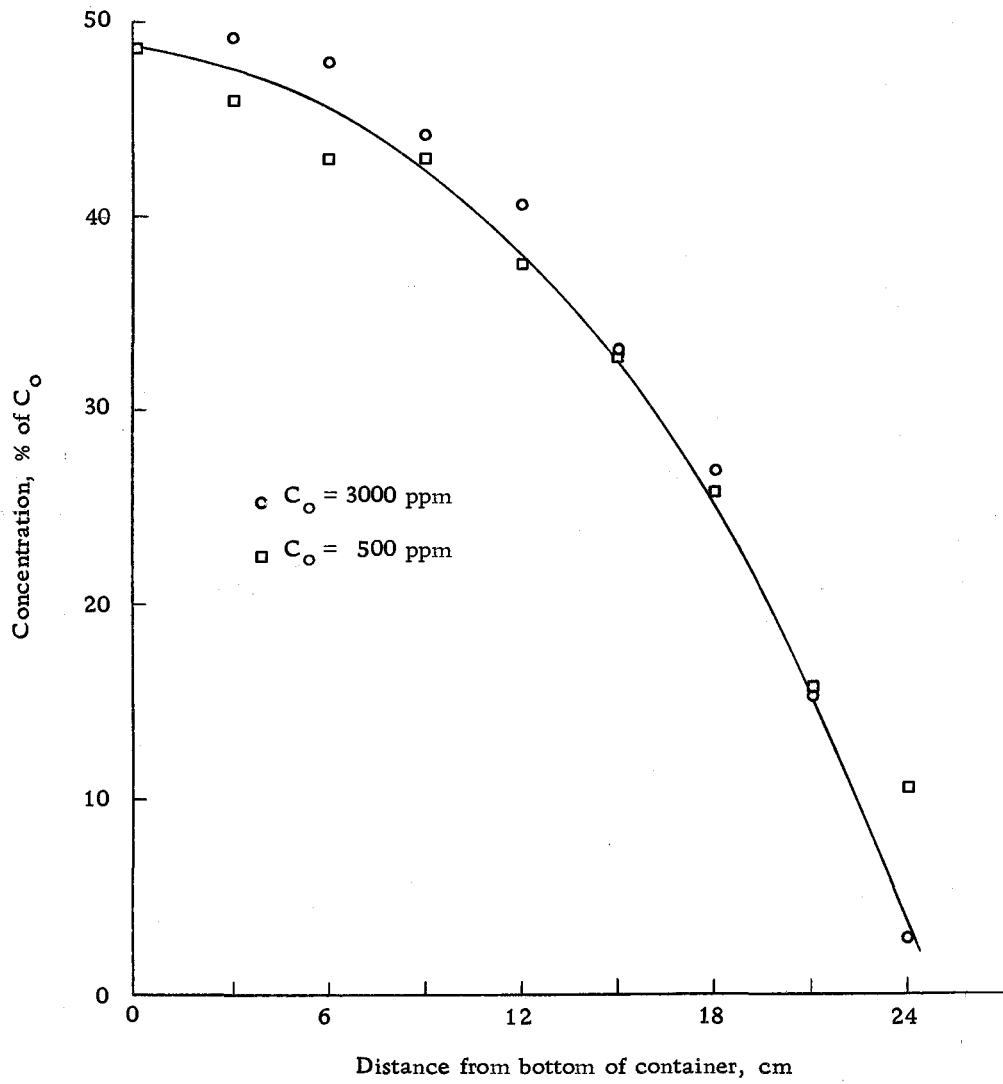


Figure 1-6. Fuller's earth settling curve; normalized vertical profile.

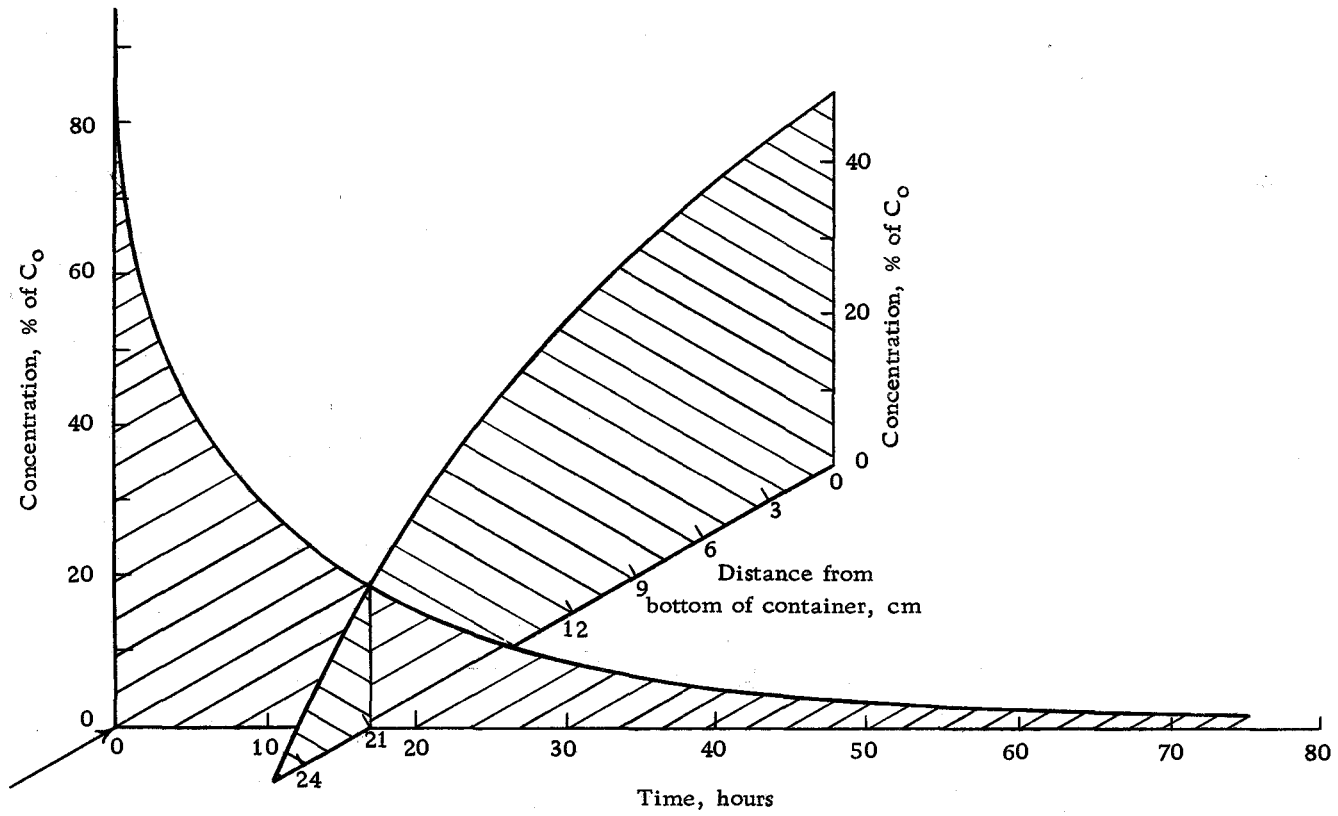


Figure 1-7. Composite normalized fuller's earth settling curve.

the determination of turbidity resulting from the suspension of the particular fuller's earth at hand by means of a Bausch and Lomb Spectronic 20. Nevertheless, the data permit significant general observations and comments to be made, although we must specify that such statements will be limited in application to suspensions containing solids of the same nature and differing only in number of particles. If the same particle size distribution exists in all suspensions of interest, then the number of particles will be directly related to the weight of suspended material (e. g. , parts per million by weight).

Perhaps the most important observation to be made is that the settling profile (concentration as a function both of distance from the bottom and of time) is essentially smooth without abrupt changes of slope. This means, of course, that first, there is no specific length of time which produces optimum clarification at any given distance from the bottom of the container. Secondly, there is no clear boundary between clarified and still-turbid areas along the vertical profile. Rather, the turbidity increases smoothly from top to bottom of the container at any time.

A reasonable conclusion to be drawn from these experiments, then, is that a decision to allow a turbid suspension to settle for an arbitrary length of time, then to decant or remove by pipet the supernatant would introduce several (normally) unknown and uncontrollable

variables. It seems that such a technique could hardly show any useful reproducibility, and, indeed, it seems possible that samples of suspensions showing all the turbidities reported by Knight (14) could conceivably have been drawn from the same container and might really have little correlation with the differences among different starting samples.

A further conclusion which may be drawn from the data is that the final turbidity after an arbitrary time of settling is dependent strictly upon the original number of particles present for a given particle nature. This is of great importance when it is desired to reduce turbidity, by settling, below some maximum level, above which turbidity interferes with an analytical determination of another component. It is clear, in this case, that a decision to allow settling for some length of time is meaningless unless the starting concentration and the depth to which the container will be sampled is specified. The only other alternative is to test the turbidity after the settling period to insure that it is at or below the maximum permissible level.

APPENDIX II

AUTOMATIC SAMPLE SELECTOR

One of three sample sources may be connected at will to the analyzer input by the appropriate positioning of two three-way stopcocks connected in series. This arrangement was established to permit arbitrary introduction into the system of a water blank, a sample of known composition, or a sample of unknown or varying composition. Such an arrangement is also useful for preparing calibration curves, using samples of known concentration. In order to facilitate replicate sampling of an array of three inputs in a systematic manner, an automatic sample selector was assembled.

The immediate goal of devising such an automatic sample selector was to permit the preparation of calibration curves without the necessity of giving the analyzer constant attention. As an example, a typical portion of a calibration curve would be prepared by sampling each of two sources of known concentration for 20 minutes apiece followed by a water blank sampled for 20 minutes, to give a total time of one hour for determining two points on the calibration curve. Further, it was deemed appropriate to repeat such a cycle so as to provide three estimates of each point. Thus it was necessary to attend the analyzer for a minimum of three hours after startup in order to obtain two points on a calibration curve with the manual

sample selection arrangement.

The criteria for the automatic sample selector then were to sample three sources in turn according to a predetermined program and to repeat this program continuously until terminated manually. In order not to have to be in constant attendance near the end of the cycle, it was desirable to arrange for the manual termination switch to have a built-in delay. Thus when the decision was made manually to terminate during any one cycle, the sample selector would automatically continue to the end of the program before shutting off. Of course, it would be necessary to provide an override switch to terminate the program immediately, should the need arise. Two additional features would also be useful, if not necessary. A set of pilot lamps should be provided to indicate which source is currently being sampled, and the sample selector should provide a pulse to the event marker terminals of the strip chart recorder each time the source being sampled is changed.

The availability of reversible motors and a cam-type timer kit in these laboratories suggested that the stopcocks in the manual selector not be replaced, but simply be coupled to the motor shafts to provide the mechanical link. The motors could then be automatically energized according to a program established on a set of switches activated by adjustable cams. The cams, mounted on a common shaft, would be programmed in terms of percentage of cycle and the

cam shaft would be rotated by a suitable combination of synchronous motor and reducing gears to give the desired cycle length.

The task of the motors would be to turn the stopcocks to a new position upon command from the programmer. Since provision would be made to adjust the length of the program and since there might be variable frictional resistance in the mechanical linkages, it would be necessary to de-energize the motors by positional limit switches. Thus each rotation of a stopcock would be initiated by time and terminated by the position of the stopcock.

With the above considerations in mind, the mechanical apparatus illustrated in Figures II-1 through II-3 was assembled on a chassis which was designed to mount adjacent to the panel from which the handles of the stopcocks of the manual sample selector protruded. Number ten rubber stoppers were slotted to accept the stopcock handles and fitted with 1/4" x 1" carriage bolts which in turn were coupled to 1/4" shafts. These shafts are supported by two lengths of 1-1/4" x 1-1/4" x 3/16" aluminum angle stock. Two cams are mounted on each shaft and activate SPDT Micro Switches (Micro Switch, Freeport, Illinois) mounted on the angle stock. The cams are adjustable and permit the switches to be used as positional limit switches for any left or right fractional rotation of each shaft. The free end of each shaft is coupled via a 2-1/2" Flexible Shaft (No. 115-253, E. F. Johnson Company, Waseca, Minnesota) to a 115 V. A. C.

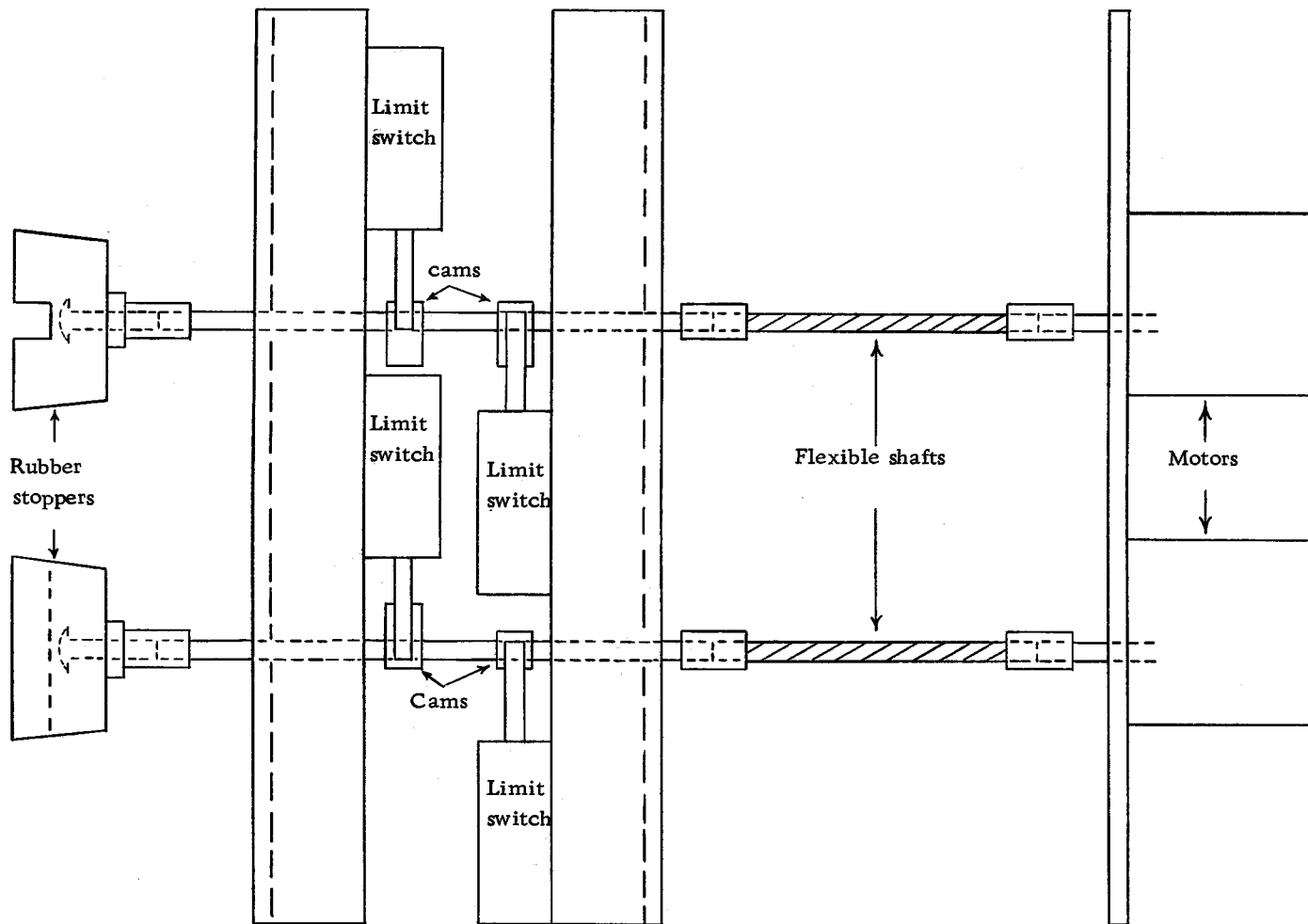


Figure II-1. Diagram of automatic sample selector, top.

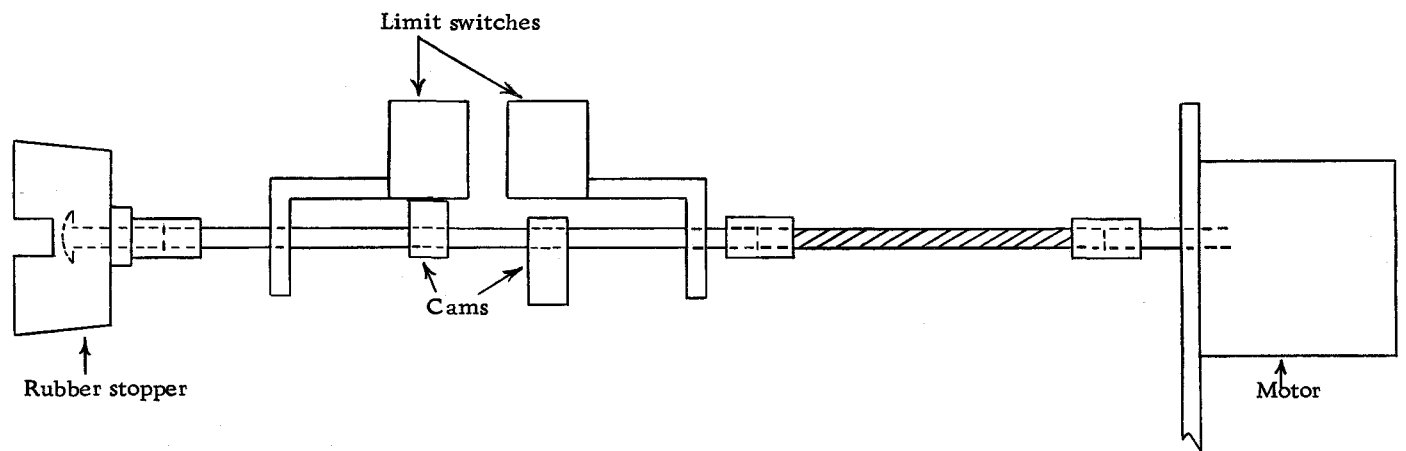


Figure II-2. Diagram of automatic sample selector, left side.

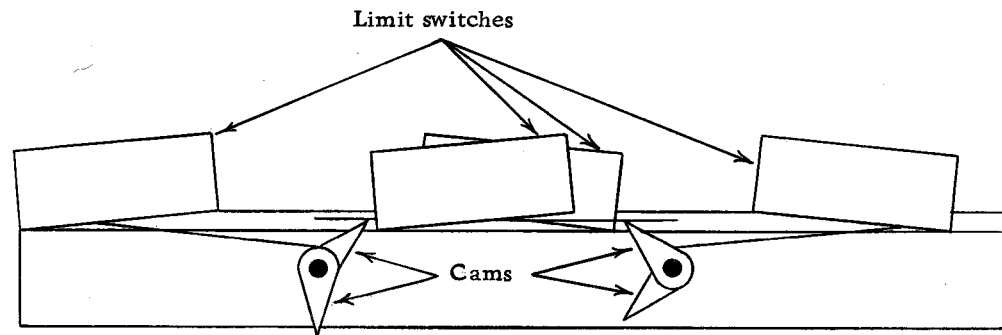


Figure II-3. Diagram of automatic sample selector, front cross section at switches.

Reversible Synchronous Motor (Type PC-DA 6 rpm, Hurst Mfg. Corp., Princeton, Indiana). These motors, when energized by the programmer, provide the stopcock drive power.

An adjustable cam timer with 12 SPDT switches was assembled from the components in the Multi-Cam Timer Kit (Industrial Timer Corp., 1407 McCarter Highway, Newark, New Jersey) to serve as the master programmer for the automatic sample selector. Each motor requires one SPDT switch on the programmer to perform the forward/reverse functions and two switches to perform the on/off function (relay activated clutch) at two different times during the program (On-forward/off and on-reverse/off). Thus programmer switches 1-3 were assigned to control motor 1, switches 4-6 to control motor 2, and switches 7-12 to indicator functions. Of the latter group, switches 7, 8, and 9 were assigned to control indicator lamps 1, 2, and 3, respectively. These lamps serve to visually indicate which source is being sampled. Switches 10-12 were assigned to activate the event marker on the Bausch and Lomb VOM-5 strip chart recorder. The four positional limit switches on the stopcock actuator chassis were assigned numbers 13 through 16.

Figure II-4 is a schematic representation of the program that was established on the Multi-Cam Timer. The program is divided into equal thirds for sampling purposes and can be briefly described as follows. The cycle begins with the rotation of stopcock 1 by

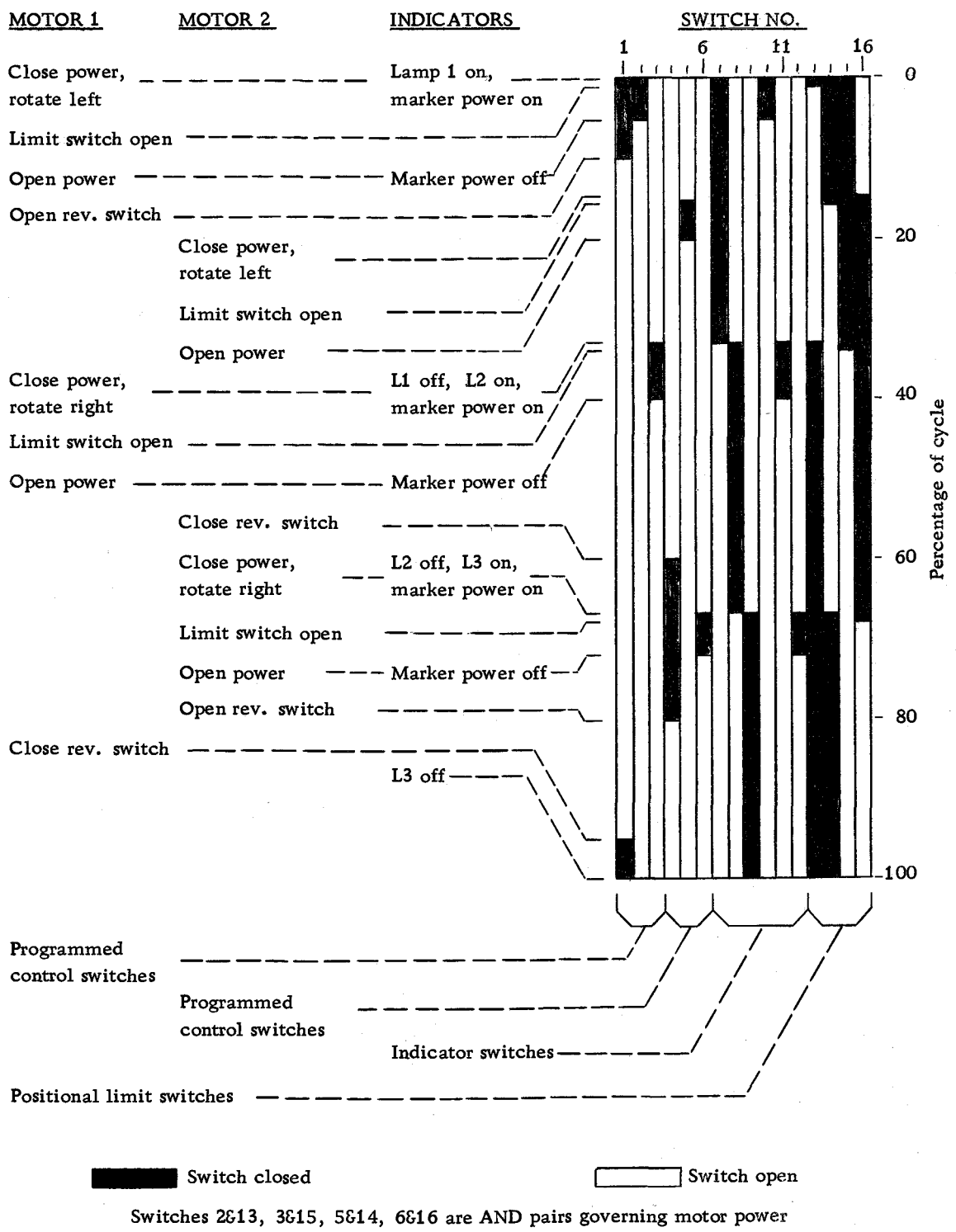


Figure II-4. Automatic sample selector program.

motor 1 to the left (normally connected to a water blank). Simultaneously a pulse goes to the event marker and lamp 1 lights. At about 15% of the cycle, stopcock 2 is reset to the left position by motor 2 and, at 33-1/3%, stopcock 1 is turned to the right, connecting to stopcock 2 (left). At this time, another pulse is sent to the event marker and lamp 1 is turned off as lamp 2 is lit. At 66-2/3% of the cycle, stopcock 2 is moved to the right position, the event marker receives a pulse, and as lamp 2 goes off, lamp 3 is lit.

Figure II-5 shows an overall schematic wiring diagram for the three chassis that comprise the automatic sample selector together with their interconnecting cables. Note that switches 14-16 are connected in parallel to perform an OR function, i. e., the event marker is energized when Sw 14 OR Sw 15 OR Sw 16 is closed. The switches which energize the motor clutches also perform logic functions. Thus switches 5 and 14 are connected in series to perform an AND function as are switches 6 and 16. The two series combinations are connected in parallel to perform an OR function, thus switches 5, 6, 14, and 16 perform both AND and OR operations, i. e., motor 2 is energized when [(Sw5 AND Sw14) OR (Sw6 AND Sw16)] are closed. Switches 2, 3, 13, and 15 similarly control the clutch of motor 1.

The mode switch on the programmer panel permits a decision to be made during any cycle to terminate at its end. (Although the program is actually terminated at the precise beginning of the next

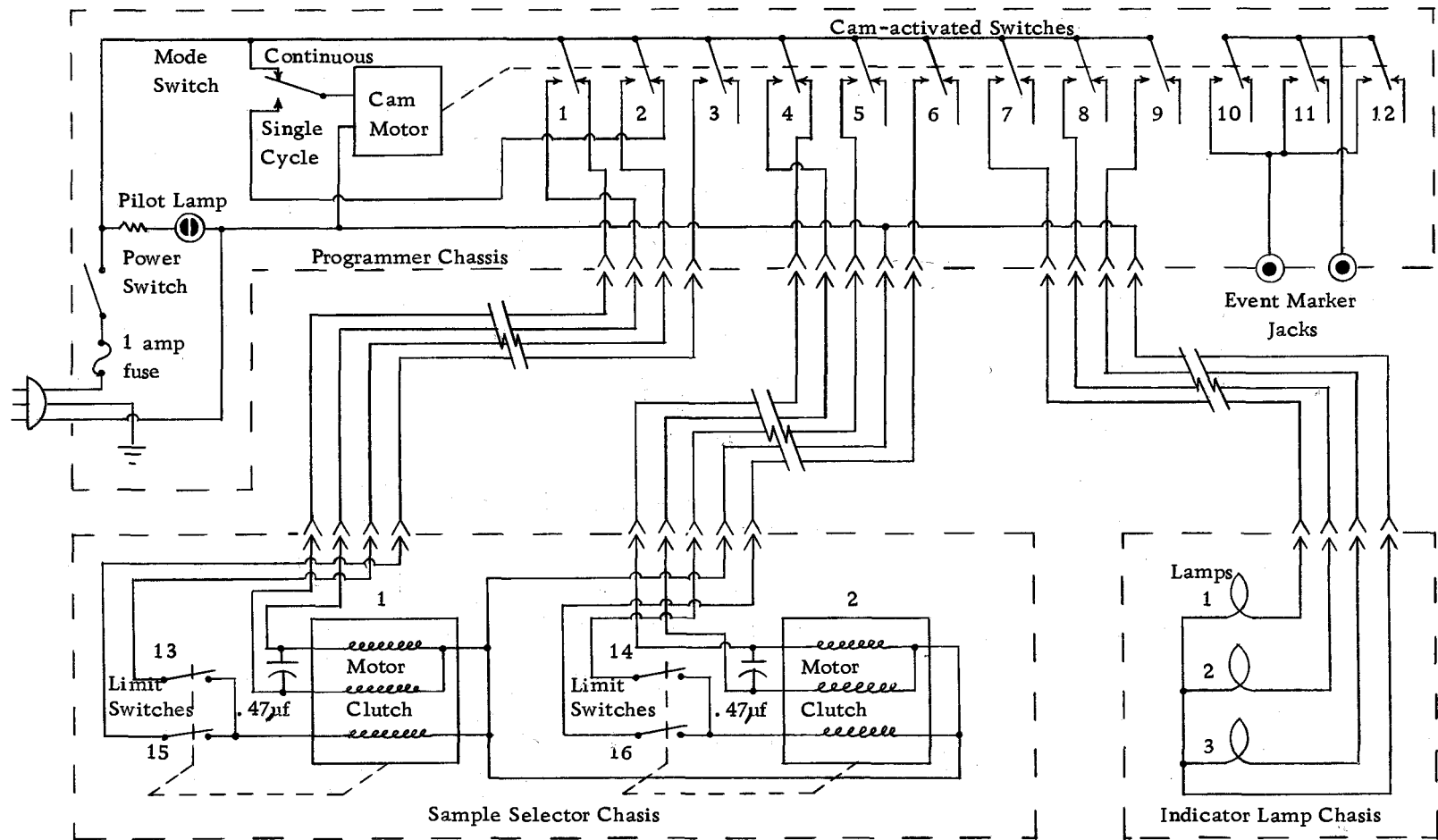


Figure II-5. Schematic wiring diagram for automatic sample selector, programmer, and indicator lamp chassis.

cycle so as to return the selector to the water blank position.) This switch functions as follows: when the mode switch is thrown from continuous to single-cycle (this must be done sometime after the first 5% of the cycle), the cam drive motor draws its power from the otherwise unused position of switch 2. Since switch 2 governs the resetting of the selector to the water blank, this switch may be regarded as the beginning-of-cycle index. At the precise moment that stopcock motor 1 is energized to return to water blank (left position), and if the mode switch is in the single cycle position the power lead to the cam drive motor is opened, and the program terminates. Of course, the program may be instantly terminated or interrupted at any time by opening the main power switch.

While the immediate use of this sample selector was to facilitate preparation of calibration curves, its construction and use provided experience in the technique of automatically initiating a process. In a modification of the analyzer described here for the purpose of field use, it will be necessary to periodically introduce samples of known concentration to provide an internal verification that the analyzer is operating properly. The automatic sample selector used here suggests a way in which this periodic checking function could be incorporated.

For dependable field operation, the stopcocks and their mechanical positioning apparatus should be replaced with a group of on/off

solenoid-activated valves. These would be activated when needed by a timer similar to the cam-type timer described here or another suitable timing device such as the Actan Programming Switch (Sealectro Corp., 225 Hoyt Street, Mamaroneck, N. Y.), which instead of being continuously variable, is programmed to open or close up to 57 contacts, each during any or all of 60 discrete fractions of each cycle.

APPENDIX III

LAMINAR FLOW EQUATIONS

To develop an equation to describe the propagation of the parabolic front which develops as a plug of fluid is moved along a tube or pipe under conditions of laminar flow, start with a fundamental equation for an elliptic paraboloid.

$$\frac{x}{a} + \frac{y^2}{b^2} + \frac{z^2}{c^2} = 1 \quad (1)$$

Now consider the special case of a paraboloid of revolution, then $b = c$ and, when $x = 0$, (1) becomes

$$\frac{y^2}{b^2} + \frac{z^2}{c^2} = \frac{y^2}{b^2} + \frac{z^2}{b^2} = 1, \quad (2)$$

the equation for a circle of radius b . Let r be substituted for b (or c) where r is the radius of the circle when $x = 0$, and let r'^2 be substituted for $(y^2 + z^2)$ where r' is the radius of the circular profile at any value of x . Further impose the condition that $x \geq 0$, then (1) becomes

$$\frac{x}{a} + \frac{r'^2}{r^2} = 1, \quad x \geq 0,$$

which is the equation for a paraboloid of revolution, maximum radius

r, with a parabolic profile in the xy or xz planes, a circular profile in the yz plane, and an x-axis intercept of a.

Now to find the volume of the paraboloid, first consider a differential cylindrical shell of length x, diameter 2r', and thickness dr'. Its volume dV is given by

$$dV = 2\pi x r' dr' \quad (4)$$

Using the method of integration by shells, the volume V of a paraboloid of revolution of maximum radius r is given by

$$V = \int_0^r dV = \int_0^r 2\pi x r' dr' \quad (5)$$

Substituting for x from (3), (5) becomes

$$\begin{aligned} V &= \int_0^r 2\pi a r' [1 - (r'^2/r^2)] dr' \\ &= \pi r^2 a/2. \end{aligned}$$

The length of a cylinder of volume equal to the volume of a paraboloid of revolution may be considered to be the mean length \bar{x} of the paraboloid. Since length is volume divided by cross sectional area,

$$\bar{x} = V/A = (\pi r^2 a/2)/\pi r^2 = a/2, \quad (7)$$

thus the mean length of the paraboloid is half its maximum or overall length.

Since the average flow rate $F = dV/dt$ may be associated with the mean length of a paraboloid moving along a cylindrical tube or pipe of cross sectional area $A = \pi r^2$,

$$F = dV/dt = A d\bar{x}/dt = \pi r^2 d\bar{x}/dt.$$

Substituting from (7) and integrating,

$$a = (2Ft/\pi r^2) + \text{Constant.} \quad (9)$$

But as t approaches zero, a approaches zero, so Constant = zero, and

$$a = 2Ft/\pi r^2. \quad (10)$$

The complete equation for the parabolic front, then, becomes

$$\frac{\pi r^2 x^2}{2Ft} + \frac{r'^2}{r^2} = 1, \quad (11)$$

where x is the distance from the origin and r' is the distance from the center of the bore of some point on the surface of a parabolic front which has moved along a tube or pipe of radius r at an average flow rate F for a time t .